



OPEN ACCESS

Original research

# Molecular heterogeneity and commonalities in pancreatic cancer precursors with gastric and intestinal phenotype

Sven-Thorsten Liffers,<sup>1,2</sup> Laura Godfrey,<sup>1,2</sup> Lisa Frohn,<sup>3</sup> Lena Haeberle,<sup>3</sup> Aslihan Yavas ,<sup>3</sup> Rita Vesce,<sup>3</sup> Wolfgang Goering,<sup>3</sup> Friederike V Opitz ,<sup>3</sup> Nickolas Stoecklein,<sup>4</sup> Wolfram Trudo Knoefel,<sup>4</sup> Anna Melissa Schlitter ,<sup>5</sup> Guenter Klöppel,<sup>5</sup> Elisa Espinet ,<sup>6,7,8</sup> Andreas Trumpp,<sup>6,7,8</sup> Jens T Siveke,<sup>1,2</sup> Irene Esposito <sup>3</sup>

► Additional supplemental material is published online only. To view, please visit the journal online (<http://dx.doi.org/10.1136/gutjnl-2021-326550>).

For numbered affiliations see end of article.

## Correspondence to

Professor Irene Esposito, Institute of Pathology, Heinrich-Heine-University Dusseldorf and University Hospital of Dusseldorf, Dusseldorf 40225, Germany; Irene.Esposito@med.uni-duesseldorf.de

S-TL and LG are joint first authors.

JTS and IE are joint senior authors.

Received 12 November 2021  
Accepted 31 July 2022



© Author(s) (or their employer(s)) 2022. Re-use permitted under CC BY-NC. No commercial re-use. See rights and permissions. Published by BMJ.

**To cite:** Liffers S-T, Godfrey L, Frohn L, et al. *Gut* Epub ahead of print: [please include Day Month Year]. doi:10.1136/gutjnl-2021-326550

## ABSTRACT

**Objective** Due to the limited number of modifiable risk factors, secondary prevention strategies based on early diagnosis represent the preferred route to improve the prognosis of pancreatic ductal adenocarcinoma (PDAC). Here, we provide a comparative morphogenetic analysis of PDAC precursors aiming at dissecting the process of carcinogenesis and tackling the heterogeneity of preinvasive lesions.

**Design** Targeted and whole-genome low-coverage sequencing, genome-wide methylation and transcriptome analyses were applied on a final collective of 122 morphologically well-characterised low-grade and high-grade PDAC precursors, including intestinal and gastric intraductal papillary mucinous neoplasms (IPMN) and pancreatic intraepithelial neoplasias (PanIN).

**Results** Epigenetic regulation of mucin genes determines the phenotype of PDAC precursors. PanIN and gastric IPMN display a ductal molecular profile and numerous similarly regulated pathways, including the Notch pathway, but can be distinguished by recurrent deletions and differential methylation and, in part, by the expression of mucin-like 3. Intestinal IPMN are clearly distinct lesions at the molecular level with a more instable genotype and are possibly related to a different ductal cell compartment.

**Conclusions** PDAC precursors with gastric and intestinal phenotype are heterogeneous in terms of morphology, genetic and epigenetic profile. This heterogeneity is related to a different cell identity and, possibly, to a different aetiology.

## INTRODUCTION

Pancreatic ductal adenocarcinoma (PDAC) is one of the most aggressive human neoplasms and represents the fourth most common cause of cancer-related deaths in Western countries.<sup>1</sup> A curative surgical approach is feasible only in about 20% of the patients.<sup>2</sup> Despite numerous progresses in the last years, the number of PDAC patients surviving longer than 5 years is disappointingly low and most patients will succumb to their disease.<sup>3–5</sup> Current treatment strategies focus on fighting the advanced disease, present in about half of the cases

## WHAT IS ALREADY KNOWN ON THIS TOPIC

- ⇒ Intraductal papillary mucinous neoplasms (IPMN) and pancreatic intraepithelial neoplasias (PanIN) are well-known pancreatic ductal adenocarcinoma (PDAC) precursors and have been characterised concerning their morphology and their immunohistochemical and genetic profile.
- ⇒ PanIN and gastric IPMN are mostly localised in the peripheral duct system and are mainly distinguished based on their size.
- ⇒ Intestinal IPMN are mostly main duct lesions with high frequency of GNAS mutations.

## WHAT THIS STUDY ADDS

- ⇒ PanIN and gastric IPMN have a very similar genetic and epigenetic profile traceable to the ductal cell compartment.
- ⇒ Differential epigenetic regulation and expression of mucin-like 3 (MUC3) and the presence of recurrent copy number variation (mainly deletions) in gastric IPMN may indicate a higher potential for progression in these lesions.
- ⇒ Intestinal IPMN display a distinct genetic landscape and higher level of genomic instability with higher proliferation rates already in low-grade lesions, suggesting a higher susceptibility for progression compared with PanIN and gastric IPMN.
- ⇒ Intestinal IPMN show an upregulation of genetic signatures related to mucin secretion and a clearly distinct epigenetic profile based on DNA methylation patterns compared with PanIN and gastric IPMN, relating them to a different adult cell type within the ductal compartment.

at diagnosis, by combining standard chemotherapy with targeted and immune-based therapies with limited benefit so far.<sup>6,7</sup>

In contrast to other solid tumours like lung, breast or colon cancer, there are only a few known

**HOW THIS STUDY MIGHT AFFECT RESEARCH, PRACTICE OR POLICY**

- ⇒ Immunophenotypical and, when necessary, molecular subtyping is fundamental in correctly classifying PDAC precursors with different risk of progression and its use in pathology reports should be enforced.
- ⇒ Despite their similarities, distinction between PanIN and gastric IPMN is relevant and should be pursued with available (eg, GNAS mutations) and, possibly, newly established markers, such as MUCL3.
- ⇒ PDAC precursor subtype-directed lineage and aetiological factor-based studies will allow identification and evaluation of lesion-specific prevention strategies.

factors that increase the risk of developing PDAC.<sup>6,8</sup> Among at least partly modifiable factors, cigarette smoking, obesity, long-standing diabetes and non-hereditary chronic pancreatitis are associated with a threefold to sixfold increased lifetime risk for PDAC. Other factors include hereditary causes with identified or still unknown gene alterations, for which effective screening strategies are still missing.<sup>9,10</sup> It seems therefore that the only effective strategy to substantially change the prognosis of this dismal disease is to detect and treat it in a very early stage, possibly at the stage of its precursor lesions.<sup>11</sup>

Intraductal and cystic lesions belong to the currently recognised precursors of PDAC and include pancreatic intraepithelial neoplasias (PanIN), intraductal papillary mucinous neoplasms (IPMN), intraductal oncocytic papillary neoplasms, intraductal tubulo-papillary neoplasms and mucinous cystic neoplasms.<sup>12,13</sup> Among them, PanIN and IPMN are the most relevant due to their frequency (PanIN) and the clinical challenge related to their treatment (IPMN). PanIN represent the longest-known and best-characterised precursors of classical PDAC, although they progress with low frequency.<sup>14,15</sup> IPMN encompass three histopathological subtypes, namely intestinal, gastric and pancreatobiliary, with different morphology, immunophenotype and, partly, biological behaviour.<sup>13</sup> Despite these differences, numerous overlapping features exist, and distinction is not always clear-cut. For example, although intestinal IPMN are usually localised in the main pancreatic duct, they may extend, or seldom even occur, in peripheral branch ducts. The same holds true for branch-duct gastric IPMN, which can extend to or occur in the main pancreatic duct. In addition, mixed immune phenotypes are detected in about 5% of the cases and recently, a possible origin of intestinal IPMN from gastric IPMN has been proposed as well.<sup>16,17</sup> In addition, the distinction between PanIN and gastric IPMN is mainly based on their size (<0.5 cm and >1 cm, respectively) and on the different frequency of GNAS mutations. However, they share a common localisation and an identical morphology and immune profile (figure 1A), rendering distinction not always straightforward in cases of small ('incipient') IPMN.<sup>18</sup> This distinction may be of clinical relevance, for example, in the setting of intraoperative examination of the pancreatic neck margin: whereas leaving behind a PanIN will not have any consequences in most cases, a residual gastric IPMN might bear a higher risk of recurrence.<sup>19,20</sup>

Recent studies have tried to shed light on the progression of precursor lesions to invasive cancer. Accordingly, the genetic evolution of PanIN has been quantified, revealing a period of about 7 years necessary for an initiating cell to develop into metastatic cancer.<sup>21</sup> However, this model is often contradicted by the clinical observation of rapidly progressive disease with

systemic dissemination preceding clinical appearance, thus suggesting the possibility of additional, not yet fully elucidated more rapid progression models such as chromothripsis rather than or in addition to linear stepwise genetic evolution.<sup>22,23</sup> A stepwise progression model is thought to play a role in IPMN as well, but the natural history of these lesions especially taking into consideration the different subtypes, remains largely unknown.<sup>24</sup>

It is therefore apparent that numerous questions regarding the development of pancreatic precursors from their cell of origin to high-grade and invasive lesions and their relation to each other remain open. In this work, we provide the first extensive genetic and epigenetic characterisation of PDAC precursors focusing on the molecular comparison between intestinal and gastric IPMN and PanIN.

**MATERIALS AND METHODS**

Additional protocols and complete procedures are described in the online supplemental material and methods section.

**Study cohort**

A tissue collection of precursor lesions of PDAC obtained from 154 patients operated on in the years 2008–2021 was established. The study cohort consists of 132 different precursor lesions and includes PanIN (n=55) and IPMN (n=77); 59 lesions (44.6%) occurred in the context of PDAC (table 1, online supplemental figure 1). All lesions were re-classified by reviewing all slides according to current criteria and nomenclature.<sup>12,25</sup> Only PanIN in pre-existent ducts were included. Representative slides from all lesions were stained with antibodies for mucin 1 (MUC1), mucin 2 (MUC2), mucin 5 (MUC5AC) and caudal type homeobox 2 (CDX2) for histopathological subtyping.<sup>13</sup> Only morphology and immunohistochemistry were considered for the distinction between PanIN and gastric IPMN and for IPMN subtyping. Diagnoses were performed by a pathologist with over 20 years' experience in pancreatic pathology (IE); difficult cases were discussed with another pathologist with over 50 years' experience in pancreatic pathology (GK). In cases with IPMN and PDAC, PDAC was defined as 'associated' if there was clear morphological evidence of its origin from the IPMN (ie, the invasive component originated from the intraductal lesion). If the IPMN was not spatially related to the PDAC, this was considered a 'concomitant' PDAC. A collective of 79 precursor lesions (66 of them being used in this study also for molecular analyses) and of 24 PDAC specimens was analysed by whole-slide immunohistochemistry to test the expression of trefoil factor 3 (TFF3) and mucin-like 3 (MUCL3) proteins (online supplemental table 1a,b).

**Estimation of DNA copy number variation by low-coverage whole-genome sequencing and methylation data**

For this analysis, 36 PanIN (28 low-grade and 8 high-grade), 38 gastric IPMN (29 low-grade and 9 high-grade) and 21 intestinal IPMN (8 low-grade and 13 high-grade) were used. Twenty-eight lesions (11 PanIN, 13 gastric IPMN and 4 intestinal IPMN) were analysed by low-coverage whole-genome sequencing (WGS). Briefly, isolated genomic DNA from formalin-fixed, paraffin-embedded (FFPE) samples was amplified with the Ampli1 WGA kit (Menarini Silicon Biosystems, Bologna, Italy) according to the manufacturer's instructions. Ten microlitres of the Ampli1 WGA product were used to clean up with 1.8 × SPRIselect beads (Beckman Coulter, Lahntal, Germany). After that, low-coverage whole-genome libraries were prepared with the Ampli1 low-pass kit (Menarini Silicon Biosystems) according to the manufacturer's

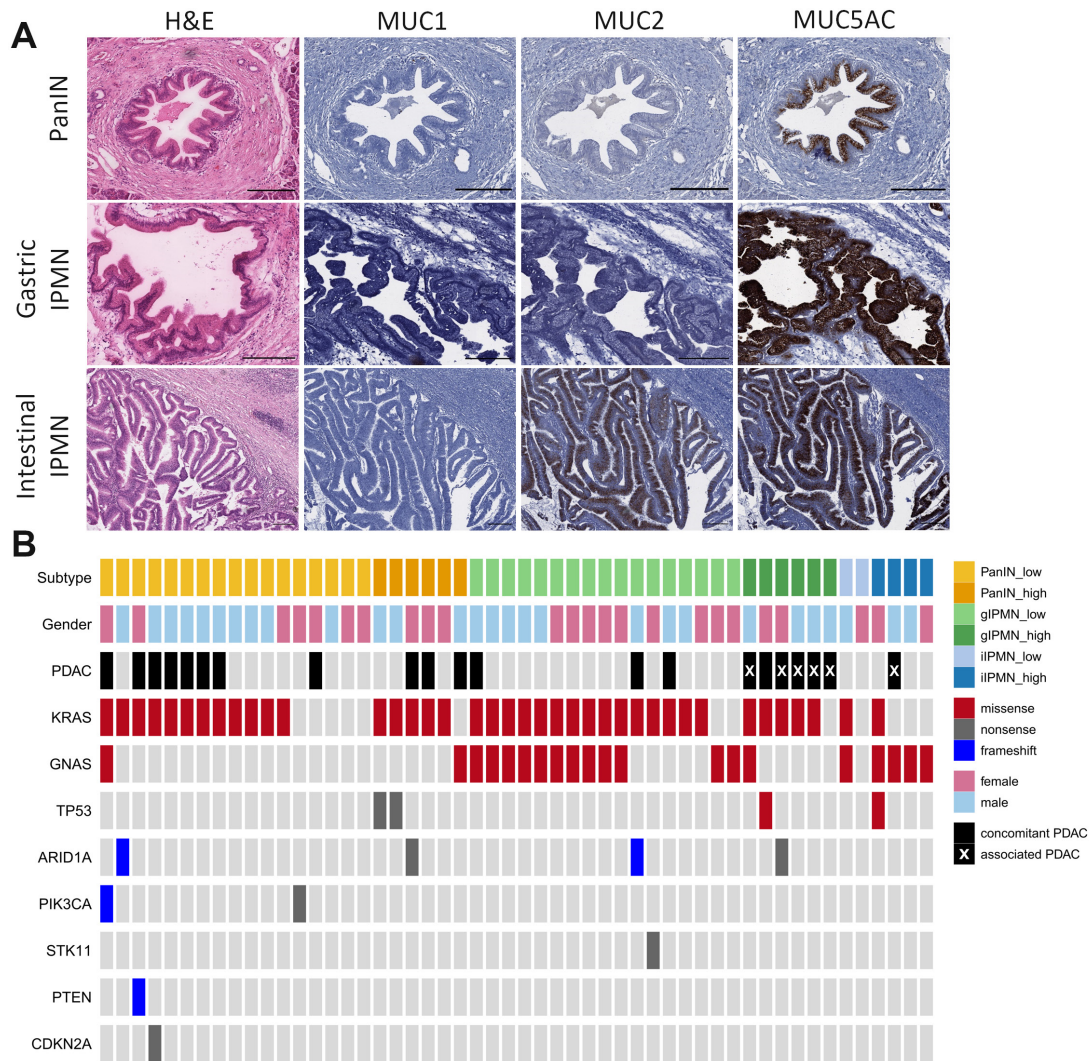


**Figure 1** Intraductal precursors of pancreatic cancer: morphology and genetics. (A) Morphology and immunohistochemistry: PanIN and gastric IPMN are distinguished according to morphology and size and display an identical immunohistochemical profile with diffuse positivity for MUC5AC and no expression of MUC1 and MUC2. Intestinal IPMN are clearly distinct lesions, both on the morphological and immunohistochemical level, characterised by positivity for MUC2 and MUC5AC. H&E and immunohistochemistry (see 'Materials and methods' section; scale bar=200 µm). (B) Targeted-next-generation sequencing analysis: low-grade and high-grade PanIN, gastric IPMN and intestinal IPMN were included in the analysis. Cases with a concomitant PDAC are indicated with a black square and those with associated PDACs are marked in addition with a white X. Labelled mutations represent pathogenic mutations according to the ClinVar database and/or the American College of Medical Genetics and Genomics guidelines with an allele frequency of  $\geq 3\%$ . Red squares represent missense mutations, grey squares are nonsense mutations and blue squares are frameshift mutations. Empty squares indicate absence of pathogenic mutations. Analysis was performed using a 21-gene custom panel on the S5 Ion Torrent platform (Phred score  $\geq 30$ , coverage  $\geq 500$ ). IPMN, intraductal papillary mucinous neoplasms; MUC1, mucin 1; MUC2, mucin 2; MUC5AC, mucin 5; PanIN, pancreatic intraepithelial neoplasias; PDAC, pancreatic ductal adenocarcinoma.

**Table 1** Study cohort

Diagnosis	Number of cases (%)	Degree of dysplasia		Cases with PDAC
		Low-grade	High-grade	
PanIN	55/132 (41.7%)	43/55 (78.2%)	12/55 (21.8%)	34/55 (61.8%)
IPMN gastric	46/132 (34.8%)	35/46 (76%)	11/46 (23.9%)	15/46 (32.6%)
IPMN intestinal	21/132 (15.9%)	8/21 (38%)	13/21 (62%)	7/21 (33.3%)
IPMN pancreatobiliary	3/132 (2.3%)	0	3/3 (100%)	2/3 (66.6%)
IPMN mixed	7/132 (5.3%)	7/7 (100%)	0	1/7 (14.3%)

IPMN, intraductal papillary mucinous neoplasms; PanIN, pancreatic intraepithelial neoplasias; PDAC, pancreatic ductal adenocarcinoma.

instructions. The final library concentration was determined on the fragment analyser (Advanced Analytical Technologies, Ames, Iowa, USA) with the Agilent high-sensitivity genomic DNA 50 kb kit (Agilent Technologies, Ratingen, Germany). An additional size selection was not done. A 100 pM equimolar library pool was created and sequenced with the Ion S5 system (ThermoFisher Scientific, Dreieich, Germany) as described in online supplemental methods.

The Ion Browser Suite mapped the sequence to the GRCh37/hg19 genome. The Ion Reporter software (V.5.12.0.0) was used for copy number determination of the low-pass sequencing. The  $\log_2$  (tumour/normal) value was calculated for each region. As a control group, six normal tissue samples consisting of acinar tissue were isolated and sequenced with the same method. Copy number regions with a  $\log_2$  ratio greater than +0.2 and less than -0.2 were considered. The median of the absolute values of all pairwise differences value was set as <0.35.

Additional 67 lesions (24 PanIN, 26 gastric IPMN and 17 intestinal IPMN) were analysed using the data from the DNA methylation profiles obtained with the Infinium Methylation EPIC BeadChip (see below, "Differential methylation analysis"). Here, the copy number variation (CNV) was estimated with the conumee package (V.1.3)<sup>26</sup> using default settings. As normal control served the combined intensities from the bulk acini samples (n=11); changes of 0.2 and -0.2 in the mean segment value were set as thresholds to define copy number gains and losses. To detect common regions between EPIC and low-pass samples, bed files were generated and compared with BEDTools (V.2.3).<sup>27</sup> A 'common' region was defined if three or more samples within the analysed precursor lesion shared the same loci. For those hits, the annotated curated NCBI RefSeq genes were retrieved from the UCSC Genome Browser (GRCh37/hg19).

### Differential methylation analysis

DNA methylation profiles were measured with the Infinium Methylation EPIC BeadChip (Illumina, San Diego, USA) at the Genomics and Proteomics Core Facility of the German Cancer Research Center Heidelberg. Methylation analysis was carried out using the R Bioconductor package ChAMP (V.2.14.0).<sup>28</sup> Briefly, IDAT files were loaded into ChAMP and preprocessed. In the first step, all probes with a detection p value >0.01 were excluded. Followed by the exclusion of probes with a bead count >3 in at least 5% of the samples, non-cg probes, single nucleotide polymorphism (SNP)-containing probes and sex probes were also filtered. Filtered datasets were normalised using the Beta Mixture Quantile dilation (BMIQ) method and batch corrected before differential analysis. Differentially methylated probes were defined by a delta of 0.2 and an adjusted p value (Benjamini-Hochberg method) of  $\leq 0.05$ . The phylogenetic tree was plotted using the R-package ape (V.5.3).

## RESULTS

### Morphology

The sample cohort consisted of 55 PanIN (41.7%), 46 gastric IPMN (34.8%) and 21 intestinal IPMN (15.9%) (table 1). Pancreatobiliary and mixed-type IPMN were excluded from further analyses due to small sample size. PanIN and gastric IPMN displayed the same immunophenotype (figure 1A) and were distinguished according to established criteria.<sup>12 25</sup>

### Gene mutations, fusion transcript analysis and chromosome copy number aberrations of PDAC precursors

Targeted next-generation sequencing was performed in 59 samples, including 7 control samples of normal acinar tissue. In detail, 23 PanIN (17 low-grade and 6 high-grade; 12 in cases without PDAC), 23 gastric IPMN (17 low-grade and 6 high-grade) and 6 intestinal IPMN (2 low-grade and 4 high-grade) were sequenced using a custom 21-gene panel (figure 1B; online supplemental table 2).

*KRAS* G12 mutations on exon 2 were present in 16/23 PanIN (69.5%), 19/23 gastric IPMN (82.6%) and 2/6 (33%) intestinal IPMN. *KRAS* Q61 mutations on exon 3 were found in one PanIN and one gastric IPMN, making up 5.1% of all *KRAS* mutated cases (online supplemental table 3). The pathogenic R201 *GNAS* mutation was present in 17/29 (58.6%) IPMN and in 2/23 PanIN (8.6%), whereas 1/29 IPMN (3.4%) displayed a *GNAS* Q227 mutation. Pathogenic *TP53* mutations were detected in four high-grade lesions (2 IPMN (2.2%) and 2 PanIN (8.7%)). In addition, *ARID1A*, *PIK3CA*, *STK11*, *PTEN* and *CDKN2A* nonsense and frameshift mutations were observed in few individual lesions (figure 1B; online supplemental table 3). The overall frequency of mutations in PanIN in specimens without PDAC was not significantly different from that of PanIN in specimens with PDAC (not shown). IPMN had a significant higher variant allele frequency (VAF) of *KRAS* and *GNAS* than PanIN (online supplemental figure 2A–B), possibly due to contamination by normal tissue in dissected PanIN lesions. Pearson's correlation analysis of double mutated (*KRAS* and *GNAS*) gastric IPMN samples confirmed a positive correlation between the VAFs of the two mutations ( $r=0.9795$ ,  $p\leq 0.0001$ , online supplemental figure 2C), indicating that these most probably occurred in the same cell.

Six cases without mutations (four PanIN, one gastric IPMN and one intestinal IPMN) were subjected to fusion transcript analysis to check for possible alternative drivers. Five samples revealed no detectable fusion transcripts (not shown); in one case (low-grade PanIN), the analysis was not possible due to insufficient RNA quality. Morphology was not predictive of the genetic status; representative examples of lesions with identical morphology and different genetic changes are shown in online supplemental figure 3.

Next, we assessed CNV by two orthogonal methods: DNA methylation array data and whole-genome low-coverage sequencing. Among the three precursor lesions, PanIN displayed the lowest number of samples affected by genomic losses and gains (n=22, 61%) followed by gastric IPMN (n=29, 76%) and intestinal IPMN (21, 100%) (table 2A). There was no relationship between the degree of dysplasia and the presence/absence of CNV (online supplemental table 4). Although intestinal IPMN showed in general higher numbers of deletions and amplifications per sample, there was a remarkable difference in the median size of deletions for gastric IPMN (4.5 Mb) compared with PanIN (0.7 Mb) and intestinal IPMN (2.3 Mb). CNV values are shown in online supplemental table 5. Furthermore, only gastric IPMN showed a loss of *TP53* (chr.:17) and *CDKN2A* (chr.:9) in multiple samples (table 2B). Deletions on chromosome 11 were solely detected in intestinal IPMN affecting the putative tumour suppressor genes *CTNND1*, *MEN1*, *ATM* and *KMT2A*. Beside this locus, intestinal IPMN were generally affected by amplifications (figure 2B and C). This finding was underpinned by the median size of 5.1 Mb/amplification compared with 1.2 Mb/amplification and 2 Mb/amplification for PanIN and gastric IPMN, respectively (table 2a). In addition, recurrent

**Table 2** (A) Overview of DNA copy number variations (CNV) of pancreatic precursor lesions, (B) detailed overview of genomic regions affected by CNV

	PanIN (n=36)		gIPMN (n=38)		iIPMN (n=21)	
Samples with CNV	22	(61%)	29	(76%)	21	(100%)
Samples with only deletions	8	(22%)	5	(13%)	1	(5%)
Samples with only amplifications	7	(19%)	12	(32%)	4	(19%)
Samples with deletions and amplifications	7	(19%)	12	(32%)	16	(76%)
Median no. of deletions/sample (95% CI)	2	(1 to 3)	2	(2 to 6)	4	(2 to 12)
Median size of deletions/sample (95% CI) Mb	0.7	(0.5 to 1.9)	4.5	(2.3 to 10.3)	2.3	(1.6 to 4.0)
Median no. of amplifications/sample (95% CI)	3	(2 to 6)	2	(2 to 4)	6.5	(2 to 19)
Median size of amplifications/sample (95% CI) Mb	1.2	(0.8 to 1.9)	2	(1.1 to 3.5)	5.1	(3.9 to 8.0)
Recurrent chromosomal regions (n≥3)	5		44		229	
Affected putative tumour suppressor genes	0		7		26	
Affected putative oncogenes	0		0		26	

Genomic location	PanIN (n=36)	gIPMN (n=38)	iIPMN (n=21)	Gene symbols	
<b>Deleted regions</b>					
chr01:010875000-013052998			3	(14%)	MTOR
chr01:015375000-016825000			3	(14%)	EPHA2
chr06:074175000-074375000		3	2	(8%)	EEF1A1
chr06:133664400-143100000		2	3	(5%)	TNFAIP3
chr06:143620678-151100000	1	3	3	(8%)	LATS1
chr09:005958053-023802212	1	4	3	(3%)	PSIP1   CDKN2A
chr10:071075000-120925000		2	4	(5%)	PTEN   TCF7L2
chr10:120925000-125869472		1	4	(3%)	FGFR2
chr11:057325000-058807232			4	(19%)	CTNND1
chr11:058807232-069089801			5	(24%)	MEN1   SF1
chr11:096437584-114325000			5	(24%)	ATM
chr11:114325000-134898258			4	(19%)	KMT2A
chr17:006225000-009675000		3	1	(8%)	GPS2   TP53
chr17:009675000-012500000		3	2	(8%)	MAP2K4
chr17:015792977-021566608		3	3	(8%)	NCOR1
<b>Amplified regions</b>					
chr01:035225000-037325000			3	(14%)	THRAP3
chr03:176225000-188875000	1	2	3	(3%)	PIK3CA
chr05:028950000-044925000			5	(24%)	NIPBL
chr06:024125000-033575000		2	3	(5%)	HLA-A   HLA-B
chr06:033575000-042725000		1	3	(3%)	CDKN1A   PIM1
chr07:000282484-007150000			5	(24%)	RAC1
chr07:054725000-055775000			5	(24%)	EGFR
chr07:061967157-074715724			4	(19%)	GTF2I
chr07:112425436-130154523			5	(24%)	MET
chr07:139404377-142048195			5	(24%)	BRAF
chr07:143397897-154270634			5	(24%)	KMT2C   CUL1
chr08:086726451-089550000			3	(14%)	CNBD1
chr08:127450000-129175000	1	6	6	(3%)	MYC
chr09:001992685-035698318			3	(14%)	PSIP1   CDKN2A
chr09:070835468-092343416			4	(19%)	GNAQ
chr09:096718222-097575000			4	(19%)	PTPDC1
chr09:097775000-114750000			4	(19%)	PTCH1
chr09:124994207-133073060			3	(14%)	SPTAN1   PPP6C
chr12:006475000-007169938	1	7	7	(3%)	CHD4
chr12:024993545-028938805	1	3	3	(3%)	KRAS
chr14:020700000-022050000			3	(14%)	CHD8

Continued

Table 2 Continued

Genomic location	PanIN (n=36)	gIPMN (n=38)	iIPMN (n=21)	Gene symbols
chr14:022800000-050175000			3 (14%)	AJUBA   FOXA1
chr14:097258910-107289540			3 (14%)	TRAF3   AKT1
chr17:061125000-062410760			3 (14%)	CD79B
chr17:062775000-063525000			3 (14%)	GNA13
chr17:068117898-077546461			3 (14%)	SOX9
chr20:008050000-016400000		1 (3%)	6 (29%)	PLCB4
chr20:016625000-021300000		1 (3%)	6 (29%)	ZNF133
chr20:030025000-034897085		1 (3%)	6 (29%)	ASXL1
chr20:036958189-042991501		1 (3%)	5 (24%)	PLCG1
chr20:052650000-061091437		1 (3%)	6 (29%)	GNAS
chr21:032825000-034475000			3 (14%)	SCAF4

CNV alterations were detected by low-coverage sequencing (n=28) and DNA methylation data (n=67), respectively. Values are n (%) unless otherwise indicated. Gain and loss of genomic regions were detected by low-coverage sequencing (n=28) and DNA methylation data (n=67), respectively. Values are n (%), putative tumour suppressors (green) and putative oncogenes (red).  
gIPMN, gastric IPMN; iIPMN, intestinal IPMN; IPMN, intraductal papillary mucinous neoplasms; PanIN, pancreatic intraepithelial neoplasias.

regions containing a putative oncogene were detected only in intestinal IPMN. Among the intestinal IPMN precursors, there was a higher prevalence of amplification for the chromosomes 7 (*EGFR*, *MET*, *BRAF*), 8 (*MYC*), 12 (*CDH4*) and 20 (*GNAS*), which were amplified in five or more cases (table 2b). The significantly higher Ki-67 proliferations rates in intestinal IPMN (online supplemental figure 5) could further support the presence of a higher level of genomic instability in intestinal IPMN.

#### Genome-wide DNA methylation analysis of PDAC precursors

DNA methylation data were generated in 79 different FFPE samples of precursor lesions, including 27 PanIN (20 low-grade and 7 high-grade), 32 gastric IPMN (24 low-grade and 8 high-grade) and 20 intestinal IPMN (8 low-grade and 12 high-grade). For comparison, we generated DNA methylome profiles from normal acinar, ductal and neuroendocrine cell compartments. Thus, acinar bulk tissue (n=11), main duct (n=11) and branch duct (n=8) cell preparations as well as FACS (fluorescence activated cell sorting)-sorted  $\beta$ -cells (n=3) from healthy pancreatic tissue were included in the analysis. Additionally, we added publicly available samples of FACS-sorted ductal cells (n=4) and FACS-sorted acinus cells (n=4) for internal control.<sup>29 30</sup>

After the data processing, 702 656 probes were used to analyse the cell type and precursor lesion-specific DNA methylation profiles. Despite differences in sample preparation between in-house and publicly available samples (ie, FFPE vs fresh frozen), multidimensional scaling revealed a coherent population of acinar bulk tissue samples and sorted acini, while spreading of ductal cells was larger (online supplemental figure 4A). A hierarchical clustering based on probes associated with known ductal and acinar markers clearly separated the normal cell populations (online supplemental figure 4B). The methylation level of CpGs located in acinar marker genes was higher in ductal cells, whereas ductal markers were hypermethylated in acinar cells. Pairwise comparison of the control groups revealed a similar amount of differentially methylated probes in acinar versus ductal cells (12.4%) and ductal versus  $\beta$ -cells (11.3%). However, based on multidimensional scaling, the distance between  $\beta$ -cells and the other two normal pancreatic cell types was larger than between acinar and ductal cells (figure 3A). The highest degree of significant differential methylation was detected between intestinal IPMN and  $\beta$ -cells (26.8%), whereas no significantly differentially methylated CpG was observed between branch and main ducts and between gastric IPMN and PanIN lesions, respectively (figure 3B). To address potential functional effects of the detected differentially

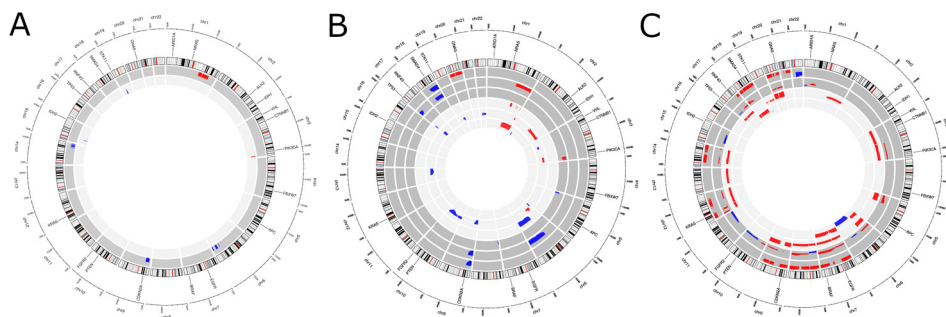


**Figure 2** Copy number variation (CNV) in PanIN, gastric and intestinal IPMN. CNVs were detected in PanIN and IPMN over the whole-genome by low-coverage sequencing. Regions in red show copy number gains and regions in blue represent copy number losses. (A) PanIN (n=11, 9 low-grade and 2 high-grade) do not possess repeated or larger regions of CNV; (B) gastric IPMN (n=13, 9 low-grade and 4 high-grade lesions) reveal three distinct repeated regions of copy number loss at chromosome 6, 9 and 18; (C) intestinal IPMN (n=4, 2 low-grade and 2 high-grade) had the highest frequency of chromosomal alterations. The broad genomic alterations generally involve entire chromosomes and are mostly located on chromosome 7, 8, 12, 18 and 20 (dark grey background=high-grade lesions, light grey background=low-grade lesions; log<sub>2</sub> value, threshold $\pm$ 0.2). IPMN, intraductal papillary mucinous neoplasms; PanIN, pancreatic intraepithelial neoplasias.

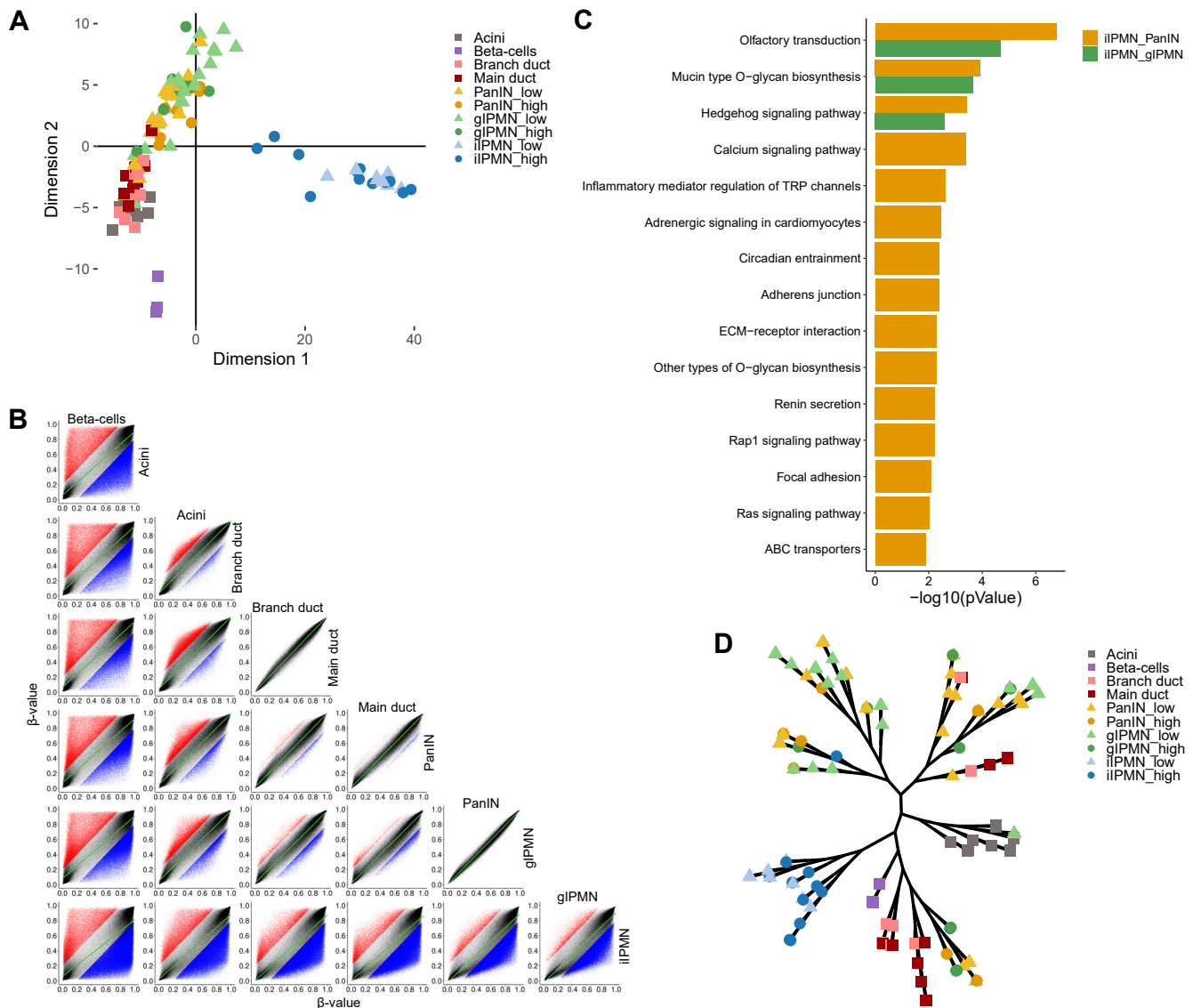


**Figure 3** DNA methylation profiling of normal pancreas cells and PDAC precursor lesions. (A) Multidimensional scaling based on the 5000 most variable CpG probes. (B) Scatter plots showing pairwise comparisons of methylated probes between indicated precursor lesions and cell types. Significantly hypermethylated probes ( $\Delta\beta \geq 0.2$ ; adjusted p value  $\leq 0.05$ ) are coloured in red and hypomethylated ( $\Delta\beta \leq -0.2$ ; adjusted p value  $\leq 0.05$ ) in blue, respectively. (C) KEGG pathway enrichment analysis of differentially methylated probes between IPMN and PanIN. (D) Phylogenetic tree displaying the relationship between precursor lesions and pancreatic cell types based on DNA methylation data. ABC, ATP-binding cassette; ECM, extracellular matrix; gIPMN, gastric IPMN; iIPMN, intestinal IPMN; IPMN, intraductal papillary mucinous neoplasms; PanIN, pancreatic intraepithelial neoplasias; PDAC, pancreatic ductal adenocarcinoma; TRP, transient receptor potential.

methylated probes (DMPs) between the different precursor lesions, we looked for enriched KEGG (Kyoto Encyclopedia of Genes and Genomes) gene sets. This analysis revealed numerous differentially enriched gene sets between PanIN and intestinal IPMN, which involved signalling pathways as well as pathways regulating cell-cell and cell-extracellular matrix interactions (figure 3C). When comparing gastric and intestinal IPMN, only three enriched gene sets were identified, including a differential regulation of the mucin type O-glycan biosynthesis and of the Hedgehog signalling pathway, among others. Notably, due to the low number of DMPs between PanIN and gastric IPMN, no significantly enriched gene set was detected, arguing for a high similarity between the two lesions, as also suggested by the phylogenetic tree analysis (figure 3D).

We next evaluated potential differences in methylation patterns between low-grade and high-grade preneoplastic precursor lesions.

Notably, we found no significant DMP between low-grade and high-grade intestinal versus gastric IPMN or between intestinal IPMN versus gastric IPMN and PanIN, respectively. When comparing low-grade and high-grade PanIN lesions, 86 significant DMPs associated with 59 genes were found between PanIN low-grade and high-grade samples, however, no candidate gene or gene network became apparent as promising candidate driver of progression (online supplemental table 6A,B).

### Transcriptome analysis of PDAC precursors

To get further insights into the distinguishing features of PanIN and IPMN, transcriptome data were generated from 41 different FFPE samples obtained from 10 PanIN (6 low-grade and 4 high-grade), 12 gastric IPMN (6 low-grade and 6 high-grade), 12 intestinal IPMN

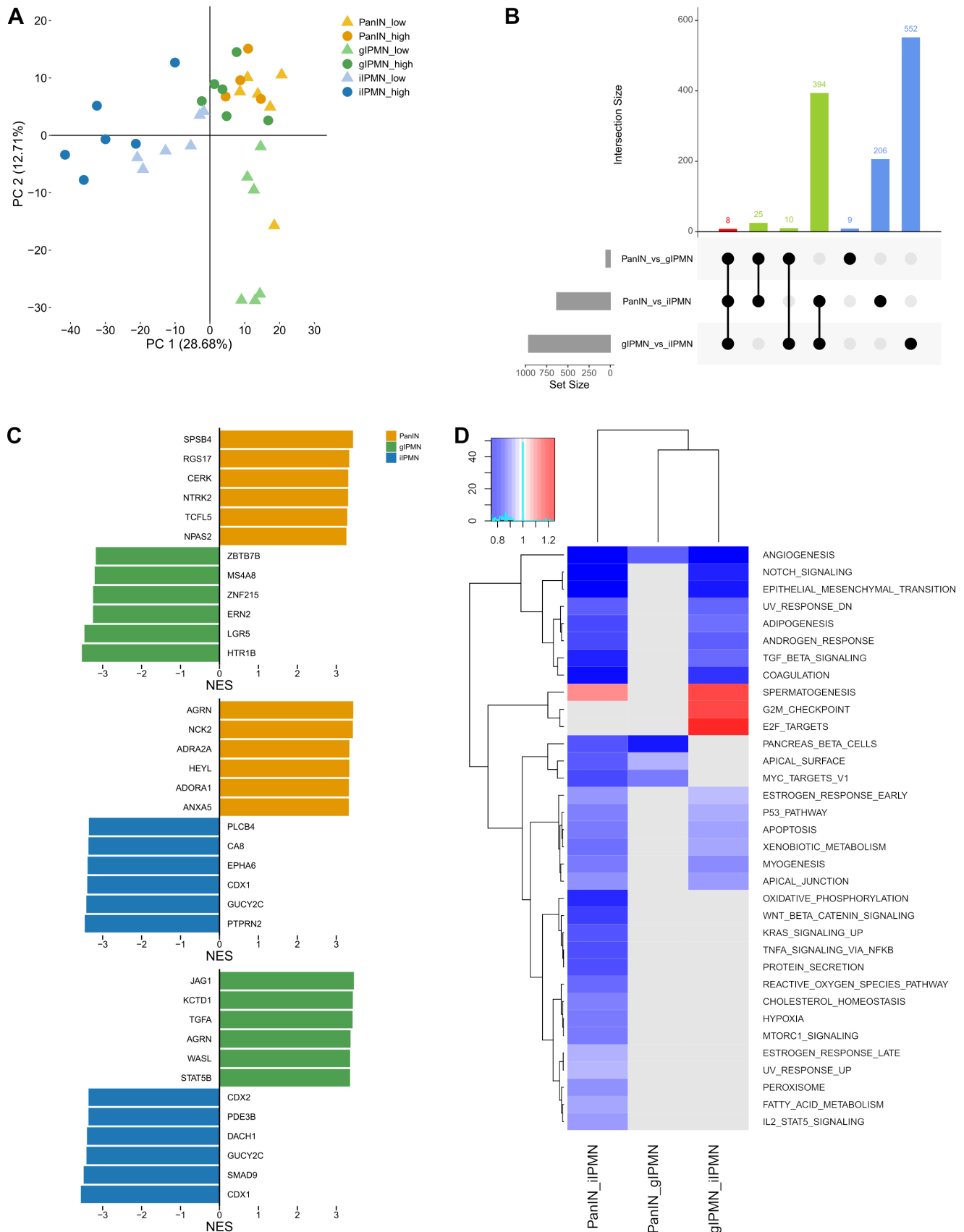


**Figure 4** Transcriptomics-based comparative analysis of precursor lesions. (A) Principal component analysis with the 500 most variable genes displaying a precursor-specific clustering. (B) Upset plot summarised the differentially expressed genes between the three precursors. (C) The precursor-specific activation of transcription factors detected by VIPER analysis based on group-wise comparisons. (D) Single sample gene set enrichments analysis indicates precursor-specific activation of *hallmark of cancer* gene sets from the MSigDB collection. gIPMN, gastric IPMN; iIPMN, intestinal IPMN; IPMN, intraductal papillary mucinous neoplasms; NES, normalised enrichment score; PanIN, pancreatic intraepithelial neoplasias.

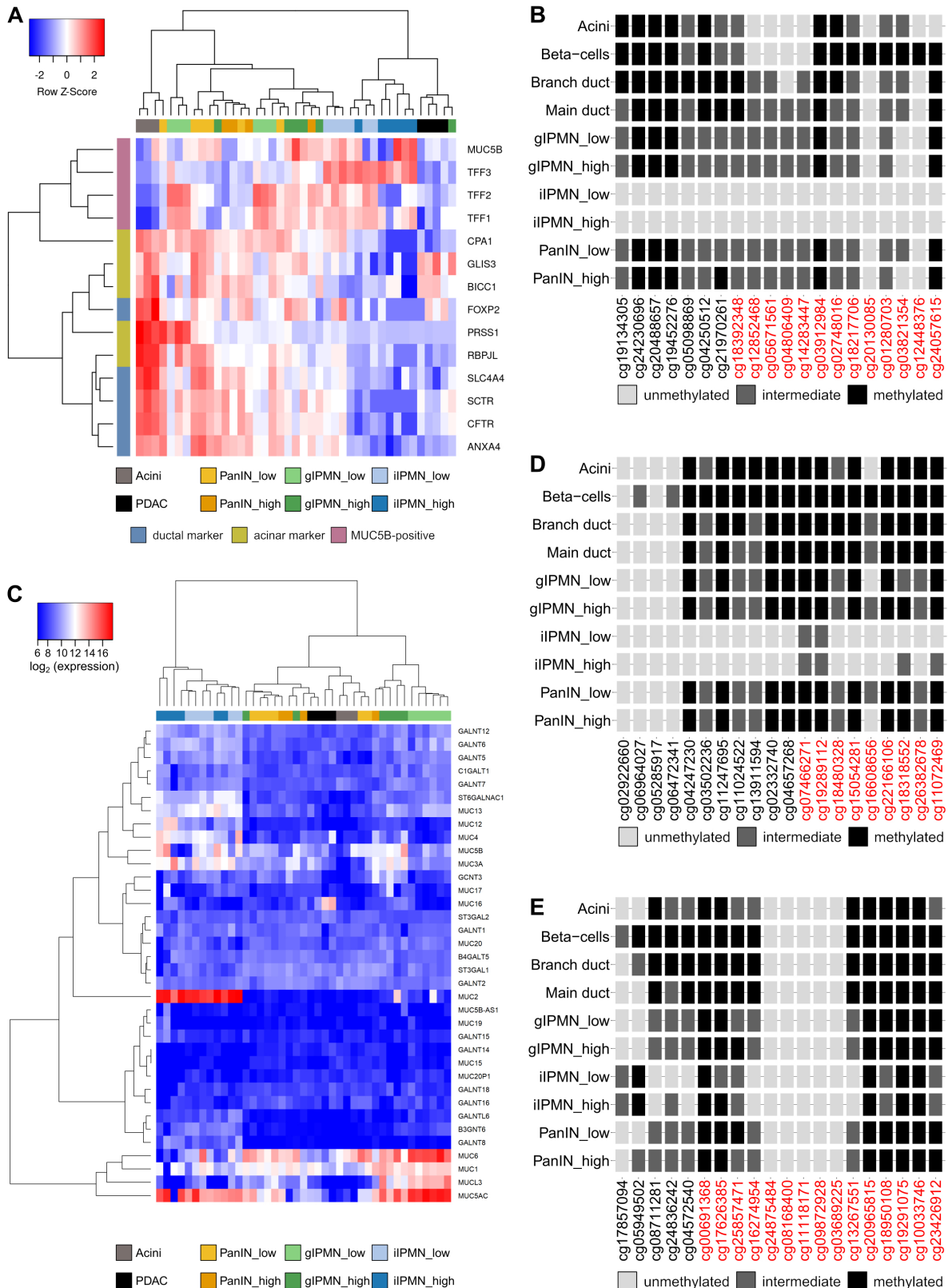


**Figure 5** Identification of different precursor subtype-specific markers. (A) Hierarchical clustering of RNA sequencing data based on published marker genes for distinct normal pancreas cell populations.<sup>29</sup> (B) Mean CpG methylation of all *TFF3* annotated probes. CpGs located in the coding region are coloured in red (unmethylated: mean  $\beta$ -value  $<0.4$ ; intermediate: mean  $\beta$ -value  $>0.4$  and  $<0.6$ ; methylated: mean  $\beta$ -value  $>0.6$ ). (C) Hierarchical clustering displaying the expression of genes involved in the Mucin type O-glycan biosynthesis and mucins expressed in precursor lesions. (D, E) Mean CpG methylation of the first 20 *MUC2* (D) and *MUC13* (E) annotated probes. CpGs located in the coding region are coloured in red (unmethylated: mean  $\beta$ -value  $<0.4$ ; intermediate: mean  $\beta$ -value  $>0.4$  and  $<0.6$ ; methylated: mean  $\beta$ -value  $>0.6$ ). gIPMN, gastric IPMN; iIPMN, intestinal IPMN; IPMN, intraductal papillary mucinous neoplasms; PanIN, pancreatic intraepithelial neoplasias; PDAC, pancreatic ductal adenocarcinoma; TFF3, trefoil factor 3.

(6 low-grade and 6 high-grade), 4 PDAC (unrelated to IPMN) and 3 samples of acinar bulk tissue. The principal component analysis showed a clear separation between intestinal IPMN, and other precursors (figure 4A). The observed pattern was comparable with the results of the DNA methylation data, further underlining the close relationship between PanIN and gastric IPMN also on the transcriptional level. Consistently, only very few genes were differentially expressed between gastric IPMN and PanIN (figure 4B). The Visualization Pipeline for RNAseq (VIPER) analysis showed a similarity in pathway activation when gastric IPMN and PanIN were compared with intestinal IPMN. This comparison displayed that in both precursor lesions (ie, gastric IPMN and PanIN) genes of the Notch signalling (namely *HEYL*—Hes-Related Family BHLH Transcription Factor With YRPW Motif Like, *JAG1*—Jagged Canonical Notch Ligand 1, *TGFA*—transforming growth factor alpha) are activated compared with intestinal IPMN (figure 4C). The activation of Notch signalling was also observed in single sample gene set enrichments (ssGSEA) based on the *hallmark of cancer* gene sets (figure 4D), arguing for distinct Notch signalling activity in gastric but not intestinal IPMN.

### Identification and validation of precursor subtype-specific markers

We further validated our data by comparing them with a recently published comprehensive transcriptomic characterisation of pancreatic cells obtained from healthy organ donors.<sup>31</sup> Here, higher expression levels of digestive enzymes, including *CPA1* (carbopeptidase A1), *PRSS1* (protease serine 1) and of relevant

transcription factors, like *FOXP2* (forkhead box P2) and *RBPJL* (Recombination Signal Binding Protein for Immunoglobulin Kappa J Region Like), were found in samples obtained from the normal pancreas (figure 5A). Interestingly, progressively decreasing expression levels were identified in some of the markers (*CPA1*, *RBPJL*), when moving from precursors usually located in the peripheral ductal system, such as PanIN and gastric IPMN, to typical main duct lesions, such as intestinal IPMN. Most interestingly, intestinal IPMN displayed an association with genes related to the subgroup of *MUC5B*-positive ductal cells, which has been identified as ‘minor’ ductal cell population in the normal pancreas.<sup>31</sup> This subtype is characterised by higher expression levels of genes related to mucous secretion. Accordingly, significantly higher levels of the trefoil factor *TFF3*, whose promoter region was selectively unmethylated, were found in intestinal IPMN compared with all other precursor lesions, both at the messenger RNA and at the protein expression level, respectively (figure 5A–B, online supplemental figure 5). Furthermore, intestinal IPMN displayed highly differentially methylated genes, such as *FOXP2*, *DCLK1* (doublecortin-like kinase 1) and *BICC2* (bicaudal C homolog 2) (online supplemental figure 6), which can be ascribed to progenitor markers, possibly suggesting the presence of a still unidentified progenitor-like cell population in the pancreatic ductal system.

Further focusing on the mucin metabolism, we found an enrichment of the O-linked glycosylation signature enriched in both IPMN subtypes by applying ssGSEA (online supplemental figure 7). As this gene set was already observed at the

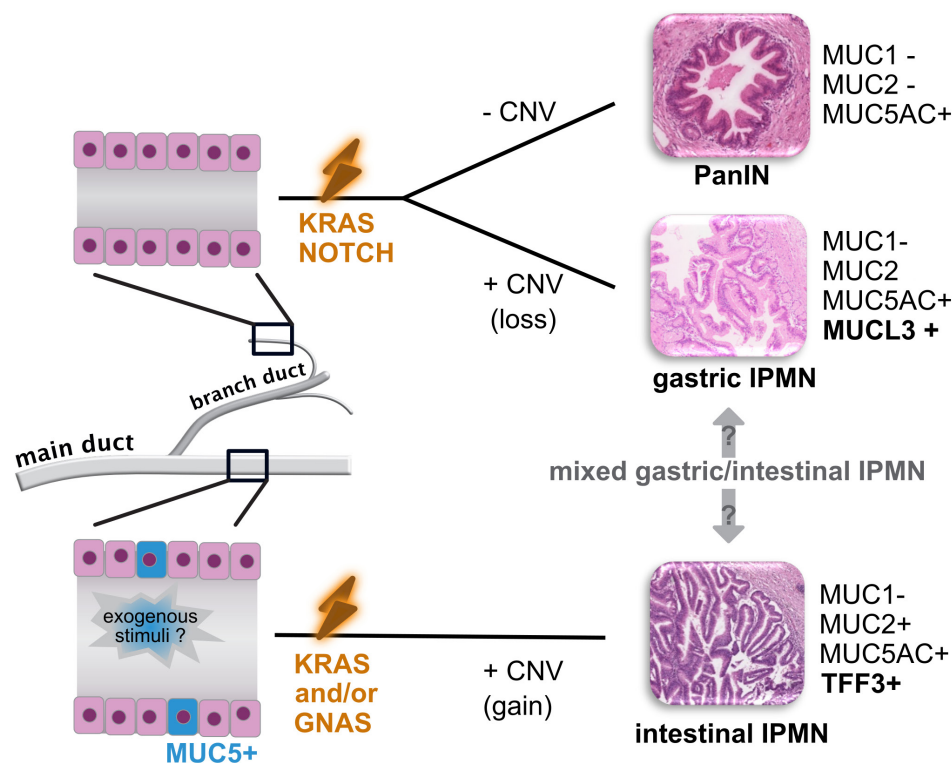


**Figure 6** Model of development of pancreatic cancer precursors. *KRAS* mutations induce a gastric phenotype characteristic of mostly peripherally located lesions, such as PanIN and gastric IPMN, which are additionally Notch-dependent. Recurrent deletions occur only in gastric IPMN. These share a very similar mucin profile with PanIN, but they can be distinguished to some extent by different MUC13 expression, with lack of expression arguing against gastric IPMN. Further stimuli, such as exogenous factors related to a different microenvironment and possibly acting on a minor MUC5B-positive ductal cell population, induce an intestinal phenotype, driven by *KRAS* and/or *GNAS* mutations, with differential regulation of the mucin type O-glycan biosynthesis, expression of MUC2, CDX2 and TFF3 and recurrent amplifications. Mixed phenotypes and/or a transition from a gastric to an intestinal phenotype may also occur. CNV, copy number variation; IPMN, intraductal papillary mucinous neoplasms; MUC1, mucin 1; MUC2, mucin 2; MUC5AC, mucin 5; PanIN, pancreatic intraepithelial neoplasias; TFF3, trefoil factor 3.

methylation level (figure 3C), we further analysed the individual gene expression and evaluated their impact in distinguishing PanIN, gastric and intestinal IPMN from each other. Beside the known precursor-specific expression of *MUC2* (figure 5C–D), *MUC5AC* and *MUC6* (figure 5C), this analysis identified for the first time *MUCL3* as a potential candidate to distinguish PanIN from gastric IPMN both at the transcriptional and methylation (figure 5E) level. Immunohistochemical analysis confirmed a more frequent *MUCL3* expression in gastric IPMN than in PanIN ( $p=0.02$ ) (online supplemental figure 5).

## DISCUSSION

In this study, pancreatic cancer precursors with gastric and intestinal phenotype were analysed using genomic, epigenomic and transcriptomic approaches to address their molecular profile and assess their cell identity and possible similarity to adult pancreatic cell compartments. A major result of our integrated genome-based approach is the evidence of distinct genomic structural patterns and of an epigenetic regulation of mucin genes underlying the different phenotype of PDAC precursors.

Gastric IPMN and PanIN show a significant overlap in their gene expression and DNA methylation profile, with numerous commonly regulated pathways, including Notch signalling, which is supported by previous functional studies on Notch signalling in PanIN-driven pancreatic carcinogenesis.<sup>32–34</sup> So far, most functional data have focused on acinar-ductal metaplasia and PanIN formation and progression. While several mouse models have been reported to elicit different subtypes of IPMN by combining the KC or KPC mouse<sup>35 36</sup> with genetic targeting of additional pathways, such as the G-protein coupled receptor (GPCR) (*guanine nucleotide binding protein, alpha stimulating (GNAS)*), transforming growth factor- $\alpha$  (TGF $\alpha$ ), SWI $^1$ ch/Sucrose Non-Fermentable (SWI/SNF), Wingless/Integrated (WNT) and phosphoinositide-3 kinase (PI3K) pathways,<sup>37</sup> the functional role of Notch signalling in the development of gastric and intestinal IPMN is not well-defined. Our finding suggests that Notch signalling is selectively involved in gastric but not in intestinal precursor development. It is tempting to speculate that PanIN and gastric IPMN have distinct precursor cells (compared with intestinal IPMN) being responsive to or requiring Notch signalling activity. In addition, they display very similar methylation profiles compared with ductal cells both from the main and the branch-duct compartment (figure 3B,D). This may appear in contrast with previous studies ascribing an essential role to *Kras* and Notch signalling for acinar-ductal reprogramming and development of PDAC precursors.<sup>38</sup> However, by comparing our results with those obtained from single cell RNA-expression analysis of normal pancreatic tissues,<sup>31</sup> we observed a retained expression of acinar markers in PanIN and gastric IPMN, which may still point towards a contribution of the acinar cell compartment to these two lesions, although minor contamination by acinar cells during the process of microdissection cannot be completely ruled out.

Interestingly, WGS and DNA methylation profiles revealed slightly more frequent (76% vs 61%) CNV in gastric IPMN than in PanIN lesions, with chromosomal regions affected by recurrent deletions only found in gastric IPMN, thus suggesting a higher impact of mutagenic factors in gastric IPMN, which potentially affect their progression.<sup>39 40</sup> The significant differential expression of *MUCL3* in gastric IPMN further consolidates the hypothesis of a higher potential for progression of these lesions compared with PanIN, since this molecule has been previously described to be overexpressed in PDAC and to

promote its progression by affecting the nuclear factor-kappa B signalling pathway,<sup>41</sup> but more data are necessary to confirm these observations. In addition, the diagnostic value *MUCL3* in distinguishing PanIN from gastric IPMN might be only relevant in case of lack of expression, which would then exclude gastric IPMN. The degree of dysplasia does not appear to be related to the presence of recurrent CNV, since the proportion of low-grade and high-grade lesions was not substantially different in the two groups. This is in contrast with previous studies, which showed infrequent and mostly non-recurrent CNV both in low-grade PanIN and IPMN<sup>42</sup> and identified a correlation between more frequent CNV and higher histological grade in IPMN.<sup>43</sup> On the other hand, CNV analysis in IPMN of mostly mixed phenotypes revealed recurrent gains in chromosome 3, 7, 8 and 12, in line with our results.<sup>44</sup>

To our knowledge, this study is the first to show that intestinal IPMN have profoundly divergent methylation profiles compared with both PanIN and gastric IPMN (figure 3A–C), suggesting a distinct cell identity. Indeed, single cell sequencing studies have revealed a certain degree of heterogeneity in the cell populations of the healthy adult pancreas.<sup>31 45</sup> A minor ductal cell population (defined as *MUC5B*-positive ductal cells), characterised by higher expression levels of genes related to mucin secretion, such as *TFF3*, has been described, which, according to our gene and protein expression data (figure 5A–B, online supplemental figure 5), could be related to intestinal IPMN. It is tempting to speculate that exposure of the ductal cell compartment to environmental carcinogens, for example, due to bile reflux as a consequence of an anatomic variation at the pancreato-biliary junction<sup>46 47</sup> or to an altered oral, gastric and intestinal microbiome,<sup>48</sup> could induce an intestinal phenotype switch as first adaptive response of a ‘susceptible’ cell type, followed by dysplasia and cancer. Since the ductal cell compartment is the only one that can achieve long-term expansion in organoids obtained from adult healthy mice,<sup>49</sup> such a ‘susceptible’ cell type might represent an adult progenitor-like cell residing in the pancreatic ducts. This model is supported by the clinical observation that intestinal IPMN are usually localised in the main pancreatic duct, where the contact with environmental carcinogens is more direct than in the periphery of the duct system. In addition, the intestinal differentiation-dysplasia-carcinoma model, possibly involving progenitor-like cells, has been already validated in other tumour types, such as Barrett adenocarcinoma of the oesophagus and gastric cancer.<sup>50</sup> Although the existence of progenitor cells in the human pancreas is still debated,<sup>51</sup> the differential methylation pattern of progenitor genes in intestinal IPMN compared with other lesion types found in this study argues for different adult duct cell types involved in these lesions and includes the activation of mucin-secretion signatures with intestinal reprogramming.

Notably, the comparison between the methylation profiles of low-grade and high-grade precursor lesions showed no apparent difference in methylated regions in the various comparison of lesion subtypes. This analysis was limited by the overall comparatively small numbers of high-grade lesions, which are rarely found in the clinical samples, and the unbalanced group sizes. However, despite these limitations, our results provide no clear evidence for a major role of differentially methylated regions between low-grade and high-grade pancreatic precursor lesions.

Based on these results and on recently published data, a model of development of gastric and intestinal pancreatic precursors can be proposed (figure 6). According to this model, *KRAS* mutations, which are very frequent genetic events both in PanIN and in primary and recurrent IPMN,<sup>52 53</sup> induce gastric reprogramming in pancreatic ductal cells independently

from their localisation. In the peripheral compartment, where PanIN and gastric IPMN are usually localised, progression and malignant transformation are rare events, probably related to Notch signalling activation, to the observed recurrent deletions in gastric IPMN and to the acquisition of additional, possibly subclonal, mutational events not detectable with ‘whole lesion’ approaches, like the one of the present study. Single cell sequencing has indeed revealed intralesional genetic heterogeneity in gastric IPMN, with subclonal mutations involving the *ARID1A* and *RNF43* genes.<sup>54</sup> These could provide a selective advantage of single cell groups within a definite lesion and explain the ‘missing’ genetic driver events in a subset of the precursor lesions investigated in the present study. Similarly, a single cell transcriptomics study performed on a small collective of IPMN of different subtypes identified cell clusters in low-grade IPMN with changes in gene expression similar to those found in high-grade lesions.<sup>55</sup> In the main duct compartment on the other hand, exposure to environmental carcinogens and to chronic inflammation induces intestinal differentiation. This can occur de novo or in a previously *KRAS*-mutated and gastric differentiated cell and is associated with higher frequency of recurrent amplifications, as shown in the CNV analysis, and with higher proliferating activity even in low-grade lesions<sup>39 40</sup> (figure 2, online supplemental figure 5). Accordingly, we found that the mucin O-glycan biosynthesis pathway, which has been shown to affect relevant processes of progression and metastasis in human cancer, including pancreatic cancer<sup>42 56</sup> is among the highest differentially regulated pathway between intestinal and gastric IPMN and between intestinal IPMN and PanIN (figure 3C). As shown in figure 6, the occurrence of mixed phenotypes, and also the evolution from gastric to intestinal IPMN, as suggested by some,<sup>16</sup> could be explained by this model. Overall, the observed distinct epigenomic patterns support further exploration of different adult cell compartments in the human pancreas, as well as aetiological and environmental factor analysis as an exciting research area.

This study has some limitations, mainly of methodological type and related to the difficulty of performing multiple, genome-wide analyses on archived paraffin material, which restricted the number of analysed samples on one side and influenced the choice of the type of analysis, for example, targeted versus whole-exome sequencing, on the other. In addition, for similar reasons, intralesional heterogeneity, which has been previously reported,<sup>44</sup> was not addressed in this study and some precursor lesions, such as pancreatobiliary IPMN, had to be excluded due to low case number.

Nevertheless, by applying multiple targeted and genome-wide analyses, we were able to provide the first comprehensive, large-scale molecular analysis of pancreatic cancer precursors with gastric and intestinal phenotype, showing their molecular heterogeneity, which is possibly related to a different cell identity and to a different aetiology. Furthermore, regardless of the above-mentioned technical limitations, we noted several overlaps in targets at the methylation and transcriptome level, as exemplified by *TFF3*, *MUC2* and *MUCL3*, even though these analyses were not all always performed in the same tissue specimens. We therefore strongly believe that studies concerning precursor lesions of PDAC should differentiate between the different entities and subtypes and not consider them as a group. Further studies are needed to better characterise susceptible cell types in the pancreatic ductal compartment as well as to identify potentially removable causes of intestinal reprogramming.

#### Author affiliations

<sup>1</sup>Bridge Institute of Experimental Tumor Therapy, West German Cancer Center, University Hospital Essen, Essen, Germany  
<sup>2</sup>Division of Solid Tumor Translational Oncology, German Cancer Consortium (DKTK, partner site Essen) and German Cancer Research Center, DKFZ, Heidelberg, Germany  
<sup>3</sup>Institute of Pathology, Heinrich-Heine University and University Hospital of Dusseldorf, Dusseldorf, Germany  
<sup>4</sup>Department of General, Visceral and Pediatric Surgery, Heinrich-Heine-University and University Hospital of Dusseldorf, Dusseldorf, Germany  
<sup>5</sup>Institute of Pathology, Technische Universitaet Muenchen, Munich, Germany  
<sup>6</sup>HI-STEM—Heidelberg Institute for Stem Cell Technology and Experimental Medicine GmbH, Heidelberg, Germany  
<sup>7</sup>Division of Stem Cells and Cancer, German Cancer Research Centre and DKFZ-ZMBH Alliance, Heidelberg, Germany  
<sup>8</sup>German Cancer Consortium, (DKTK), Heidelberg, Germany

**Correction notice** This article has been corrected since it published Online First. The formatting of table 2 has been corrected and figure 3 updated.

**Twitter** Irene Esposito @IEspositoPATH

**Acknowledgements** We thank the microarray unit of the DKFZ Genomics and Proteomics Core Facility for providing the Illumina Human Methylation arrays and related services. PF Cheung and K Savvatakis are acknowledged for their help in preparing FACS-sorted cells from FFPE tissues. We would like to acknowledge the support of the Biobank of the University Hospital of Dusseldorf, Germany.

**Contributors** S-TL performed the EPIC-based CNV analysis and the analysis of the methylome and transcriptome data and wrote the manuscript. LG analysed the methylome data and the provided comparison with the single-cell data and wrote the manuscript. LF collected the samples, performed the low-pass WGS and the targeted NGS, she prepared the DNA/RNA for further analyses by manual or laser-assisted microdissection and performed part of the immunostaining. LH evaluated the cohort and the immunohistochemical results and wrote the manuscript. AY contributed to morphological and immunohistochemical analyses and wrote the paper. RV performed and evaluated immunohistochemistry. WG and FVO evaluated the panel sequencing and performed and evaluated the fusion transcript analyses. NS contributed to the study design and the planning and interpretation of the WGS experiments. WTK contributed to the study design, to the sample collection and to the data interpretation. AMS contributed to sample collection and analysis and to the study design. GK contributed to the study design and results interpretation and wrote the paper. EE and AT contributed to the methylome analysis and interpretation of the results. JTS planned and supervised the methylome and CNV analysis, contributed to the interpretation of the results and wrote the manuscript. IE conceived the study, planned all experiments, performed the morphological re-evaluation, supervised the WGS and NGS analysis, the sample preparation for further analysis and the immunohistochemistry, interpreted the results, wrote and submitted the manuscript. IE and JTS act as guarantors of the manuscript.

**Funding** This work was supported by grants of the German Research Foundation (DFG) to IE (grant N° ES285/6-1 and ES 285/8-1). IE is further supported by the European Commission (H2020, Grant Agreement N° 824946–SIMBIT). JTS is supported by the German Cancer Consortium (DKTK), by the Deutsche Forschungsgemeinschaft (DFG, German Research Foundation; #405344257/ SI 1549/3-2 and SI1549/4-1), by the German Cancer Aid (#70112505/PIPAC, #70113834/PREDICT-PACA) and by the German Federal Ministry of Education and Research (BMBF; 01KD2206A/SATURN3). Part of this work represents the doctoral thesis of one of the authors (LF).

**Competing interests** None declared.

**Patient and public involvement** Patients and/or the public were not involved in the design, or conduct, or reporting, or dissemination plans of this research.

**Patient consent for publication** Not applicable.

**Ethics approval** This study was approved by the ethic committee of the University Hospital of Dusseldorf, Germany (ethic no. 3821).

**Provenance and peer review** Not commissioned; externally peer reviewed.

**Data availability statement** RNAseq data are available in a public, open access repository. EPIC data are available upon reasonable request.

**Supplemental material** This content has been supplied by the author(s). It has not been vetted by BMJ Publishing Group Limited (BMJ) and may not have been peer-reviewed. Any opinions or recommendations discussed are solely those of the author(s) and are not endorsed by BMJ. BMJ disclaims all liability and responsibility arising from any reliance placed on the content. Where the content includes any translated material, BMJ does not warrant the accuracy and reliability of the translations (including but not limited to local regulations, clinical guidelines, terminology, drug names and drug dosages), and is not responsible for any error and/or omissions arising from translation and adaptation or otherwise.

**Open access** This is an open access article distributed in accordance with the Creative Commons Attribution Non Commercial (CC BY-NC 4.0) license, which permits others to distribute, remix, adapt, build upon this work non-commercially, and license their derivative works on different terms, provided the original work is properly cited, appropriate credit is given, any changes made indicated, and the use is non-commercial. See: <http://creativecommons.org/licenses/by-nc/4.0/>.

#### ORCID iDs

Aslihan Yavas <http://orcid.org/0000-0002-8408-3063>  
 Friederike V Opitz <http://orcid.org/0000-0002-5025-3781>  
 Anna Melissa Schlitter <http://orcid.org/0000-0001-6431-2036>  
 Elisa Espinet <http://orcid.org/0000-0002-0690-9878>  
 Irene Esposito <http://orcid.org/0000-0002-0554-2402>

#### REFERENCES

- American Cancer Society. *Cancer facts & figures*. Atlanta, 2020.
- Kleeff J, Korc M, Apte M, et al. Pancreatic cancer. *Nat Rev Dis Primers* 2016;2:16022.
- Balachandran VP, Łuksza M, Zhao JN, et al. Identification of unique neoantigen qualities in long-term survivors of pancreatic cancer. *Nature* 2017;551:512–6.
- Stark AP, Sacks GD, Rochefort MM, et al. Long-Term survival in patients with pancreatic ductal adenocarcinoma. *Surgery* 2016;159:1520–7.
- Strobel O, Lorenz P, Hinz U, et al. Actual five-year survival after upfront resection for pancreatic ductal adenocarcinoma. *Ann Surg* 2022;275:962–71.
- Wood LD, Canto MI, Jaffe EM, et al. Pancreatic cancer: pathogenesis, screening, diagnosis, and treatment. *Gastroenterology* 2022;163:386–402.
- Park W, Chawla A, O'Reilly EM. Pancreatic cancer: a review. *JAMA* 2021;326:851–62.
- Ryan DP, Hong TS, Bardeesy N. Pancreatic adenocarcinoma. *N Engl J Med Overseas Ed* 2014;371:1039–49.
- Rawla P, Sunkara T, Gaduputi V. Epidemiology of pancreatic cancer: global trends, etiology and risk factors. *World J Oncol* 2019;10:10–27.
- Goggins M, Overbeek KA, Brand R, et al. Management of patients with increased risk for familial pancreatic cancer: updated recommendations from the International cancer of the pancreas screening (CAPS) Consortium. *Gut* 2020;69:7–17.
- Tomasetti C, Li L, Vogelstein B. Cancer etiology, and cancer prevention. *Science* 2017;355:1330–4.
- WHO Classification of Tumours Editorial Board (eds.). WHO Classification of Tumours. In: *Digestive system tumours*. 5th Edition, Volume 1. Lyon, 2019.
- Klöppel G, Basturk O, Schlitter AM, et al. Intraductal neoplasms of the pancreas. *Semin Diagn Pathol* 2014;31:452–66.
- Hruban RH, Adsay NV, Albores-Saavedra J. Pancreatic intraepithelial neoplasia: a new nomenclature and classification system for pancreatic duct lesions. *Am J Surg Pathol* 2001;25:579–86.
- Peters MLB, Eckel A, Mueller PP, et al. Progression to pancreatic ductal adenocarcinoma from pancreatic intraepithelial neoplasia: results of a simulation model. *Pancreatol* 2018;18:928–34.
- Omori Y, Ono Y, Kobayashi T, et al. How does intestinal-type intraductal papillary mucinous neoplasm emerge? CDX2 plays a critical role in the process of intestinal differentiation and progression. *Virchows Arch* 2020;477:21–31.
- Roth S, Zamzow K, Gaida MM, et al. Evolution of the immune landscape during progression of pancreatic intraductal papillary mucinous neoplasms to invasive cancer. *EBioMedicine* 2020;54:102714.
- Matthaei H, Wu J, Dal Molin M, et al. GNAS sequencing identifies IPMN-specific mutations in a subgroup of diminutive pancreatic cysts referred to as "incipient IPMNs". *Am J Surg Pathol* 2014;38:360–3.
- Matthaei H, Hong S-M, Mayo SC, et al. Presence of pancreatic intraepithelial neoplasia in the pancreatic transection margin does not influence outcome in patients with R0 resected pancreatic cancer. *Ann Surg Oncol* 2011;18:3493–9.
- Marchegiani G, Mino-Kenudson M, Ferrone CR, et al. Patterns of recurrence after resection of IPMN: who, when, and how? *Ann Surg* 2015;262:1108–14.
- Yachida S, Jones S, Bozic I, et al. Distant metastasis occurs late during the genetic evolution of pancreatic cancer. *Nature* 2010;467:1114–7.
- Rhim AD, Mirek ET, Aiello NM, et al. Emt and dissemination precede pancreatic tumor formation. *Cell* 2012;148:349–61.
- Notta F, Chan-Seng-Yue M, Lemire M, et al. A renewed model of pancreatic cancer evolution based on genomic rearrangement patterns. *Nature* 2016;538:378–82.
- Noè M, Niknafs N, Fischer CG, et al. Genomic characterization of malignant progression in neoplastic pancreatic cysts. *Nat Commun* 2020;11:4085.
- Basturk O, Hong S-M, Wood LD, et al. A revised classification system and recommendations from the Baltimore consensus meeting for neoplastic precursor lesions in the pancreas. *Am J Surg Pathol* 2015;39:1730–41.
- ZMc HV. Enhanced copy-number variation analysis using Illumina DNA methylation arrays. R package version 1.9.0. Available: <http://bioconductor.org/packages/conumee/>
- Quinlan AR, Hall IM. BEDTools: a flexible suite of utilities for comparing genomic features. *Bioinformatics* 2010;26:841–2.
- Tian Y, Morris TJ, Webster AP, et al. Champ: updated methylation analysis pipeline for Illumina BeadChips. *Bioinformatics* 2017;33:3982–4.
- Espinet E, Gu Z, Imbusch CD, et al. Aggressive PDACs show hypomethylation of repetitive elements and the execution of an intrinsic IFN program linked to a ductal cell of origin. *Cancer Discov* 2021;11:638–59.
- Moss J, Magenheim J, Neiman D, et al. Comprehensive human cell-type methylation atlas reveals origins of circulating cell-free DNA in health and disease. *Nat Commun* 2018;9:5068.
- Tosti L, Hang Y, Debnath O, et al. Single-nucleus and in situ RNA-sequencing reveal cell topographies in the human pancreas. *Gastroenterology* 2021;160:1330–44.
- Miyamoto Y, Maitra A, Ghosh B, et al. Notch mediates TGF alpha-induced changes in epithelial differentiation during pancreatic tumorigenesis. *Cancer Cell* 2003;3:565–76.
- Mazur PK, Einwächter H, Lee M, et al. Notch2 is required for progression of pancreatic intraepithelial neoplasia and development of pancreatic ductal adenocarcinoma. *Proc Natl Acad Sci U S A* 2010;107:13438–43.
- Hidalgo-Sastre A, Brodylo RL, Lubeseder-Martellato C, et al. Hes1 controls exocrine cell plasticity and restricts development of pancreatic ductal adenocarcinoma in a mouse model. *Am J Pathol* 2016;186:2934–44.
- Hingorani SR, Wang L, Multani AS, et al. Trp53R172H and KrasG12D cooperate to promote chromosomal instability and widely metastatic pancreatic ductal adenocarcinoma in mice. *Cancer Cell* 2005;7:469–83.
- Hingorani SR, Petricoin EF, Maitra A, et al. Preinvasive and invasive ductal pancreatic cancer and its early detection in the mouse. *Cancer Cell* 2003;4:437–50.
- Li J, Wei T, Zhang J, et al. Intraductal papillary mucinous neoplasms of the pancreas: a review of their genetic characteristics and mouse models. *Cancers* 2021;13:5296.
- De La O J-P, Emerson LL, Goodman JL, et al. Notch and KRAS reprogram pancreatic acinar cells to ductal intraepithelial neoplasia. *Proc Natl Acad Sci U S A* 2008;105:18907–12.
- Hovhannisyan G, Harutyunyan T, Aroutiounian R, et al. Dna copy number variations as markers of mutagenic impact. *Int J Mol Sci* 2019;20:4723.
- Arlt MF, Wilson TE, Glover TW. Replication stress and mechanisms of CNV formation. *Curr Opin Genet Dev* 2012;22:204–10.
- Yan J, Chen G, Zhao X, et al. High expression of diffuse panbronchiolitis critical region 1 gene promotes cell proliferation, migration and invasion in pancreatic ductal adenocarcinoma. *Biochem Biophys Res Commun* 2018;495:1908–14.
- Gupta R, Leon F, Rauth S, et al. A systematic review on the implications of O-linked glycan branching and truncating enzymes on cancer progression and metastasis. *Cells* 2020;9:446.
- Mateos RN, Nakagawa H, Hirono S, et al. Genomic analysis of pancreatic juice DNA assesses malignant risk of intraductal papillary mucinous neoplasm of pancreas. *Cancer Med* 2019;8:4565–73.
- Fischer CG, Beleva Guthrie V, Braxton AM, et al. Intraductal papillary mucinous neoplasms arise from multiple independent clones, each with distinct mutations. *Gastroenterology* 2019;157:1123–37.
- Muraro MJ, Dharmadhikari G, Grün D, et al. A single-cell transcriptome atlas of the human pancreas. *Cell Syst* 2016;3:385–94.
- Adachi T, Tajima Y, Kuroki T, et al. Bile-reflux into the pancreatic ducts is associated with the development of intraductal papillary carcinoma in hamsters. *J Surg Res* 2006;136:106–11.
- Muraki T, Reid MD, Pehlivanoglu B, et al. Variant anatomy of the biliary system as a cause of pancreatic and peri-ampullary cancers. *HPB* 2020;22:1675–85.
- Kiss B, Mikó E, Sebő Éva, et al. Oncobiosis and microbial metabolite signaling in pancreatic adenocarcinoma. *Cancers* 2020;12:1068.
- Huch M, Bonfanti P, Boj SF, et al. Unlimited in vitro expansion of adult bi-potent pancreas progenitors through the Lgr5/R-spondin axis. *Embo J* 2013;32:2708–21.
- Hayakawa Y, Nakagawa H, Rustgi AK, et al. Stem cells and origins of cancer in the upper gastrointestinal tract. *Cell Stem Cell* 2021;28:1343–61.
- Alvarez Fallas ME, Pedraza-Arevalo S, Cujba A-M, et al. Stem/Progenitor cells in normal physiology and disease of the pancreas. *Mol Cell Endocrinol* 2021;538:111459.
- Hata T, Suenaga M, Marchionni L, et al. Genome-Wide somatic copy number alterations and mutations in high-grade pancreatic intraepithelial neoplasia. *Am J Pathol* 2018;188:1723–33.
- Pea A, Yu J, Rezaee N, et al. Targeted DNA sequencing reveals patterns of local progression in the pancreatic remnant following resection of intraductal papillary mucinous neoplasm (IPMN) of the pancreas. *Ann Surg* 2017;266:133–41.
- Kuboki Y, Fischer CG, Beleva Guthrie V, et al. Single-cell sequencing defines genetic heterogeneity in pancreatic cancer precursor lesions. *J Pathol* 2019;247:347–56.
- Bernard V, Semaan A, Huang J, et al. Single-Cell transcriptomics of pancreatic cancer precursors demonstrates epithelial and microenvironmental heterogeneity as an early event in neoplastic progression. *Clin Cancer Res* 2019;25:2194–205.
- Pan S, Brentnall TA, Chen R. Glycoproteins and glycoproteomics in pancreatic cancer. *World J Gastroenterol* 2016;22:9288–99.

## 1 Supplemental data

## 2 Methods

### 3 Immunohistochemistry

4 Staining was performed manually or using the Ventana BenchMark Ultra automated IHC/ISH  
5 slide staining system (Ventana Medical Systems Inc., Tucson, USA) (suppl. table 1a). The  
6 cytoplasmic expression of TFF3 and MUCL3 was evaluated using the immunoreactivity scoring  
7 system (IRS) based on staining intensity (0: negative, 1: mild, 2: moderate, 3: intense) and the  
8 percentage of stained cells (0: no positive cells, 1: <10% positive cells, 2: 10-50% positive cells,  
9 3: 51-80% positive cells, 4: >80% positive cells). The final score (0-12) was found by multiplying  
10 the positive cells proportion score (0-4) and the staining intensity score (0-3). The mean value  
11 of Ki67 proliferation rate of five randomly selected high power (40x) fields (HPFs) was  
12 calculated using the percentage of stained cells.

### 13 DNA/ RNA Isolation from FFPE samples

14 For genomic DNA or total RNA Isolation, 5-8 8- $\mu$ m-thick tissue sections were prepared, and  
15 lesions were dissected manually or by laser-capture microdissection (LMD), depending on  
16 their size to ensure adequate cellularity (>80%) for subsequent molecular analysis. For LMD,  
17 cresyl violet staining was done before using the Palm Microbeam System (Carl Zeiss,  
18 Oberkochen, Germany) according to the manufacturer's instructions. In some samples  
19 containing larger lesions, manual microdissection was used, as previously described.[1] The  
20 obtained cell clusters were isolated using the QIAamp DNA micro Kit or the GeneRead FFPE  
21 DNA Kit for DNA and the RNeasy FFPE Kit for RNA (all from Qiagen, Hilden, Germany) following  
22 the manufacturer's instructions. The genomic DNA quality control was performed by  
23 quantitative PCR using the Power SYBR™ Green PCR Master Mix on a StepOnePlus™ Real-Time  
24 PCR System. Quantification was performed with a self-designed primer assay (HML-2 for: 5'  
25 AAACGCCAATCCTGAGTGTC-3'; HML-2 rev: 5' CATAGCTCCTCCGATTCAT-3'). These primers  
26 are complementary to long terminal repeats (LTRs) of the HML 2 human endogenous  
27 retroviruses and have a length of about 115 bp.

## 1 Targeted NGS

2 A PDAC-Panel with two primer pools was created by the Ion AmpliSeq™ Designer (v5.6,  
3 ThermoFisher Scientific, Dreieich, Germany). The panel consists of 217 amplicons of 21 genes  
4 covering hot-spot mutational sites of 18 and the whole coding sequence of 3 (*ARID1A*, *TP53*  
5 and *RNF43*) additional genes relevant for PDAC (suppl. table 2). Barcoded libraries from gDNA  
6 (up to 10 ng per pool) were prepared using the Ion AmpliSeq Library kit 2.0 with Ion Xpress™  
7 Barcode adapters. The Ion library TaqMan™ Quantitation Kit was used for quantification of  
8 the libraries. The libraries were pooled and amplified in an emulsion PCR reaction using the  
9 Ion 520™ & Ion 530™ Kit-OT2. The resulting Ion Sphere particles (ISPs) were loaded on a 520™  
10 or 530™ Chip and sequenced on the Ion S5™ system (all reagents from ThermoFisher).

11 The results of the next generation sequencing from the Ion S5™ system were aligned to the  
12 human reference genome (GRCh37/hg19) using the S5 Ion Torrent Server VM (ThermoFisher).  
13 The Ion Reporter software (Version 5.12.0.0) was used for variant calling and annotations of  
14 the DNA panel sequencing. The parameters for variant calling were set equal for all samples.  
15 Following thresholds were defined: 3% allele frequency with a minimum coverage of 500 and  
16 a Phred Score of  $\geq 30$ . Detected variants were validated using the Integrative Genomics Viewer  
17 (IGV), ClinVar database from National Institutes of Health (NIH) and University of California  
18 Santa Cruz (UCSC) Genome Browser. Variants not present in the above mentioned databases  
19 were classified according to the American College of Medical Genetics and Genomics (ACMG)  
20 guidelines using the ACMG database (varsome.com; v7.3.7).[2]

## 21 Fusion transcript analysis

22 50 ng of isolated RNA were used for cDNA synthesis by QuantiTect Reverse Transcription Kit  
23 (Qiagen) and were subsequently subjected to library preparation using the Oncomine  
24 Comprehensive Assay Plus RNA (ThermoFisher) targeting over 1,300 isoforms of 49 tumor  
25 driver genes including approximately 200 known *BRAF* fusion transcripts. NGS was performed  
26 (as described above) and data analysis was done using the Oncomine Comprehensive Plus  
27 w2.1 - Fusion workflow implemented within the IonReporter Software package (V5.18;  
28 ThermoFisher).

## 29 Isolation of epithelial cells from the main pancreatic duct and from peripheral (branch) ducts

1 Specimens were obtained fresh from the operating theater and immediately subjected to  
2 gross examination. The main pancreatic duct was probed, and the specimen dissected by a  
3 pathologist along the probe. The main duct was then carefully dissected with a scissor and  
4 then fixed in 10% buffered formalin and embedded in paraffin. Peripheral tissue blocks were  
5 prepared, and branch-ducts were isolated by LMD, as described above. DNA extraction was  
6 performed as described above.

### 7 **Generation of $\beta$ -cells**

8  $\beta$ -cell populations from FFPE tissue were generated from 50- $\mu$ m-thick sections. Tissue sections  
9 were dewaxed with xylol and rehydrated in descending ethanol concentrations. Antigen  
10 retrieval was done at 80°C for one hour in a pressure cooker before tissue was digested with  
11 1% (w/v) collagenase Ia (Sigma, Steinheim, Germany) and 1%(w/v) dispase (Gibco, Grand  
12 Island, USA) for 45 min at 37°C to obtain single cells. The cell suspension was subsequently  
13 filtered (30  $\mu$ m mesh) and the cells were collected by centrifugation. Single cells were stained  
14 Insulin (Abcam, Cambridge, UK; 1:200). The stained cells were sorted with a BD FACS Aria™  
15 III System. DNA was isolated from the sorted cells as described above.

### 16 **Transcriptome analysis**

17 After total RNA isolation, the samples were shipped to Macrogen (Seoul, Korea) for  
18 sequencing. Libraries from total RNA were prepared using the Illumina TruSeq™ Stranded  
19 mRNA Library Prep kit and sequenced with 2 x 100 bp on the Illumina NovaSeq 6000 (Illumina  
20 Inc, San Diego, USA). The raw data processing of the transcriptome data was performed by  
21 Macrogen. Briefly, adapter and low-quality base trimming was carried out with Trimmomatic  
22 (v0.38).[3] Trimmed reads were mapped against the GRCh38/hg38 human reference genome  
23 using the Bowtie2 (v2.3.4.1) aligner.[4] Afterwards, the aligned reads were assembled with  
24 Cufflinks (v2.2.1).[5] After assembly the abundance of gene was calculated in read counts per  
25 gene. Before differential gene expression analysis lowly expressed genes were filtered from  
26 the data set. Therefore, genes which showed a lower read count as 0.5 transcripts per million  
27 reads and were missing in more than one sample per group were excluded from further  
28 analysis. The filtered raw count matrix was normalized and batch-corrected using the DESeq2  
29 package (v3.14).[6] Finally, differentially expressed genes were calculated pairwise and  
30 defined as followed  $\log_2$  fold change of  $< -1$  and  $> 1$ , respectively, and the significance level of

1 the adjusted p-value was set to < 0.05. PCA, heatmap and expression plots were calculated  
2 based on the variance stabilizing transformation output of DESeq2

### 3 **Pathway analysis**

4 Gene set enrichment analysis

5 For methylation data, enrichment of KEGG terms was estimated for all differentially  
6 methylated probes (DMP) in a pair-wise manner. DMPs were defined as displaying a beta  
7 value change of 0.4 and an adjusted p-value < 0.05. Gene set enrichment was calculated with  
8 the gometh function of the missMethyl package (v.1.26.1).[7]

9 The single sample Gene Set Enrichment Analysis (ssGSEA) was performed only for RNA seq  
10 derived data. Briefly, the normalized enrichment scores (NES) were calculated on the variance  
11 stabilized transformation data with the GSVA package (v.1.40.1).[8] Differentially activated  
12 gene sets were calculated between the different precursor lesions as described by Larsen *et*  
13 *al.* with a p-value of < 0.05.[9]

14 VIPER analysis

15 The activation of transcription factors was calculated with the VIPER algorithm (v1.26.0).[9]  
16 For the analysis, the paad regulon was taken from the arcane.networks package (1.18.0).  
17 Activated transcription factors were defined as displaying a p-value < 0.005 and a NES score  
18 of >3 or >-3.

### 19 **Statistical analysis**

20 Statistical analysis was performed using the GraphPad Prism 8 software (GraphPad Software  
21 Inc., San Diego, USA) or R v. 3.6.0 (R Core Team 2018). Statistical significance in  
22 immunohistochemistry was determined by Kruskal-Wallis test with Dunn's multiple  
23 comparison test. Results are presented as means  $\pm$  standard error of the mean (SEM). P values  
24 less than 0.05 were considered statistically significant (\* p< 0.05; \*\* p < 0.01; \*\*\* p<0.001).

## 1 References

- 2 1 Schlitter AM, Born D, Bettstetter M, *et al.* Intraductal papillary neoplasms of the bile  
3 duct: Stepwise progression to carcinoma involves common molecular pathways. *Mod*  
4 *Pathol* 2014;27:73–86.
- 5 2 Richards S, Aziz N, Bale S, *et al.* Standards and guidelines for the interpretation of  
6 sequence variants: a joint consensus recommendation of the American College of  
7 Medical Genetics and Genomics and the Association for Molecular Pathology. *Genet*  
8 *Med* 2015;17:405–24.
- 9 3 Bolger AM, Lohse M, Usadel B. Trimmomatic: a flexible trimmer for Illumina sequence  
10 data. *Bioinformatics*. 2014;30:2114-2120.
- 11 4 Langmead B, Salzberg SL. Fast gapped-read alignment with Bowtie 2. *Nat Methods*  
12 2012;9:357-9.
- 13 5 Li H, Handsaker B, Wysoker A, *et al.* The sequence alignment/map format and  
14 SAMtools. *Bioinformatics* 2009;25:2078-9.
- 15 6 Love MI, Huber W, Anders S. Moderated estimation of fold change and dispersion for  
16 RNA-seq data with DESeq2. *Genome Biol* 2014;15:550.
- 17 7 Phipson B, Maksimovic J, Oshlack A. missMethyl: an R package for analyzing data from  
18 Illumina's HumanMethylation450 platform. *Bioinformatics* 2016;32:286-8.
- 19 8 Hänzelmann S, Castelo R, Guinney J. GSVA: gene set variation analysis for microarray  
20 and RNA-seq data. *BMC Bioinformatics* 2013;14:7.
- 21 9 Larsen BM, Kannan M, Langer LF, *et al.* A pan-cancer organoid platform for precision  
22 medicine. *Cell Rep* 2021;36:109429.
- 23 10 Alvarez MJ, Shen Y, Giorgi FM, *et al.* Functional characterization of somatic mutations  
24 in cancer using network-based inference of protein activity. *Nat Genet* 2016;48:838-  
25 47.

26

1 **Supplementary tables**2 **Supplementary table 1a: Antibodies and protocols for immunohistochemistry.**

Antibody	Type	Dilution	Antigen Demasking	Source
Anti-MUC1	Mo Mono	1:100	CC1	Biocare
Anti-MUC2	Mo Mono	1:100	CC1	Dako
Anti-MUC5AC	Mo Mono	1:1000	CC1	Chemicon
Anti-CDX2	Mo Mono	1:40	CC1	BioGenex
Anti-MIB1	Mo Mono	1:100	CC1	Dako
Anti-TFF3	Rb Mono	1:2000	EDTA buffer pH 9	Abcam
Anti-MUCL3	Rb Poly	1:500	Citrate buffer pH 6	LSBio

3 \*Rb: rabbit. Mo: mouse Mono: monoclonal. Poly: polyclonal. CC1: Cell Conditioning 1 (Ventana Medical System, Tucson, AZ,  
4 USA).

5 **Supplementary table 1b: Tissue collective used for Ki67, TFF3 and anti-MUC13 staining.**

Type of lesion	Number of lesions
<b>PanIN</b>	<b>31</b>
Low grade	26
High grade	5
<b>Gastric IPMN</b>	<b>28</b>
Low grade	20
High grade	8
<b>Intestinal IPMN</b>	<b>20</b>
Low grade	9
High grade	11
<b>PDAC</b>	<b>24</b>

6

## 1 Supplementary table 2: Genes and amplicons in targeted NGS.

Gene Symbol	Chr	Ion AmpliSeq Fwd Primer (5'-3')	Ion AmpliSeq Rev Primer (5'-3')	Amplicon ID
ALK	chr2	TCTCTCGGAGGAAGGACTTGAG	GCCCAGACTCAGCTCAGTTAAT	CHP2_ALK_1
ALK	chr2	ACAGGGTACCAGGAGATGATGTAAG	GGAAGAGTGGCCAAGATTGGA	CHP2_ALK_2
APC	chr5	GAGAGAACGCGGAATTGGTCTA	GTATGAATGGCTGACACTTCTCCA	CHP2_APC_1
APC	chr5	AGCACTGATGATAAACACCTCAAGTT	ATCTTCTTGACACAAAGACTGGCT	CHP2_APC_2
APC	chr5	TTCAATATCATCTTTGTCATCAGCTGAA	TTTGGTTCTAGGGTGTGTGAC	CHP2_APC_3
APC	chr5	GCAGACTGCAGGGTTCTAGTT	GTGAAGTACAGAAAGTACATCTGCT	CHP2_APC_4
APC	chr5	AGCCCCAGTGATCTCCAGATA	CCCTCTGAAGTGCAGCATTACT	CHP2_APC_5
APC	chr5	AGAGGGTCCAGGTTCTCCA	TCATTTCTGAACTGGAGGCATT	CHP2_APC_6
APC	chr5	ATGAAACAGAATCAGAGCAGCCTAAA	CGTGATGACTTTGTTGGCATGG	CHP2_APC_7
ARID1A	chr1	CAAAATGAACAACAAGGCAGATGGG	TCAGAGACTATCTAGTCCGGTGTCT	ARID1A_10.112972
ARID1A	chr1	CAGCTAACTTACTGGACTTGAGAATTTTT	GAGTCAAGACAAAAATCACTACCTTGG	ARID1A_10.135473
ARID1A	chr1	CATGATGGGAACTGGACCTCCTTA	TTAGCTGTGATGTGACTCTGAAGAAAT	ARID1A_10.143283
ARID1A	chr1	CCCCAGCCTACGGCTTC	CCCCCGTAGGGCTCCA	ARID1A_1.1.15178
ARID1A	chr1	CCTAGGCCCGCCCTGA	GGCTCCGGCCGTAGGGT	ARID1A_1.1.16654
ARID1A	chr1	CAGTCAAGAGACTTCTGAGACCCTTA	CAGATAACGGTCCACCCACATC	ARID1A_11.181180
ARID1A	chr1	CCGCTGGGAAAGGAGCTG	GCCTAGGGCCCGCTTC	ARID1A_1.1.20289
ARID1A	chr1	CTATGCCTCTATGTGTCTGTGAAG	GTACCACATGAAGCCAGTGAGTAC	ARID1A_11.248116
ARID1A	chr1	ACAACTCTACTACCCAACC	CTGCTGAGCGAAGGACGA	ARID1A_1.1.2481
ARID1A	chr1	CTCCAGAAATCCAGTTCTTCTACTACA	ATAGAGGTCCAGAGGTTTCTACC	ARID1A_11.279375
ARID1A	chr1	CTCAGCAGCGCTTCGGG	GGGCCCGCCACTGTAGT	ARID1A_1.1.36612
ARID1A	chr1	CTCGGAGCTGAAGAAAGCCG	GCTCTCGGCCCGCTCT	ARID1A_1.1.38056
ARID1A	chr1	GAGCCGTCTGCCGTCG	GGAGTGTACTGGTGGTTGGG	ARID1A_1.1.42139
ARID1A	chr1	GGCCCCAGCAGAAGCTCTCAC	AGCCCGGAGTGCCACCTC	ARID1A_1.1.52554
ARID1A	chr1	GGCTGCCGGCTCCAAGC	GCTGGCGACGTGAGCA	ARID1A_1.1.54514
ARID1A	chr1	GGGATCATGGCCGCGCA	CCGGCGGCTGCCTTCAT	ARID1A_1.1.54590
ARID1A	chr1	TTATCTGGCCTTCACTGAGGAGAA	CTCACCTGAGTCAATCCACCAAT	ARID1A_11.550938
ARID1A	chr1	AGCCGGACTGAAGAAGCTCG	GGCCCGGCTGAGTGAG	ARID1A_1.1.6484
ARID1A	chr1	CTCGCCCGGACCCCTCAG	GCCAGACAATGGCAGCTCC	ARID1A_1.2.19161
ARID1A	chr1	GGGTACCAGGGCTACCC	GGGCTCATGGGCGCTG	ARID1A_1.2.26067
ARID1A	chr1	GATATACCTCGACTCCTTTGGTTTGG	AGGGTCTTCTCCCGTTCAAT	ARID1A_12.293039
ARID1A	chr1	GCCAGCTCCTTGAAAAGCAGTATATC	GACCCATCCTTACCAGGAGAG	ARID1A_12.311881
ARID1A	chr1	AGACATCTTTCAGCTGTGATT	CACAGATCCTTGGCATATCCTGTTG	ARID1A_12.73402
ARID1A	chr1	CCGGCGGACATGGCCTC	CCTCCCACTCAGCTGTGTA	ARID1A_1.2.9363
ARID1A	chr1	CTCAACTTGTATCTGTCCACAGC	CTGCTCTGGCCTTACCTCATG	ARID1A_13.224100
ARID1A	chr1	CTCCTGCGTGTCTTTGTTATATTGG	TGGAGTCATGGAATCCGCTT	ARID1A_13.228066
ARID1A	chr1	GAGGAGACTTAAAGCCACCAACTC	CAAGGAGTCCCATGCACTTATCT	ARID1A_13.262576
ARID1A	chr1	GCCTTGTAGATCCTCTGCTAAGAAG	GCCCTGCATAGATCCTGATCC	ARID1A_13.286741
ARID1A	chr1	CTTAATGATGGAAGTACTCCACATTC	CAAGTCAAATAGCAATCAGATCAGTCA	ARID1A_14.234479
ARID1A	chr1	TGACTCAAACCTGGGTATCA	CATTTCACTGGCCCTGTCTTACG	ARID1A_14.440936
ARID1A	chr1	GACCACGACAGCACTATCCCTA	TCATGTTCCCTCAGGCCCTATT	ARID1A_15.209989
ARID1A	chr1	TCACCCTTGCCTTTCTACG	TCACTGTGCATAAGGACCTCCA	ARID1A_15.321878
ARID1A	chr1	CCAATTTTGTAGGACGGAGCCT	CACCGAGACCAGGCTTACTC	ARID1A_15.99688

ARID1A	chr1	CTAATCCTGTGTTCTTTGCCTCCT	TTTTCAAGGCGAACCTGCATG	ARID1A_16.147847
ARID1A	chr1	GGATGTATTCTCCTAGCCGCTAC	TTGGGTGGAGAACTGATTGCCATA	ARID1A_16.243588
ARID1A	chr1	AGCGTGCCATACAGCACT	GGCAGTGGCAGGATAGGCA	ARID1A_18.122838
ARID1A	chr1	AACCGCACCTCTCCTAGC	TCCCGCGAATCATGGG	ARID1A_18.17117
ARID1A	chr1	CAGATGAAATGCTGCACACAGATC	GATACCTGAGGAATGTGATTCTGCAT	ARID1A_18.249269
ARID1A	chr1	CAGGTATCCAGCCCTGCTC	TGCTATGTGCGAGGCAGGT	ARID1A_18.260793
ARID1A	chr1	CCACTGCCACAGCTGCTAC	GCTGAGCAACCTCAGCTGAT	ARID1A_18.303487
ARID1A	chr1	AAGGCTCGTGGCCTTCCC	GTGCGTTCTCCATTGGC	ARID1A_18.33212
ARID1A	chr1	CTGTGTCCACCAAGCATCTGG	GGCACGCTGTACATCTCC	ARID1A_18.457891
ARID1A	chr1	GCAAACATGCCACCACAAATGATG	TGTTCCGGTTCACGCCATGATAG	ARID1A_18.536845
ARID1A	chr1	GCCTTCCCCTCAGCAAGATGTATA	GGTCTCGGCCAACTGGAATG	ARID1A_18.584475
ARID1A	chr1	ACATAGCACCTGCCCTGT	GGGAGATTAGGCAACCGAATG	ARID1A_18.63843
ARID1A	chr1	TGCTCAGCAAGGCACCATG	CGAGCCTTCGTGGTTGG	ARID1A_18.820768
ARID1A	chr1	TTGTCTCTGCCTTAGAATTACAAGCG	GCTGGGCAGCTTGTGCT	ARID1A_18.880618
ARID1A	chr1	AGACGACATGGAGGTTTATTCAGG	CCCAGGCACTGATACTCA	ARID1A_19.54023
ARID1A	chr1	ATCTTCAGAGTAGCTTCACTGATGGG	GTTGATGGTATCTAATGCCATGTG	ARID1A_19.79292
ARID1A	chr1	CAACATCCTGCTGTATGATGACAAC	GGCATGGAAGATATCTACAAGAGAGAAA	ARID1A_19.96133
ARID1A	chr1	ATCCTGGGAGGTTTCAGCAA	GAAGCTGGCTTGCCTTGC	ARID1A_20.1.247050
ARID1A	chr1	CCAGTTCAGAGAATAGTGAGGA	GCAGCAGGCCACTGTCAAA	ARID1A_20.1.351511
ARID1A	chr1	CCCTCGGAAGCATGTGACAAC	CTTGATGGCCTCTGAACCTTAGC	ARID1A_20.1.374770
ARID1A	chr1	CCTGTGCTCACTGGCGGAT	GGCCCTCCTGGTCTGTTG	ARID1A_20.1.397870
ARID1A	chr1	CGAAGCCTGTCAATTTGTGCCA	GTTAGTGGTGCCTGCTTCCG	ARID1A_20.1.400147
ARID1A	chr1	CTGTTCTTAGGCCACTTTTCTCC	CCCAGGATCCAGTAGCGTT	ARID1A_20.1.464959
ARID1A	chr1	GAGGAAGTAGTTGAAAATGATGAGGAGA	TCCACCACAAATGGATCATTCTTCTGTA	ARID1A_20.1.565326
ARID1A	chr1	GCAGCAAGTTTCCATTGGCATTAG	AGGCTTCGAATGGTATTGGACAC	ARID1A_20.1.612574
ARID1A	chr1	GCCTGATTGAGATCTTTGGCATTAAAA	ACTTCTCTTCTTCTTCTTCTAGTTTA	ARID1A_20.1.637352
ARID1A	chr1	GGGCCCCACCTGATGGA	GTTCCGGTGGCTCTGTGC	ARID1A_20.1.733579
ARID1A	chr1	GTGGTGGACTGCTCAGATAAGCT	AGCTCTGTCTTGTCTCGAAGT	ARID1A_20.1.787955
ARID1A	chr1	ACCGGAACATCAAGATCCTAGAG	CCCTGGGTGTTGGACATC	ARID1A_20.1.90003
ARID1A	chr1	ATGGTGCGCTTCTCAGT	CGGCAAGGCTGCTCTAG	ARID1A_20.2.152846
ARID1A	chr1	CAGTGCAAGAGGCGAGTATCG	CCGCATCATGTCCACACTAGTTG	ARID1A_20.2.222602
ARID1A	chr1	CCACTAATTATGAAAAGGAGGAGGAA	CCGAGATGTTGGCGAGTGTA	ARID1A_20.2.247152
ARID1A	chr1	CCTTGCCGCCACACAGTT	CAACAGCCGTGATTCTGACA	ARID1A_20.2.313338
ARID1A	chr1	CTTGAGATGCTCCGGGAA	AGGGCAAACTGCCAGTGTA	ARID1A_20.2.409280
ARID1A	chr1	CTTCAGCTGAAGCCAGGAC	CGACCATAGTGTATACAATTCT	ARID1A_20.2.432258
ARID1A	chr1	AAACTCAGCATCCAGGACAACAAT	GCCAGGTTGGCCAGCAGTA	ARID1A_20.2.5295
ARID1A	chr1	ACCCAGGGCTGCTGCTCAT	TCTCAAGCAGTCCCACCA	ARID1A_20.2.54967
ARID1A	chr1	GGCTGTTGGACATCTCGGT	GTTTTGCATAAATAAGGGCAACAGTC	ARID1A_20.2.603909
ARID1A	chr1	GGGCAGTTGGACCTATCTCCATAC	CTGAGTTTGTGAGGGTTTCAA	ARID1A_20.2.613243
ARID1A	chr1	TGGACGAGAACCCTCAGAGTTTAC	GCTGTGATGACTGGCAATCAAAA	ARID1A_20.2.760156
ARID1A	chr1	CATGGGCGGCTCTTATAC	TAGTAGCACTGTAAATTAAGTGGCCA	ARID1A_2.198073
ARID1A	chr1	CTAACCCATACTCGCAGCAACA	TCACAATCACCATCTACTGCTG	ARID1A_2.263887
ARID1A	chr1	GCCATCCAGTCCAATGGATCAG	CCTGCATGGTATCGGGTAC	ARID1A_2.310812
ARID1A	chr1	AAACCTGTGTAAGTGGTTATATATTCAGT	CCATATGGCTGAGGTCATCTTG	ARID1A_2.6808
ARID1A	chr1	AGTCCAGCAAACTGCCTATTC	ACCCAGAGTTAATGGTCTTAAGTG	ARID1A_3.115759

ARID1A	chr1	CAGCAAAGTCTCACCTCAG	GGGATGGCTGCTGGGAGTAT	ARID1A_3.189854
ARID1A	chr1	CAGCTCCACATCAGCAGTC	AGCCTGCTGGGAGAGCGT	ARID1A_3.203145
ARID1A	chr1	CAGGCTCAGTCTCCTACCA	GCAGGAGGCAGGGATATCTT	ARID1A_3.210697
ARID1A	chr1	TGCTTCTATACTCATCATCAGTGCAT	CTTTGCTGGTTGTAATATGGAGTCTG	ARID1A_3.663071
ARID1A	chr1	TTTTCTTTCTACAGATTCCTCCTT	CTGCTGCTGATACGAAGGTTG	ARID1A_3.701387
ARID1A	chr1	AGCAGCAGCCACAGTCTCAA	TGAGCCTGTGGCTGTGAGTA	ARID1A_3.77267
ARID1A	chr1	CCATCACAGCTTTTGTCTTTCTGTGTAG	ACCTTCAGAAGGTGCAGAAATACT	ARID1A_4.173246
ARID1A	chr1	CTGGCCTTACATAATACTTTTCGC	GATGCCTGAGACCCAAATGAATC	ARID1A_4.215850
ARID1A	chr1	GAGGGCAAGAAGATGAACCTGAG	AGGTCAAATTAGTAAACTTCCAACCA	ARID1A_4.255932
ARID1A	chr1	GAGTCTGGAGTGAGCACATC	CGAGAGTGGTCTGAGCGA	ARID1A_5.220317
ARID1A	chr1	AGAATCTTTCTGCCTAATATACTAATCCATG	AGGAGACTGAGCTGGATTACTCT	ARID1A_5.34011
ARID1A	chr1	AGTCTCTTTCTCTCTCATACCT	CAGTCACTTTCCCTCTCCCTAA	ARID1A_5.70816
ARID1A	chr1	GATATGCTTATGTTGTTCTTTGTCTGGA	CACTCAAATGTCTGCCCTAGCTC	ARID1A_6.227771
ARID1A	chr1	AGCCATTTCTAGCTCTGAATTAACCTCC	TCGATCTTGGGCAATGCTTGAT	ARID1A_6.45476
ARID1A	chr1	CAGCCTTATCTCCGCGTCAG	ACTGTTTTCTCTCACCCTGAT	ARID1A_7.149596
ARID1A	chr1	CAGGATAAGGATGGAGAGCATTGTTC	TGTGTATCTGTCTCCGGAA	ARID1A_7.152412
ARID1A	chr1	CATGGCCAATATGCCACCTCA	ATAATACATTTCTTGCACTGACACCCT	ARID1A_8.210031
ARID1A	chr1	CCAATGCCAACTACCCAGTG	GGCCATGTTAGGGCCATAAGG	ARID1A_8.229785
ARID1A	chr1	GTTGCTAGTGAGTGACTAACCAAGTC	GGCTGTCCATGCATTTGACCTC	ARID1A_8.517555
ARID1A	chr1	AGGATGAGTCACGCCTCCATG	GGCCTTACCTGTTTTGGATAGAGTTG	ARID1A_8.91537
ARID1A	chr1	AGCACTATTTGGCTCCAGTTCAAATC	GGTTGATCATGCCAGCCATACTATTA	ARID1A_9.65769
BRAF	chr7	CATACTTACCATGCCACTTTCCCTT	TTTCTTTTCTGTTGGCTTGACTTGA	CHP2_BRAF_1
BRAF	chr7	CCACAAATGGATCCAGACAACGT	GCTTGCTCTGATAGGAAAATGAGATCTA	CHP2_BRAF_2
CDKN2A	chr9	CACCAGCGTGTCCAGGAA	CCCTGGCTCTGACCATTCTGT	CHP2_CDKN2A_1
CDKN2A	chr9	CATCTATGCGGGCATGGTACT	CGCTGGTGGTGTCTG	CHP2_CDKN2A_2
CTNNB1	chr3	ACTGTTTCTGATTTATAGCTGATTTGATGGA	CCTCTTCTCAGGATTGCCTTT	CHP2_CTNNB1_1
EGFR	chr7	CCTCATTGCCCTCAACACAGT	TCAGTCCGGTTTTATTGTCATCATAGTT	CHP2_EGFR_1
EGFR	chr7	CACCAGTACCAGATGGATGT	CCCAAAGACTCTCCAAGATGGGATA	CHP2_EGFR_2
EGFR	chr7	AGACATGCATGAACATTTTTCTCCAC	TCCAGACCAGGGTGTGTTTTTC	CHP2_EGFR_3
EGFR	chr7	TGTGGAGCTCTTACACCCA	GTGCCAGGGACCTTACCTTATAC	CHP2_EGFR_4
EGFR	chr7	ACGTCTTCTCTCTCTGTCA	CTGAGGTTCAGAGCCATGGA	CHP2_EGFR_5
EGFR	chr7	CATGCGAAGCCACACTGAC	ACATAGTCCAGGAGGCA	CHP2_EGFR_6
EGFR	chr7	GACTATGTCCGGGAACACAAAGA	CCCATGGCAAACCTTGCTA	CHP2_EGFR_7
EGFR	chr7	CGCAGCATGTCAAGATCACAGAT	GCATGTGTTAAACAATACAGCTAGTG	CHP2_EGFR_8
FBXW7	chr4	TGACAATGTTTAAAGTGGTAGCTGTT	ACTCATTGATAGTTGTAACCAACACA	CHP2_FBXW7_1
FBXW7	chr4	CCTGTGACTGCTGACCAAACCTTTA	CACATCTTCTTATAGGTGCTGAAAGG	CHP2_FBXW7_2
FBXW7	chr4	CCCAACCATGACAAGATTTTCCC	GGTCATCACAATGAGAGACAACATCA	CHP2_FBXW7_3
FBXW7	chr4	ACTAACAAACCCTCTGCCATCATA	TCTGCAGAGTTGTTAGCGGTT	CHP2_FBXW7_4
FBXW7	chr4	GTAGAATCTGCATTCCAGAGACAA	TCTCTTGATACATCAATCCGTGTTTGG	CHP2_FBXW7_5
FGFR2	chr10	CATCACTGTAAACCTTGACAGACAAAC	TGGTCTCTCATTCTCCCATCCC	CHP2_FGFR2_1
FGFR2	chr10	CATCCTCTCTCAACTCCAACAGG	AGTGGATCAAGCACGTGGAAAA	CHP2_FGFR2_2
FGFR2	chr10	GCTTCTTGGTCTGTCTTCTTCTT	CTCCTCTGTGATCTGCAATCT	CHP2_FGFR2_3
FGFR2	chr10	TGGAAGCCAGCCATTTCTAAA	GATGATGAAGATGATGGGAAACACAAG	CHP2_FGFR2_4
GNAS	chr20	TTGGTGAGATCCATTGACCTCAATTT	TGAATGTCAAGAAACCATGATCTGT	CHP2_GNAS_1
GNAS	chr20	CCTCTGGAATAACAGCTGTCC	TGATCCCTAACAAACACAGAAGCAA	CHP2_GNAS_2

IDH1	chr2	CCAACATGACTTACTTGATCCCCAT	ATCACCAAATGGCACCATACGA	CHP2_IDH1_1
IDH2	chr15	ACCCTGGCCTACCTGGTC	AGTTCAAGCTGAAGAAGATGTGGAA	CHP2_IDH2_1
KRAS	chr12	CAAAGAATGGCTGCACCAGTAATAT	AGGCCTGCTGAAAATGACTGAATATAA	CHP2_KRAS_1
KRAS	chr12	TCCTCATGTACTGGTCCCTCATT	GTAAAAGGTGCACTGTATAATCCAGACT	CHP2_KRAS_2
KRAS	chr12	CAGACTGTATTTATTTTCAGTGTACTTACCT	GACTCTGAAGATGTACCTATGGTCTTA	CHP2_KRAS_3
NRAS	chr1	CCTCACCTCTATGGTGGGATCATAT	GTTCTTGCTGGTGTGAAATGACTG	CHP2_NRAS_1
NRAS	chr1	TTGCCTGTCTCATGTATTGG	CACCCCAGGATTCTTACAGAAAA	CHP2_NRAS_2
NRAS	chr1	GCACAAATGCTGAAAGCTGTACC	CAAGTGTGATTGCCAACAAAGGA	CHP2_NRAS_3
PIK3CA	chr3	CCATAAAGCATGAACTATTTAAAGAAGCAAGA	GGTTGAAAAAGCCGAAGGTCAC	CHP2_PIK3CA_1
PIK3CA	chr3	TGGAATGCCAGAACTACAATCTTTTGAT	AAGATCCAATCCATTTTGTGTGC	CHP2_PIK3CA_10
PIK3CA	chr3	TGGATCTCCACACAATTAACAGCAT	TGCTGTTTATGGATTGTGCAATTC	CHP2_PIK3CA_11
PIK3CA	chr3	CCCTTTTTAAAGTAATTGAACCAAGTAGGC	TTTAAGATTACGAAGGATTGGTTAGACAGAA	CHP2_PIK3CA_2
PIK3CA	chr3	GACGATTTCCACAGCTACAC	AGCATCAGCATTTGACTTTACCTTATCA	CHP2_PIK3CA_3
PIK3CA	chr3	CATAGGTGGAATGAATGGCTGAATTATG	TCAATCAGCGGTATAATCAGGAGTTTTT	CHP2_PIK3CA_4
PIK3CA	chr3	TCCCATTATTATAGAGATGATTGTTGAATTTTCT	CAAAACAAGTTTATATTTCCCATGCCA	CHP2_PIK3CA_5
PIK3CA	chr3	GCTTTGAATCTTTGGCCAGTACCT	CATAAGAGAGAAGGTTTGACTGCCATA	CHP2_PIK3CA_6
PIK3CA	chr3	CAGAGTAACAGACTAGCTAGAGACAATGA	GCACTTACCTGTGACTCCATAGAAA	CHP2_PIK3CA_7
PIK3CA	chr3	CACGATCTTTTAGATCTGAGATGCACA	CCTTTTGTGTTTTCATCTTCTCTCTG	CHP2_PIK3CA_8
PIK3CA	chr3	GATGCAGCCATTGACCTGTTTAC	AGAAAACCATTACTTGTCCATCGTCT	CHP2_PIK3CA_9
PTEN	chr10	GCCATCTCTCCTCCTTTTTCTT	GCCGCAGAAATGGATACAGGTC	CHP2_PTEN_1
PTEN	chr10	TGTTAATGGTGGCTTTTGTGTTGTTGT	TCTACCTCACTCTAACAAAGCAGATAACT	CHP2_PTEN_2
PTEN	chr10	CCATAACCCACACAGCTAGAA	TGCCCGATGTAATAAATATGCACAT	CHP2_PTEN_3
PTEN	chr10	GGCTACGACCCAGTTACCATAG	TGCCACTGGTCTATAATCCAGATGAT	CHP2_PTEN_4
PTEN	chr10	TGAGATCAAGATTGCAGATACAGAATCC	ACCTTTAGCTGGCAGACCAC	CHP2_PTEN_5
PTEN	chr10	AGGTGAAGATATATTCTCCAATTCAGGAC	TTGGATATTTCTCCAATGAAAGTAAAGTAC	CHP2_PTEN_6
PTEN	chr10	CACTTTTGGGTAATACATTCTCATACCAGGA	TATACTGCAAATGCTATCGA	CHP2_PTEN_7
PTEN	chr10	GCAGTATAGAGCGTGCAGATAATGA	CATCACATACACAAGTCAACAACCC	CHP2_PTEN_8
RNF43	chr17	CCAAACACATCTGGAGCACACT	GCCTGACCCTCAATGACCTCTT	RNF43_1.100174
RNF43	chr17	CCGCTTTTGTAGTGGTGGT	TGACTTTGACCCCTAGTGTACT	RNF43_2.1.213215
RNF43	chr17	ACAACCACTGGCTGTGAA	GCACCCAGCTTCCAGATT	RNF43_2.1.22754
RNF43	chr17	CGGTGTCAGAATCCATTAGAAAG	GACAAGAGGCTGCTACCAGAAA	RNF43_2.1.264668
RNF43	chr17	CTCTCCCTACCACCCACTT	GTGGTTGTGCTGACTCCTC	RNF43_2.1.277654
RNF43	chr17	CTGGGTGCACAGTTGCATC	CCCTGGCCAGTTGACG	RNF43_2.1.308947
RNF43	chr17	GAAACCTGGGTTTCCCTGT	GGGTCCATGGCAGCAGTTC	RNF43_2.1.342797
RNF43	chr17	AAAGTCACTGCTTAGGGAGCT	AGAAAGCTATTGCACAGAACGC	RNF43_2.1.4249
RNF43	chr17	GGGACCAAGGATATGCCACACT	TGCAAAAATCCAGCCTCTCTGC	RNF43_2.1.479773
RNF43	chr17	GGGCACTGTGGTTAGAGAG	AAAAGCGTTCCAGTGGCA	RNF43_2.1.483268
RNF43	chr17	GTGACTTGCTGATCAGGAGAAGGT	GTTTCCAGCCATGTCCACTACC	RNF43_2.1.554471
RNF43	chr17	TTTTTGCAAGTTGAACAGACTGCT	CAAGTACCAGATCCAATCAGC	RNF43_2.1.716452
RNF43	chr17	CTCCAGATCCACTGCTGTCA	TTCCCCAGAGCTGCACATC	RNF43_2.2.168519
RNF43	chr17	GTAGGCTGATGTCCTGTCAG	GCTTGCCAGTGCCTCTA	RNF43_2.2.335644
RNF43	chr17	GTGCTGTGAGGTGGATTGGAG	CCCACGACCTGGTCCCTT	RNF43_2.2.348341
RNF43	chr17	GTGATGCCGAGGGCCCAT	CAGGTGCAAGACTCCACCTC	RNF43_2.2.359855
RNF43	chr17	AGGTGGTAGTGGGATGGC	TGCTTTCTGAATGCATTCTGTAGG	RNF43_2.2.62203
RNF43	chr17	CCTCTACTGTGATGTTGAACATG	CCTGATTCTGGCAATCCTATGG	RNF43_3.144168

RNF43	chr17	AAGCCACATTCTAGACCTGTCTG	CTCTTTTCTCCAGGACTACGG	RNF43_3.9926
RNF43	chr17	TCCTCCAGACAGATGGCACA	CCCAATCTGAGCCCCATTCT	RNF43_4.332752
RNF43	chr17	TTCAATCTCCCAGTCTGGTCAT	AGCTGGCCACCAGGAGGTA	RNF43_4.381754
RNF43	chr17	TACTCCTTCTTCTCCCTAACCCAC	ATGATGTGTGGATCCTAATGACAGT	RNF43_5.252108
RNF43	chr17	AAGCCAGGATGATCACAAGATGG	CTCAAGGGAACCTCCAGTTAGCTAT	RNF43_5.9080
RNF43	chr17	CCCTGAGAGCTTTATCTTCTCCATC	GACCTCAGCCCAACCTCTACT	RNF43_6.126819
RNF43	chr17	GTCTGGAGGTCTAGTGTGCT	TGGGCACCTTCCCCCTGTA	RNF43_6.251138
RNF43	chr17	ATCAGCTTCTCAGCGTCATTACC	CTGGATGGAGGAAGATAAAGCTCTCA	RNF43_6.62210
RNF43	chr17	CACAGGACAAAGTAGGGCTAAGTG	AAGCTGATGGAGTTTGTGTACAAGAA	RNF43_6.83735
RNF43	chr17	CCAGCTTGACGATGCTGATGAAT	TGGTACTCTCCCTAGAAAATGGAGAG	RNF43_8.145848
RNF43	chr17	GTGTAGGGCGAAGTGTGAGTC	CCTAACCCAAGTCTGTCTCTCTG	RNF43_8.334246
RNF43	chr17	ATTTCCACTTCTCTCAGACCAAGTCAT	CCTGTCACTGGCTAGCAAGGTA	RNF43_8.99948
RNF43	chr17	GCAAACACACCTTCCAAAGTGAGATT	TGGACGCACAGGACTGGTAC	RNF43_9.251835
RNF43	chr17	ACAAAAGAAGAAAGACATATTTCAAACAGATG	TTATCAGAGTGATCCCTTGAAAATGG	RNF43_9.43347
RNF43	chr17	AGCTTTCTGTCTGCTGATCTTCA	GTATGTATGGTTGAAGTGCATTGCTG	RNF43_9.83487
SMAD4	chr18	CTCATGTGATCTATGCCGCT	AGTCTACTTACCAATCCAGGTGATACA	CHP2_SMAD4_1
SMAD4	chr18	TGCTACTTCTGAATTGAAATGGTTCA	GATTACTACCATTACTCTGCAGTGTT	CHP2_SMAD4_2
SMAD4	chr18	ATGGTGAAGGATGAATATGTGCATGA	GCTGGTAGCATTAGACTCAGATGG	CHP2_SMAD4_3
SMAD4	chr18	GTGAAGGACTGTTGCAGATAGCAT	AAGGCCACATGGGTTAATTTG	CHP2_SMAD4_4
SMAD4	chr18	TTTCTTTAGGGCTTTCACAATGA	CTGAGAAGTGACCCATAATCCATT	CHP2_SMAD4_5
SMAD4	chr18	GCTCCTGAGTATTGGTGTCCAT	CCTGTGGACATTGGAGAGTTGA	CHP2_SMAD4_6
SMAD4	chr18	TGTAATTTCTTTTTCTTCTAAGGTTGCACATAG	ACTTGGGTAGATCTTATGAACAGCAT	CHP2_SMAD4_7
SMAD4	chr18	AGGCTTTGATTGCGTCAGTGT	GCTGGAGCTATTCCACTACTG	CHP2_SMAD4_8
SMAD4	chr18	GCTGCTGGAATTGGTGTGATG	AGTACTCGTCTAGGAGCTGGAG	CHP2_SMAD4_9
STK11	chr19	GAGCTGATGTCGGTGGGTAT	CTCCGAGTCCAGCACCTC	CHP2_STK11_1
STK11	chr19	CTCCAGGCAGCTGCAA	CCGGTGGTGAGCAGCAG	CHP2_STK11_2
STK11	chr19	CCGGTGGCACCTCAA	CTGGTCCGGCAGGTGTC	CHP2_STK11_3
STK11	chr19	AACATCACACGGGTCTGTAC	GATGAGGCTCCACCTTTCAG	CHP2_STK11_4
STK11	chr19	GAAGAAACATCCTCCGGCTGAA	ACCGTGAAGTCTGAGTGTAGA	CHP2_STK11_5
TP53	chr17	TCCACTCACAGTTTCCATAGGTCT	GTTGGAAGTGTCTCATGCTGGAT	CHP2_TP53_1
TP53	chr17	GGCTGTCCAGAATGCAAGAA	GATGAAGCTCCAGAATGCCA	CHP2_TP53_2
TP53	chr17	TGCACAGGGCAGGTCTTG	CCGTCTCCAGTTGCTTTATCTGT	CHP2_TP53_3
TP53	chr17	ACCAGCCTGTCTCTCT	GTGCAGCTGTGGTTGATTC	CHP2_TP53_4
TP53	chr17	CCAGTTGCAAACAGACCTCA	AGGCCTCTGATTCCTCACTGAT	CHP2_TP53_5
TP53	chr17	GGCTCCTGACCTGGAGTCTT	CTCATCTTGGCCTGTGTTATCTC	CHP2_TP53_6
TP53	chr17	CGCTTCTGTCTGCTTCT	TTCTTTTTCTATCTGAGTAGTGGT	CHP2_TP53_7
TP53	chr17	GGAAGGGCTGAGGTCACT	CCCCTCTCTGTTGCTGC	CHP2_TP53_8
VHL	chr3	CTCCAGGTCATCTTCTGCAAT	GTACCTCGGTAGCTGTGGATG	CHP2_VHL_1
VHL	chr3	GTGGCTCTTAAACCTTTGCT	GTCAGTACCTGGCAGTGTGATA	CHP2_VHL_2
VHL	chr3	GGCAAAGCCTCTTGTCTGTTTC	TGACGATGTCCAGTCTCCTGTAAT	CHP2_VHL_3

1

1 **Supplementary table 3: Mutation profile of precursor lesions detected by targeted NGS.**

Grade	Gene	Sample	Variant	VAF [%]	Variant Effect	Transcript
low-grade PanIN	<i>ARID1A</i>	<b>113</b>	Gln802fs	4.83	frameshift/insertion	NM_006015.5
	<i>CDKN2A</i>	74	Arg58Ter	3.48	nonsense	NM_001195132.1
	<i>GNAS</i>	127	Arg201His	20.17	missense	NM_000516.5
	<i>KRAS</i>	52	Gly12Val	15.38	missense	NM_033360.3
		<b>55</b>	Gly12Val	9.66	missense	NM_033360.3
		<b>56</b>	Gly12Asp	6.13	missense	NM_033360.3
		69	Gln61His	4.08	missense	NM_033360.3
		74	Gly12Asp	12.05	missense	NM_033360.3
		<b>111</b>	Gly12Val	11.19	missense	NM_033360.3
		125	Gly12Val	4.29	missense	NM_033360.3
		127	Gly12Asp	18.24	missense	NM_033360.3
		128	Gly12Asp	3.42	missense	NM_033360.3
		129	Gly12Asp	3.7	missense	NM_033360.3
		<b>113</b>	Gly12Arg	4.18	missense	NM_033360.3
		<b>113</b>	Gly12Val	8.75	missense	NM_033360.3
		<b>43</b>	Gly12Val	12.88	missense	NM_033360.3
	<i>PIK3CA</i>	68	Arg349Ter	3.74	nonsense	NM_006218.3
127		Phe83fs	4.52	frameshift/deletion	NM_006218.3	
<i>PTEN</i>		128	Asn323fs	22.37	frameshift/deletion	NM_000314.6
high-grade PanIN	<i>ARID1A</i>	73	Trp2091Ter	7.46	nonsense	NM_006015.4
	<i>GNAS</i>	96	Arg201His	3.42	missense	NM_000516.5
	<i>KRAS</i>	73	Gly12Asp	8.29	missense	NM_033360.3
		<b>80</b>	Gly12Val	16.59	missense	NM_033360.3
		101	Gly12Asp	13.7	missense	NM_033360.3
		<b>104</b>	Gly12Asp	5.15	missense	NM_033360.3
		<b>114</b>	Gly12Val	18.3	missense	NM_033360.3

	<i>TP53</i>	<b>80</b>	Arg213Ter	34.5	nonsense	NM_000546.5
		<b>104</b>	Arg196Ter	4.04	nonsense	NM_000546.5
low-grade IPMN gastric	<i>ARID1A</i>	21	Asp1850fs	7.45	frameshift/insertion	NM_006015.5
	<i>GNAS</i>	<b>2</b>	Arg201His	33.98	missense	NM_000516.5
		<b>7</b>	Arg201Cys	11.34	missense	NM_000516.5
		<b>35</b>	Arg201His	41.52	missense	NM_000516.5
		<b>62</b>	Arg201Cys	15.56	missense	NM_000516.5
		<b>86</b>	Arg201His	30.46	missense	NM_000516.5
		89	Arg201His	5.56	missense	NM_000516.5
		<b>94</b>	Arg201His	21.97	missense	NM_000516.5
		<b>97</b>	Arg201Cys	33.81	missense	NM_000516.5
		<b>99</b>	Arg201His	25.08	missense	NM_000516.5
		<b>110</b>	Arg201Cys	22.37	missense	NM_000516.5
		<b>112</b>	Arg201His	24.32	missense	NM_000516.5
		<b>54</b>	Arg201Cys	23.16	missense	NM_000516.5
	<i>KRAS</i>	21	Gly12Val	18.86	missense	NM_033360.3
		<b>2</b>	Gly12Val	35.1	missense	NM_033360.3
		<b>7</b>	Gly12Val	12.14	missense	NM_033360.3
		<b>35</b>	Gly12Asp	38.57	missense	NM_033360.3
		<b>39</b>	Gly12Val	35	missense	NM_033360.3
		<b>61</b>	Gly12Val	18.03	missense	NM_033360.3
		<b>62</b>	Gly12Val	18.5	missense	NM_033360.3
		64	Gly12Val	9.01	missense	NM_033360.3
		<b>86</b>	Gly12Val	27.81	missense	NM_033360.3
		89	Gln61His	36.49	missense	NM_033360.3
		<b>94</b>	Gly12Asp	21.16	missense	NM_033360.3
		<b>97</b>	Gly12Asp	33.68	missense	NM_033360.3

		<b>99</b>	Gly12Val	26.83	missense	NM_033360.3
		<b>110</b>	Gly12Val	24.76	missense	NM_033360.3
		<b>57</b>	Gly12Arg	6.96	missense	NM_033360.3
	<i>STK11</i>	<b>61</b>	Tyr60Ter	61.89	nonsense	NM_000455.4
high-grade IPMN gastric	<i>ARID1A</i>	130	Gln2115Ter	30.84	nonsense	NM_006015.5
	<i>GNAS</i>	51	Arg201Cys	31.03	missense	NM_000516.5
	<i>KRAS</i>	51	Gly12Val	33.12	missense	NM_033360.3
		65	Gly12Asp	16.51	missense	NM_033360.3
		66	Gly12Asp	33.64	missense	NM_033360.3
		130	Gly12Asp	22.65	missense	NM_033360.3
		131	Gly12Asp	23.98	missense	NM_033360.3
	<i>TP53</i>	65	Arg248Trp	17.99	missense	NM_000546.5
low-grade IPMN intestinal	<i>GNAS</i>	<b>92</b>	Arg201Cys	80.59	missense	NM_000516.5
	<i>KRAS</i>	<b>92</b>	Gly12Arg	37.95	missense	NM_033360.3
high-grade IPMN intestinal	<i>GNAS</i>	<b>33</b>	Arg201Cys	45.42	missense	NM_000516.5
		<b>88</b>	Arg201Cys	36.81	missense	NM_000516.5
		<b>90</b>	Arg201His	35.51	missense	NM_000516.5
		17	Gln227Lys	42.36	missense	NM_000516.5
	<i>KRAS</i>	<b>88</b>	Gly12Ser	33.81	missense	NM_033360.3
	<i>TP53</i>	<b>88</b>	Met237Thr	49.16	missense	NM_000546.5

1 PanIN/IPMN in cases without associated/concomitant PDAC are indicated in bold.

2

3

4

5

1 **Supplementary table 4. Distribution of CNV-positive and negative precursor lesions**  
 2 **according to the degree of dysplasia.**

		<i>CNV pos</i>	<i>CNV neg</i>
<i>PanIN</i>	<b>Low-grade</b>	16 (57%)	12 (43%)
	<b>High-grade</b>	6 (75%)	2 (25%)
<i>Gastric IPMN</i>	<b>Low-grade</b>	22 (76%)	7 (24%)
	<b>High-grade</b>	6 (75%)	3 (25%)
<i>Intestinal IPMN</i>	<b>Low-grade</b>	8 (100%)	0
	<b>High-grade</b>	13 (100%)	0

3 Percentages refers to the total number of cases in each group

4

5

6

7

8

9

10

11

12

13

14

**Supplementary table 5: Overview of log<sub>2</sub> copy number ratios sorted in ascending order. Values of genomic alterations were detected by low-coverage sequencing (n=28) and DNA methylation data (n=67), respectively.**

Genomic location	affected samples (n)	PanIN (n=36)	gIPMN (n=38)			iIPMN (n=21)		
<b>deleted regions</b>								
chr01:010875000-013052998	3					-0.26	-0.25	-0.24
chr01:015375000-016825000	3					-0.26	-0.25	-0.20
chr06:074175000-074375000	5		-0.29	-0.22	-0.21	-0.44	-0.24	
chr06:133664400-143100000	5		-0.37	-0.28		-0.50	-0.45	-0.28
chr06:143620678-151100000	7	-0.21	-0.37	-0.34	-0.29	-0.50	-0.45	-0.28
chr09:005958053-023802212	5	-0.23	-0.51	-0.36	-0.36	-0.24		
chr10:071075000-120925000	6		-0.45	-0.22		-0.36	-0.30	-0.28
chr10:120925000-125869472	5		-0.30			-0.41	-0.30	-0.28
chr11:057325000-058807232	4					-0.44	-0.40	-0.27
chr11:058807232-069089801	5					-0.44	-0.40	-0.28
chr11:096437584-114325000	5					-0.51	-0.44	-0.40
chr11:114325000-134898258	4					-0.51	-0.44	-0.28
chr17:006225000-009675000	4		-0.50	-0.32	-0.21	-0.23		
chr17:009675000-012500000	5		-0.53	-0.31	-0.21	-0.50	-0.22	
chr17:015792977-021566608	6		-0.58	-0.23	-0.21	-0.49	-0.32	-0.25
<b>amplified regions</b>								
chr01:035225000-037325000	3					0.25	0.33	0.61

chr03:176225000-188875000	6	0.26	0.21	0.23	0.28	0.38	0.44				
chr05:028950000-044925000	5				0.24	0.25	0.31	0.74	0.79		
chr06:024125000-033575000	5		0.25	0.36	0.31	0.35	0.56				
chr06:033575000-042725000	4		0.42		0.32	0.34	0.56				
chr07:000282484-007150000	5				0.22	0.30	0.32	0.36	0.41		
chr07:054725000-055775000	5				0.21	0.26	0.27	0.33	0.36		
chr07:061967157-074715724	4				0.27	0.32	0.36	0.37			
chr07:112425436-130154523	5				0.21	0.33	0.36	0.38	0.57		
chr07:139404377-142048195	5				0.22	0.32	0.36	0.33	0.58		
chr07:143397897-154270634	5				0.24	0.33	0.34	0.38	0.59		
chr08:086726451-089550000	3				0.21	0.31	0.36				
chr08:127450000-129175000	7	0.42			0.21	0.27	0.29	0.36	0.56	0.66	
chr09:001992685-035698318	3				0.24	0.32	0.61				
chr09:070835468-092343416	4				0.22	0.26	0.32	0.60			
chr09:096718222-097575000	4				0.21	0.24	0.32	0.60			
chr09:097775000-114750000	4				0.22	0.26	0.32	0.61			
chr09:124994207-133073060	3				0.22	0.32	0.61				
chr12:006475000-007169938	8	0.21			0.24	0.33	0.56	0.71	0.88	0.89	1.70
chr12:024993545-028938805	4	0.21			0.21	0.38	1.32				
chr14:020700000-022050000	3				0.21	0.28	0.33				
chr14:022800000-050175000	3				0.22	0.25	0.35				
chr14:097258910-107289540	3				0.25	0.22	0.36				
chr17:061125000-062410760	3				0.32	0.32	0.74				
chr17:062775000-063525000	3				0.32	0.34	0.49				
chr17:068117898-077546461	3				0.21	0.32	0.38				

chr20:008050000-016400000	7	0.24	0.22	0.23	0.24	0.26	0.33	0.84
chr20:016625000-021300000	7	0.25	0.22	0.23	0.25	0.28	0.33	0.82
chr20:030025000-034897085	7	0.26	0.22	0.22	0.23	0.31	0.33	0.81
chr20:036958189-042991501	6	0.26	0.22	0.23	0.35	0.33	0.79	
chr20:052650000-061091437	7	0.23	0.22	0.22	0.23	0.33	0.35	0.80
chr21:032825000-034475000	3		0.21	0.26	0.30			

1

1 **Supplementary table 6a: Differentially methylated probes in low- and high-grade pancreatic**  
 2 **cancer precursors.**

	Low-grade samples	High-grade samples	DMPs (hypermethylated in high-grade)	DMP associated genes (hypermethylated in high-grade)
iPMN	8	12	0	0
gIPMN	24	8	0	0
PanIN	20	7	86 (62)	59 (45)

3 iIPMN: intestinal IPMN; gIPMN: gastric IPMN

4

5 **Supplementary table 6b: Genes associated with significantly hyper- or hypomethylated CpG**  
 6 **in PanIN high-grade**

Genes associated with at least one significantly hypermethylated CpG	Genes associated with at least one significantly hypomethylated
TAC1	GLRX
AKAP13	BCL11B
POLR1D	ITFG3
GLYATL3	IFT140
HOXA5	CTNNA3
ZIC2	RUNX1
SIM2	SPARCL1
ARID4B	PHLDB1
MON2	NINJ2
CNKSR3	METTL9
SP8	SLC51A
ADD2	EMID2
HOXB1	CACNA1A
ST3GAL6	C19orf35
FBN2	
ZIK1	
LRP1B	
NTRK3	
GLI3	
NTM	
RASGRF1	
FAM46C	

NXPH1	
LBX2	
LOC101929710	
ADRA1A	
GRIK3	
PARP8	
KIAA1026	
SLC6A15	
IRX1	
GRIA4	
TLE4	
DGKI	
PACSIN2	
DOK5	
ZIC4	
MYLK	
DAPK1	
C5orf66-AS1	
AMER3	
CPEB1	
ST6GAL2	
INA	
AP2A2	

1

## 1 **Supplementary Figure Legends**

### 2 **Supplementary figure 1: Overview of lesions and methods**

3 55 PanINs, 46 gastric IPMNs (gIPMN) and 21 intestinal IPMNs (iIPMN) were subjected to 4  
4 main analyses: targeted next generation sequencing (n=52), low-coverage whole-genome  
5 sequencing (n=28), genome-wide DNA methylation analysis (n=79) and transcriptome analysis  
6 (n=34). Each circle of the diagram represents one of the mentioned methods and includes the  
7 number of samples used for related analyses. The samples that could not be placed into the  
8 diagram were shown at the right bottom corner of the figure. Pancreatobiliary and mixed-type  
9 IPMNs were excluded from further analyses due to small sample size.

### 10 **Supplementary figure 2: Allele frequency of *KRAS* and *GNAS* mutations in different precursor 11 lesions.**

12 (A) VAF of *KRAS* mutations; (B) VAF of *GNAS* mutations; (C) scatterplot of the VAF of the *KRAS*  
13 mutations (G12) against the VAF of *GNAS* mutations (R201) detected in low- and high-grade  
14 gastric IPMN. The grey lines represent the 95% confidence interval of the Pearson's correlation  
15 coefficient  $r$  (n=9). (Kruskal-Wallis-test \*  $p < 0.05$ ; \*\*  $p < 0.01$ ; \*\*\*  $p < 0.001$ ).

16

### 17 **Supplementary figure 3: Morphology of lesions with different genetic status according to 18 targeted NGS**

19 Representative HE images of low- and high-grade PanINs, gastric IPMNs and intestinal IPMNs  
20 with variable mutation profiles detected by targeted NGS are shown. No specific morphology  
21 was identified related to the mutation status between the samples in the same diagnostic  
22 group. In particular, gastric lesions with *GNAS* mutations (case 127, 96, 99 and 112) did not  
23 show relevant intestinal differentiation; only in case 112, focal (<5% of the cells) expression of  
24 *MUC2* and *CDX2* was observed (not shown). Scale bars represent 200  $\mu\text{m}$ . Detailed mutation  
25 profile of the samples is provided in Suppl. Table 3.

### 26 **Supplementary figure 4: Quality control of DNA methylation data derived from normal 27 pancreas cell preparations.**

28 (A) Multi-dimensional scaling of the 1000 most variable probes. (B) Hierarchical clustering of  
29 probes for known acinar and ductal marker genes.

1

2 **Supplementary figure 5: Proliferation activity, expression of TFF3 and of MUCL3 protein in**  
3 **PanIN, IPMN and PDAC.**

4 Representative images (A) and related graphs (B-D) of IHC staining performed in whole tissue  
5 sections in 31 PanIN, 28 gastric IPMN, 20 intestinal IPMN and 24 PDAC. Intestinal IPMNs and  
6 PDACs showed higher proliferation rates with Ki67 staining than PanIN and gastric IPMN. TFF3  
7 was strongly expressed in intestinal IPMN. Gastric IPMN revealed higher expression of MUCL3  
8 compared to PanIN. Scale bars represent 100  $\mu$ m. (IRS: immunoreactivity score) (\* $p < 0.05$ ).

9

10 **Supplementary figure 6: Hierarchical clustering of DNA methylation data based on published**  
11 **marker genes for distinct normal pancreas cell populations.** The mean methylation beta-  
12 value for all gene associated probes is displayed, respectively.

13

14 **Supplementary figure 7: Differentially activated gene sets.** Displayed pathways were  
15 detected by pairwise comparison between the indicated lesions. Odds ratios below 0.8  
16 indicate the activation in the first listed lesion whereas 1.1 is associated with the second  
17 group. The analyzed gene sets based on the KEGG pathway (A) and hallmarks (B) from  
18 the MSigDB.

19

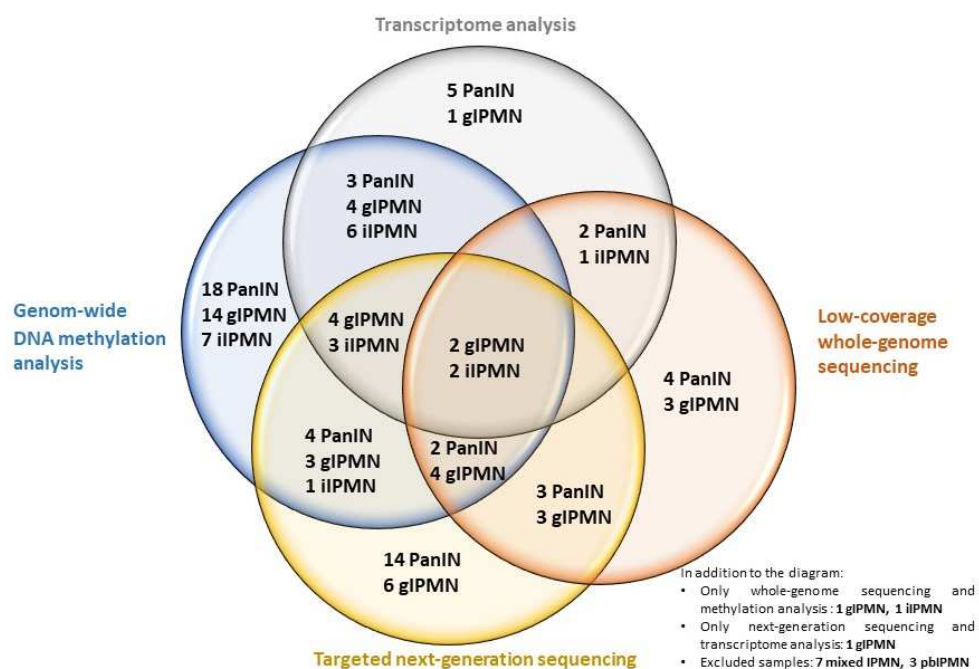
20

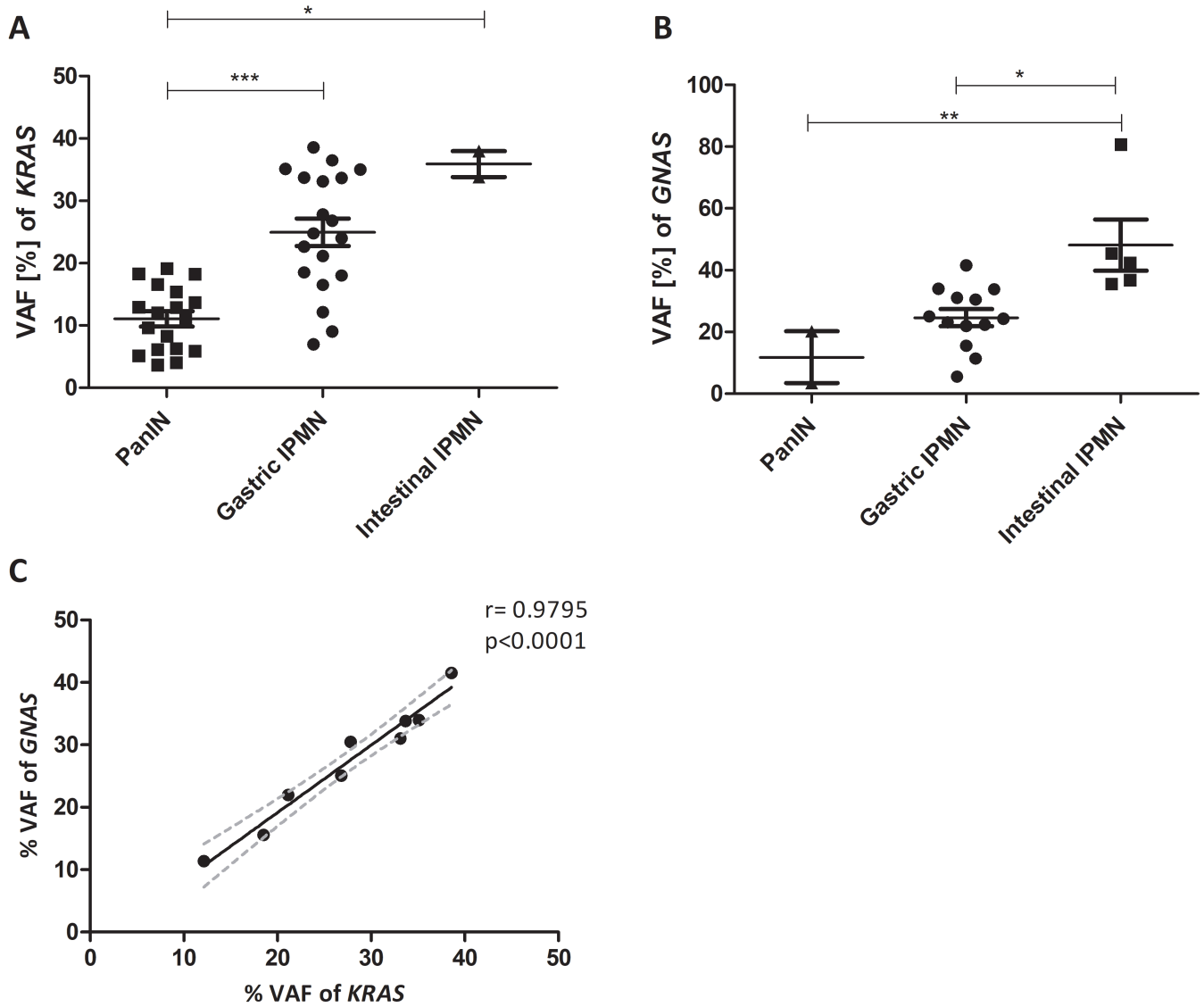
21

22

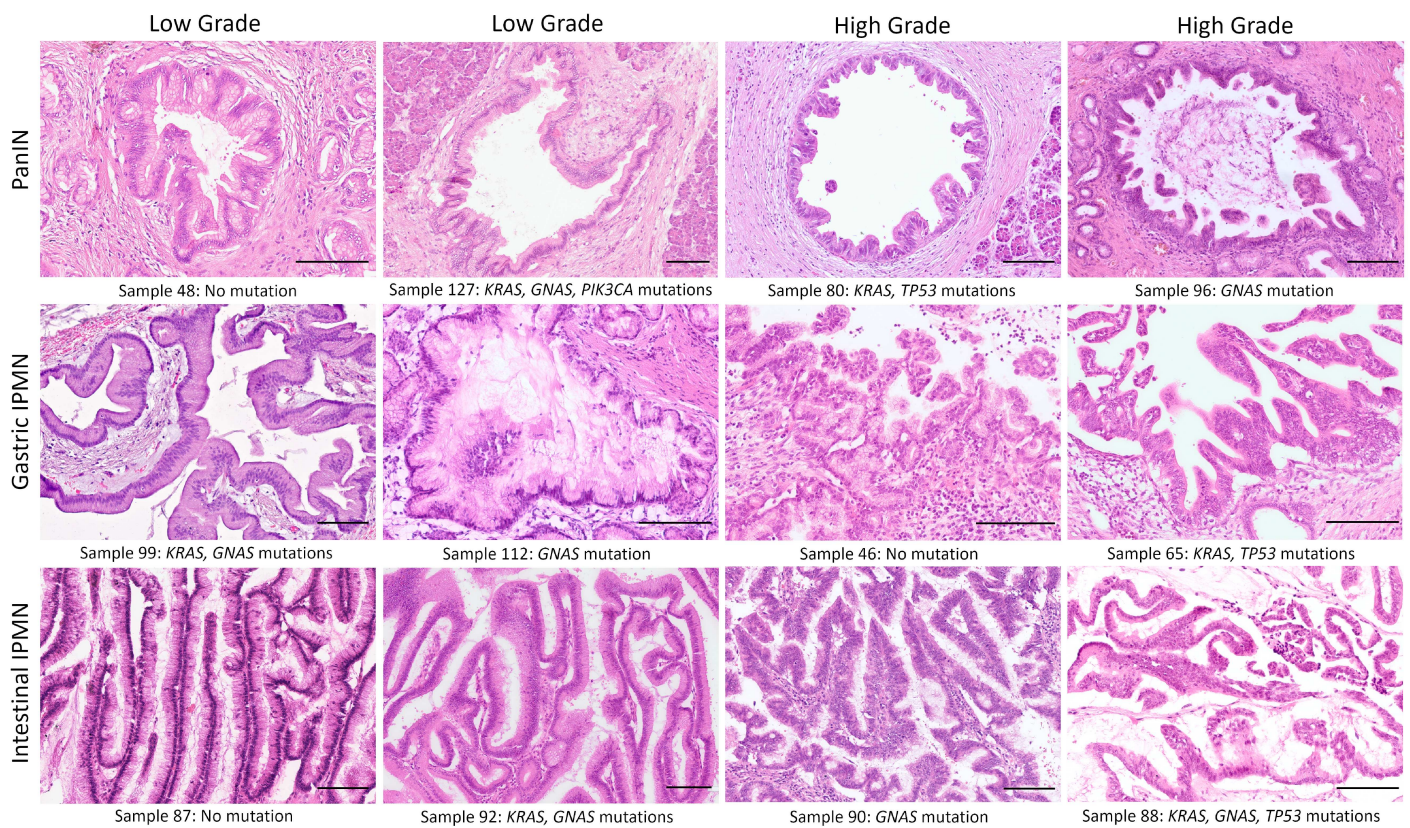
23

## Suppl. Figure 1.jpg

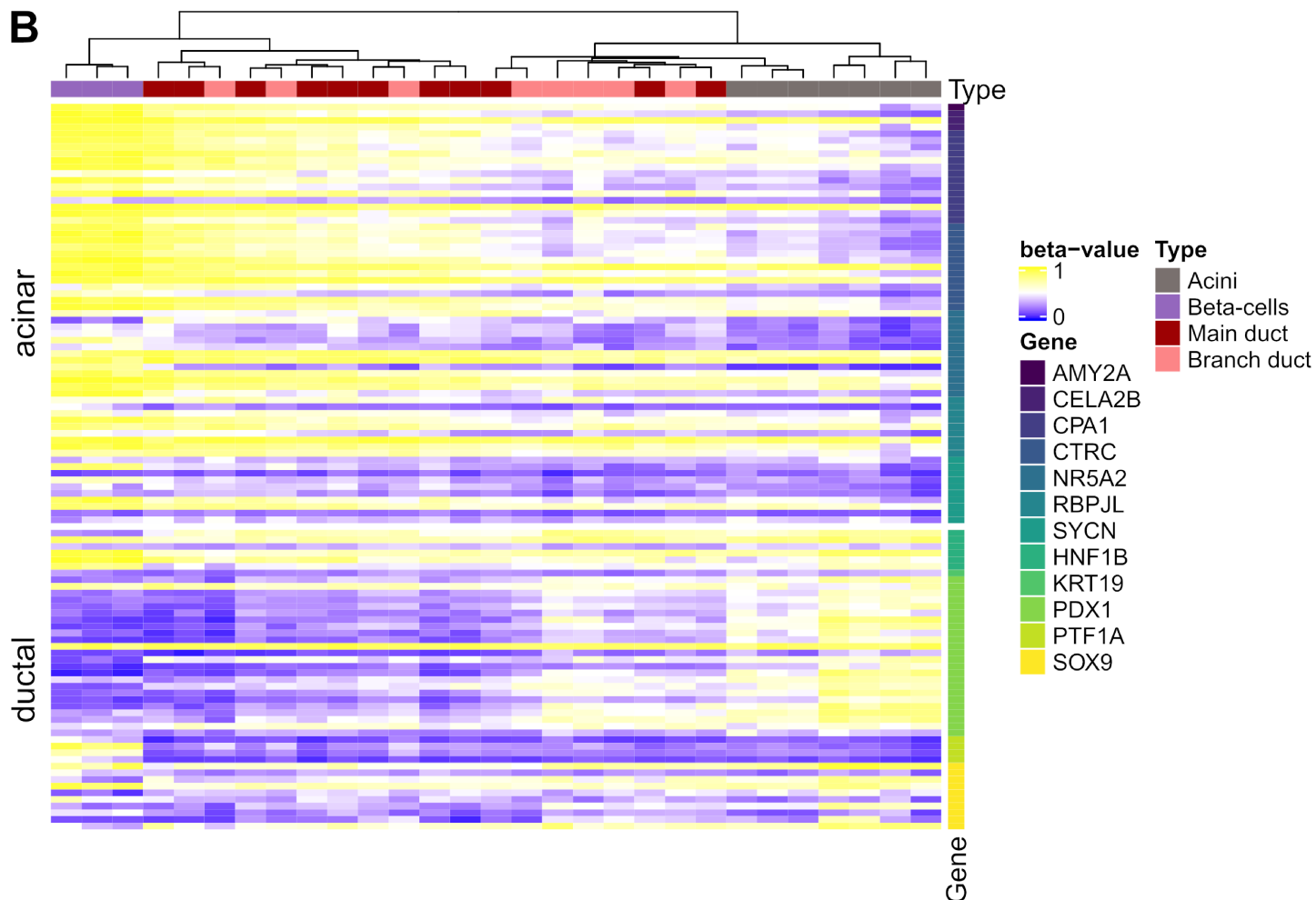
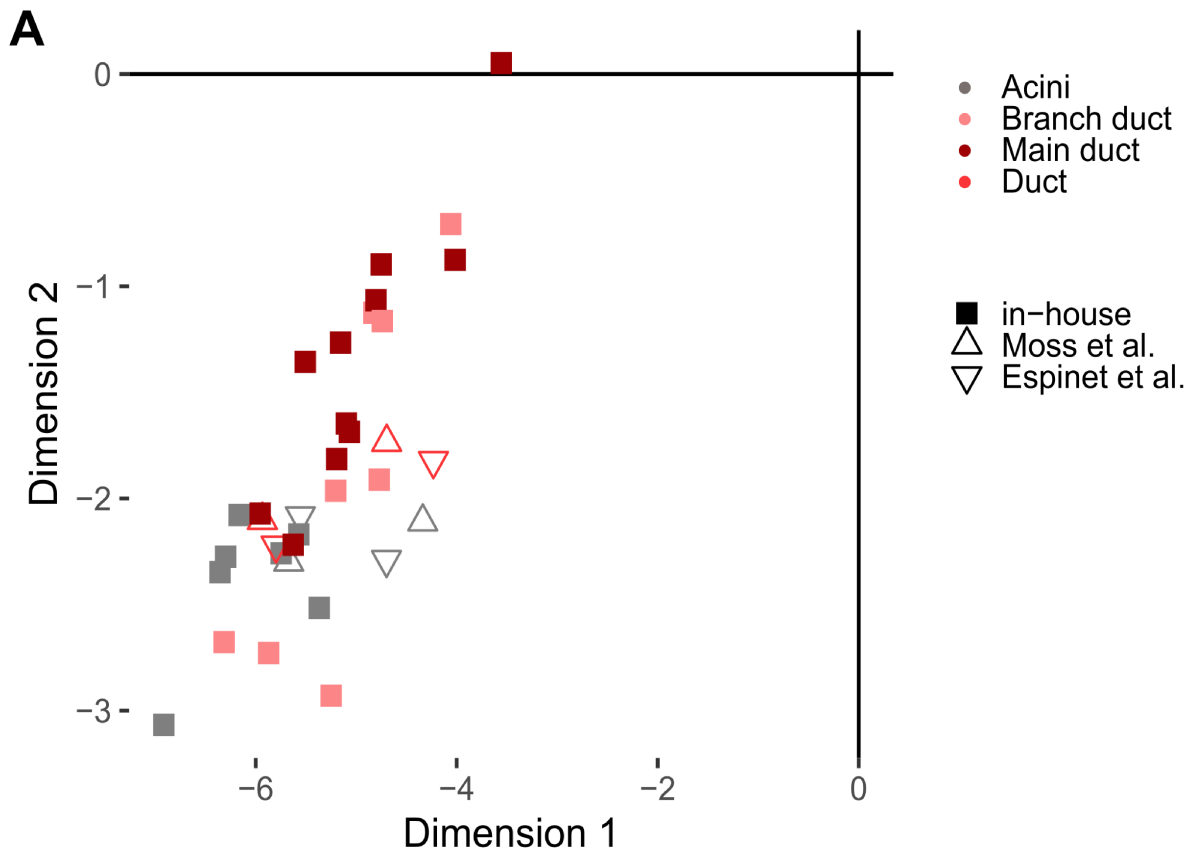


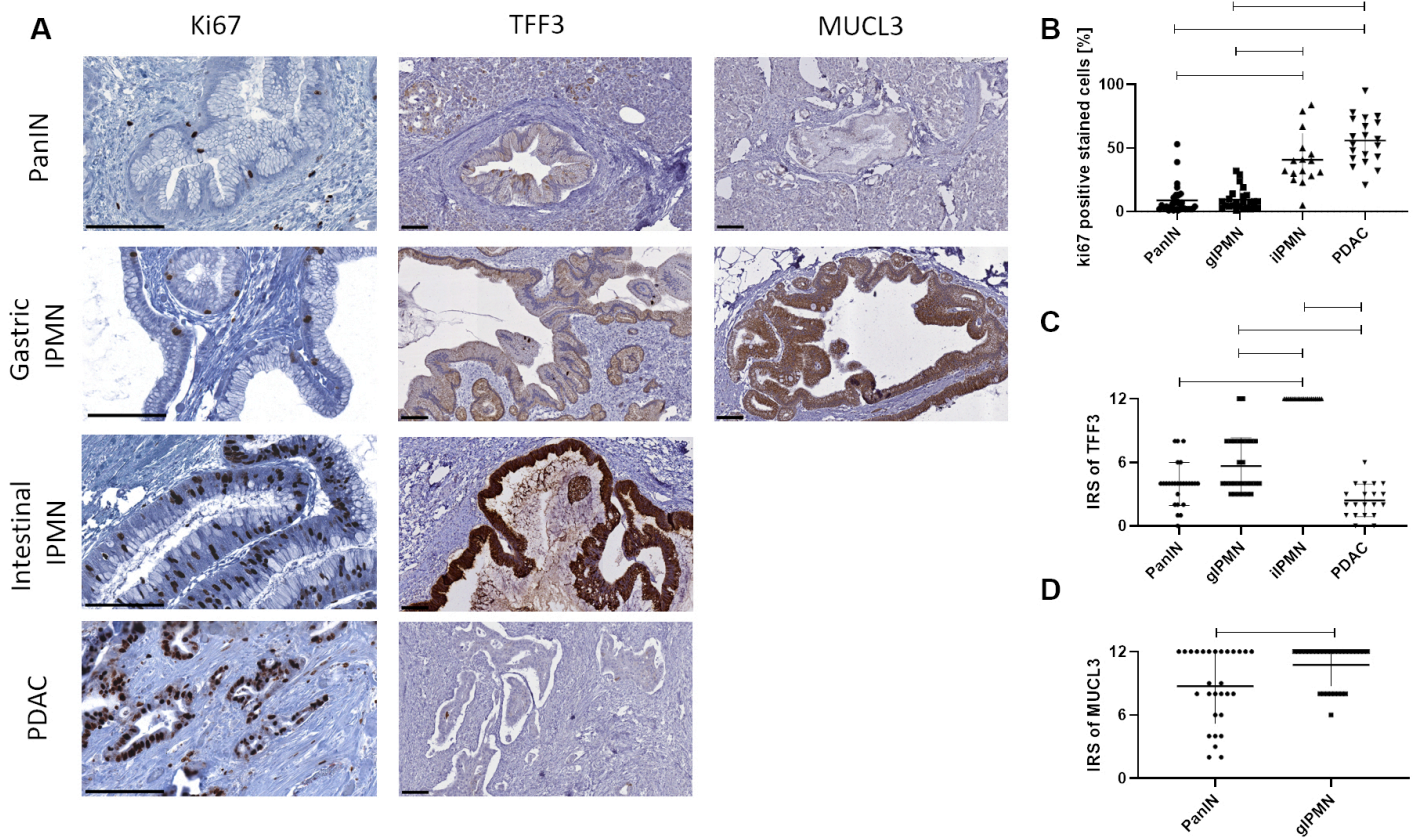


## Suppl. Figure 3.tif

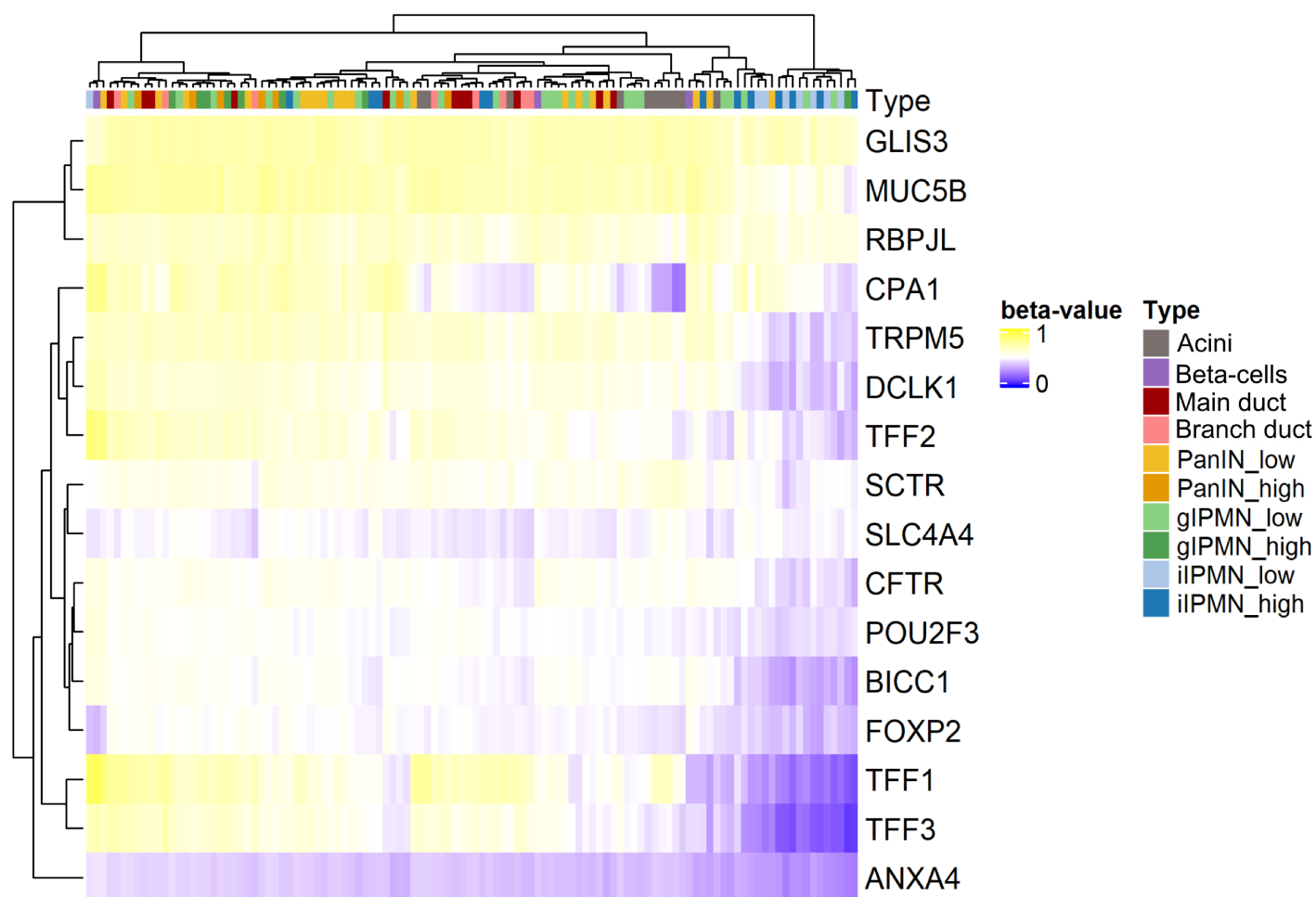


Layer



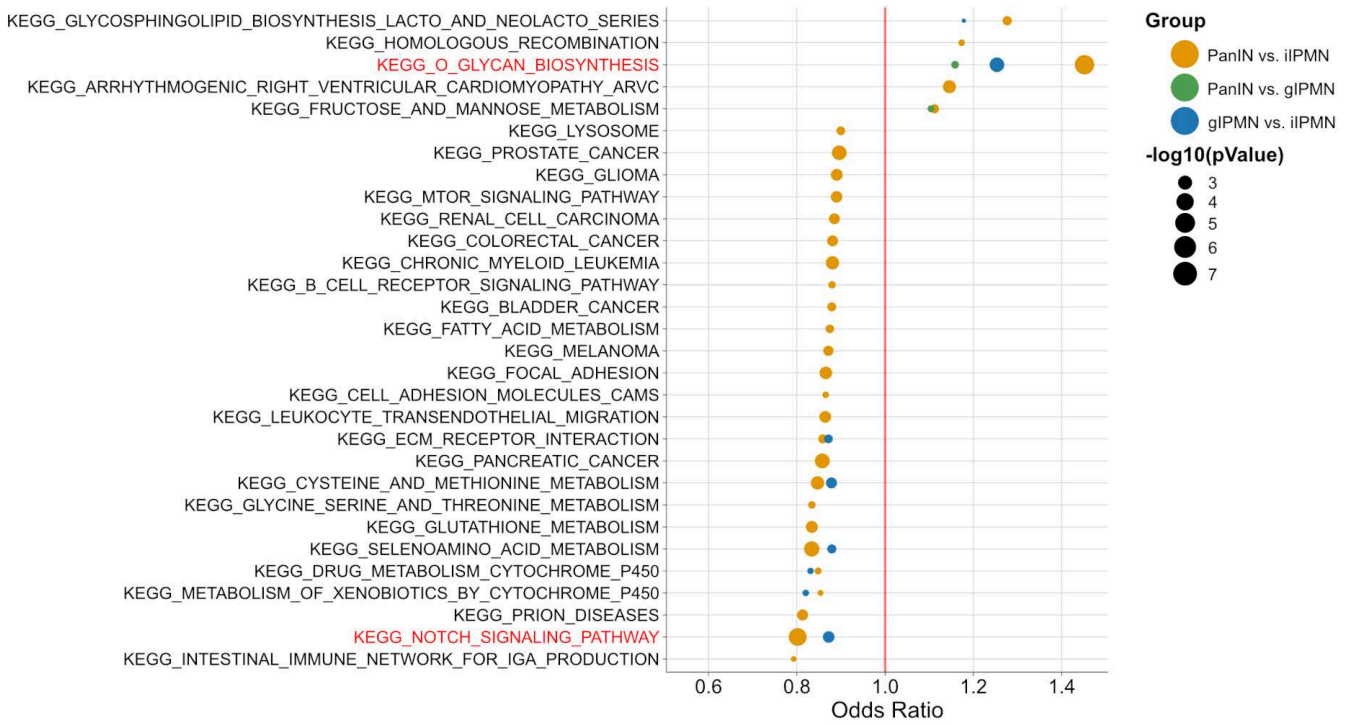


Layer

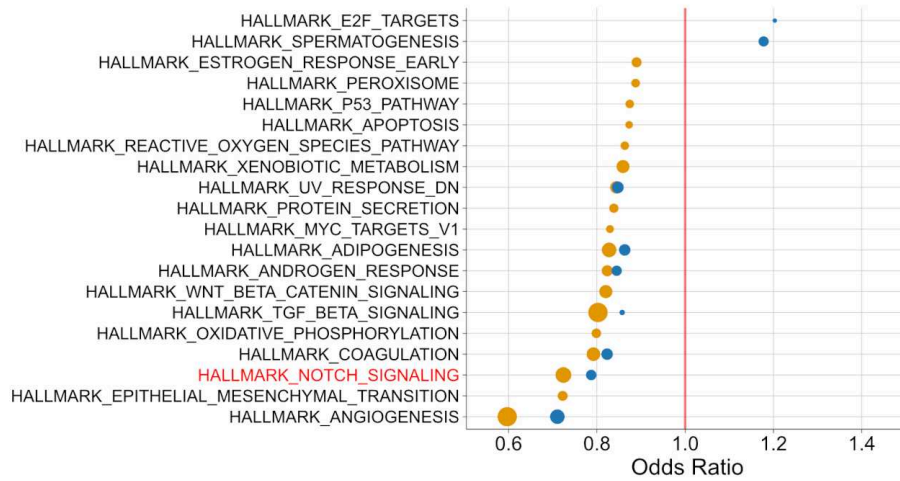


Suppl. Figure 7.tiff

**A**



**B**



## 1 Supplemental data

## 2 Methods

### 3 Immunohistochemistry

4 Staining was performed manually or using the Ventana BenchMark Ultra automated IHC/ISH  
5 slide staining system (Ventana Medical Systems Inc., Tucson, USA) (suppl. table 1a). The  
6 cytoplasmic expression of TFF3 and MUCL3 was evaluated using the immunoreactivity scoring  
7 system (IRS) based on staining intensity (0: negative, 1: mild, 2: moderate, 3: intense) and the  
8 percentage of stained cells (0: no positive cells, 1: <10% positive cells, 2: 10-50% positive cells,  
9 3: 51-80% positive cells, 4: >80% positive cells). The final score (0-12) was found by multiplying  
10 the positive cells proportion score (0-4) and the staining intensity score (0-3). The mean value  
11 of Ki67 proliferation rate of five randomly selected high power (40x) fields (HPFs) was  
12 calculated using the percentage of stained cells.

### 13 DNA/ RNA Isolation from FFPE samples

14 For genomic DNA or total RNA Isolation, 5-8 8- $\mu$ m-thick tissue sections were prepared, and  
15 lesions were dissected manually or by laser-capture microdissection (LMD), depending on  
16 their size to ensure adequate cellularity (>80%) for subsequent molecular analysis. For LMD,  
17 cresyl violet staining was done before using the Palm Microbeam System (Carl Zeiss,  
18 Oberkochen, Germany) according to the manufacturer's instructions. In some samples  
19 containing larger lesions, manual microdissection was used, as previously described.[1] The  
20 obtained cell clusters were isolated using the QIAamp DNA micro Kit or the GeneRead FFPE  
21 DNA Kit for DNA and the RNeasy FFPE Kit for RNA (all from Qiagen, Hilden, Germany) following  
22 the manufacturer's instructions. The genomic DNA quality control was performed by  
23 quantitative PCR using the Power SYBR™ Green PCR Master Mix on a StepOnePlus™ Real-Time  
24 PCR System. Quantification was performed with a self-designed primer assay (HML-2 for: 5'  
25 AAACGCCAATCCTGAGTGTC-3'; HML-2 rev: 5' CATAGCTCCTCCGATCCAT-3'). These primers  
26 are complementary to long terminal repeats (LTRs) of the HML 2 human endogenous  
27 retroviruses and have a length of about 115 bp.

## 1 Targeted NGS

2 A PDAC-Panel with two primer pools was created by the Ion AmpliSeq™ Designer (v5.6,  
3 ThermoFisher Scientific, Dreieich, Germany). The panel consists of 217 amplicons of 21 genes  
4 covering hot-spot mutational sites of 18 and the whole coding sequence of 3 (*ARID1A*, *TP53*  
5 and *RNF43*) additional genes relevant for PDAC (suppl. table 2). Barcoded libraries from gDNA  
6 (up to 10 ng per pool) were prepared using the Ion AmpliSeq Library kit 2.0 with Ion Xpress™  
7 Barcode adapters. The Ion library TaqMan™ Quantitation Kit was used for quantification of  
8 the libraries. The libraries were pooled and amplified in an emulsion PCR reaction using the  
9 Ion 520™ & Ion 530™ Kit-OT2. The resulting Ion Sphere particles (ISPs) were loaded on a 520™  
10 or 530™ Chip and sequenced on the Ion S5™ system (all reagents from ThermoFisher).

11 The results of the next generation sequencing from the Ion S5™ system were aligned to the  
12 human reference genome (GRCh37/hg19) using the S5 Ion Torrent Server VM (ThermoFisher).  
13 The Ion Reporter software (Version 5.12.0.0) was used for variant calling and annotations of  
14 the DNA panel sequencing. The parameters for variant calling were set equal for all samples.  
15 Following thresholds were defined: 3% allele frequency with a minimum coverage of 500 and  
16 a Phred Score of  $\geq 30$ . Detected variants were validated using the Integrative Genomics Viewer  
17 (IGV), ClinVar database from National Institutes of Health (NIH) and University of California  
18 Santa Cruz (UCSC) Genome Browser. Variants not present in the above mentioned databases  
19 were classified according to the American College of Medical Genetics and Genomics (ACMG)  
20 guidelines using the ACMG database (varsome.com; v7.3.7).[2]

## 21 Fusion transcript analysis

22 50 ng of isolated RNA were used for cDNA synthesis by QuantiTect Reverse Transcription Kit  
23 (Qiagen) and were subsequently subjected to library preparation using the Oncomine  
24 Comprehensive Assay Plus RNA (ThermoFisher) targeting over 1,300 isoforms of 49 tumor  
25 driver genes including approximately 200 known *BRAF* fusion transcripts. NGS was performed  
26 (as described above) and data analysis was done using the Oncomine Comprehensive Plus  
27 w2.1 - Fusion workflow implemented within the IonReporter Software package (V5.18;  
28 ThermoFisher).

## 29 Isolation of epithelial cells from the main pancreatic duct and from peripheral (branch) ducts

1 Specimens were obtained fresh from the operating theater and immediately subjected to  
2 gross examination. The main pancreatic duct was probed, and the specimen dissected by a  
3 pathologist along the probe. The main duct was then carefully dissected with a scissor and  
4 then fixed in 10% buffered formalin and embedded in paraffin. Peripheral tissue blocks were  
5 prepared, and branch-ducts were isolated by LMD, as described above. DNA extraction was  
6 performed as described above.

### 7 **Generation of $\beta$ -cells**

8  $\beta$ -cell populations from FFPE tissue were generated from 50- $\mu$ m-thick sections. Tissue sections  
9 were dewaxed with xylol and rehydrated in descending ethanol concentrations. Antigen  
10 retrieval was done at 80°C for one hour in a pressure cooker before tissue was digested with  
11 1% (w/v) collagenase Ia (Sigma, Steinheim, Germany) and 1%(w/v) dispase (Gibco, Grand  
12 Island, USA) for 45 min at 37°C to obtain single cells. The cell suspension was subsequently  
13 filtered (30  $\mu$ m mesh) and the cells were collected by centrifugation. Single cells were stained  
14 Insulin (Abcam, Cambridge, UK; 1:200). The stained cells were sorted with a BD FACS Aria™  
15 III System. DNA was isolated from the sorted cells as described above.

### 16 **Transcriptome analysis**

17 After total RNA isolation, the samples were shipped to Macrogen (Seoul, Korea) for  
18 sequencing. Libraries from total RNA were prepared using the Illumina TruSeq™ Stranded  
19 mRNA Library Prep kit and sequenced with 2 x 100 bp on the Illumina NovaSeq 6000 (Illumina  
20 Inc, San Diego, USA). The raw data processing of the transcriptome data was performed by  
21 Macrogen. Briefly, adapter and low-quality base trimming was carried out with Trimmomatic  
22 (v0.38).[3] Trimmed reads were mapped against the GRCh38/hg38 human reference genome  
23 using the Bowtie2 (v2.3.4.1) aligner.[4] Afterwards, the aligned reads were assembled with  
24 Cufflinks (v2.2.1).[5] After assembly the abundance of gene was calculated in read counts per  
25 gene. Before differential gene expression analysis lowly expressed genes were filtered from  
26 the data set. Therefore, genes which showed a lower read count as 0.5 transcripts per million  
27 reads and were missing in more than one sample per group were excluded from further  
28 analysis. The filtered raw count matrix was normalized and batch-corrected using the DESeq2  
29 package (v3.14).[6] Finally, differentially expressed genes were calculated pairwise and  
30 defined as followed  $\log_2$  fold change of  $< -1$  and  $> 1$ , respectively, and the significance level of

1 the adjusted p-value was set to < 0.05. PCA, heatmap and expression plots were calculated  
2 based on the variance stabilizing transformation output of DESeq2

### 3 **Pathway analysis**

4 Gene set enrichment analysis

5 For methylation data, enrichment of KEGG terms was estimated for all differentially  
6 methylated probes (DMP) in a pair-wise manner. DMPs were defined as displaying a beta  
7 value change of 0.4 and an adjusted p-value < 0.05. Gene set enrichment was calculated with  
8 the gometh function of the missMethyl package (v.1.26.1).[7]

9 The single sample Gene Set Enrichment Analysis (ssGSEA) was performed only for RNA seq  
10 derived data. Briefly, the normalized enrichment scores (NES) were calculated on the variance  
11 stabilized transformation data with the GSVA package (v.1.40.1).[8] Differentially activated  
12 gene sets were calculated between the different precursor lesions as described by Larsen *et*  
13 *al.* with a p-value of < 0.05.[9]

14 VIPER analysis

15 The activation of transcription factors was calculated with the VIPER algorithm (v1.26.0).[9]  
16 For the analysis, the paad regulon was taken from the arcane.networks package (1.18.0).  
17 Activated transcription factors were defined as displaying a p-value < 0.005 and a NES score  
18 of >3 or >-3.

### 19 **Statistical analysis**

20 Statistical analysis was performed using the GraphPad Prism 8 software (GraphPad Software  
21 Inc., San Diego, USA) or R v. 3.6.0 (R Core Team 2018). Statistical significance in  
22 immunohistochemistry was determined by Kruskal-Wallis test with Dunn's multiple  
23 comparison test. Results are presented as means  $\pm$  standard error of the mean (SEM). P values  
24 less than 0.05 were considered statistically significant (\* p< 0.05; \*\* p < 0.01; \*\*\* p<0.001).

## 1 References

- 2 1 Schlitter AM, Born D, Bettstetter M, *et al.* Intraductal papillary neoplasms of the bile  
3 duct: Stepwise progression to carcinoma involves common molecular pathways. *Mod*  
4 *Pathol* 2014;27:73–86.
- 5 2 Richards S, Aziz N, Bale S, *et al.* Standards and guidelines for the interpretation of  
6 sequence variants: a joint consensus recommendation of the American College of  
7 Medical Genetics and Genomics and the Association for Molecular Pathology. *Genet*  
8 *Med* 2015;17:405–24.
- 9 3 Bolger AM, Lohse M, Usadel B. Trimmomatic: a flexible trimmer for Illumina sequence  
10 data. *Bioinformatics*. 2014;30:2114-2120.
- 11 4 Langmead B, Salzberg SL. Fast gapped-read alignment with Bowtie 2. *Nat Methods*  
12 2012;9:357-9.
- 13 5 Li H, Handsaker B, Wysoker A, *et al.* The sequence alignment/map format and  
14 SAMtools. *Bioinformatics* 2009;25:2078-9.
- 15 6 Love MI, Huber W, Anders S. Moderated estimation of fold change and dispersion for  
16 RNA-seq data with DESeq2. *Genome Biol* 2014;15:550.
- 17 7 Phipson B, Maksimovic J, Oshlack A. missMethyl: an R package for analyzing data from  
18 Illumina's HumanMethylation450 platform. *Bioinformatics* 2016;32:286-8.
- 19 8 Hänzelmann S, Castelo R, Guinney J. GSEA: gene set variation analysis for microarray  
20 and RNA-seq data. *BMC Bioinformatics* 2013;14:7.
- 21 9 Larsen BM, Kannan M, Langer LF, *et al.* A pan-cancer organoid platform for precision  
22 medicine. *Cell Rep* 2021;36:109429.
- 23 10 Alvarez MJ, Shen Y, Giorgi FM, *et al.* Functional characterization of somatic mutations  
24 in cancer using network-based inference of protein activity. *Nat Genet* 2016;48:838-  
25 47.

26

1 **Supplementary tables**2 **Supplementary table 1a: Antibodies and protocols for immunohistochemistry.**

Antibody	Type	Dilution	Antigen Demasking	Source
Anti-MUC1	Mo Mono	1:100	CC1	Biocare
Anti-MUC2	Mo Mono	1:100	CC1	Dako
Anti-MUC5AC	Mo Mono	1:1000	CC1	Chemicon
Anti-CDX2	Mo Mono	1:40	CC1	BioGenex
Anti-MIB1	Mo Mono	1:100	CC1	Dako
Anti-TFF3	Rb Mono	1:2000	EDTA buffer pH 9	Abcam
Anti-MUCL3	Rb Poly	1:500	Citrate buffer pH 6	LSBio

3 \*Rb: rabbit. Mo: mouse Mono: monoclonal. Poly: polyclonal. CC1: Cell Conditioning 1 (Ventana Medical System, Tucson, AZ,  
4 USA).

5 **Supplementary table 1b: Tissue collective used for Ki67, TFF3 and anti-MUC13 staining.**

Type of lesion	Number of lesions
<b>PanIN</b>	<b>31</b>
Low grade	26
High grade	5
<b>Gastric IPMN</b>	<b>28</b>
Low grade	20
High grade	8
<b>Intestinal IPMN</b>	<b>20</b>
Low grade	9
High grade	11
<b>PDAC</b>	<b>24</b>

6

## 1 Supplementary table 2: Genes and amplicons in targeted NGS.

Gene Symbol	Chr	Ion AmpliSeq Fwd Primer (5'-3')	Ion AmpliSeq Rev Primer (5'-3')	Amplicon ID
ALK	chr2	TCTCTCGGAGGAAGGACTTGAG	GCCCAGACTCAGCTCAGTTAAT	CHP2_ALK_1
ALK	chr2	ACAGGGTACCAGGAGATGATGTAAG	GGAAGAGTGGCCAAGATTGGA	CHP2_ALK_2
APC	chr5	GAGAGAACGCGGAATTGGTCTA	GTATGAATGGCTGACACTTCTCCA	CHP2_APC_1
APC	chr5	AGCACTGATGATAAACACCTCAAGTT	ATCTTCTTGACACAAAGACTGGCT	CHP2_APC_2
APC	chr5	TTCAATATCATCTTTGTCATCAGCTGAA	TTTGGTTCTAGGGTGTGTGAC	CHP2_APC_3
APC	chr5	GCAGACTGCAGGGTTCTAGTT	GTGAAGTACAGAAAGTACATCTGCT	CHP2_APC_4
APC	chr5	AGCCCCAGTGTCTCCAGATA	CCCTCTGAAGTGCAGCATTACT	CHP2_APC_5
APC	chr5	AGAGGGTCCAGGTTCTCCA	TCATTTCTGAACTGGAGGCATT	CHP2_APC_6
APC	chr5	ATGAAACAGAATCAGAGCAGCCTAAA	CGTGATGACTTTGTTGGCATGG	CHP2_APC_7
ARID1A	chr1	CAAAATGAACAACAAGGCAGATGGG	TCAGAGACTATCTAGTCCGGTGTCT	ARID1A_10.112972
ARID1A	chr1	CAGCTAACTTACTGGACTTGAGAATTTTT	GAGTCAAGACAAAAATCACTACCTTGG	ARID1A_10.135473
ARID1A	chr1	CATGATGGGAACTGGACCTCCTTA	TTAGCTGTGATGTGACTCTGAAGAAAT	ARID1A_10.143283
ARID1A	chr1	CCCCAGCCTACGGCTTC	CCCCCGTAGGGCTCCA	ARID1A_1.1.15178
ARID1A	chr1	CCTAGGCCCGCCCTGA	GGCTCCGGCCGTAGGGT	ARID1A_1.1.16654
ARID1A	chr1	CAGTCAAGAGACTTCTGAGACCCTTA	CAGATAACGGTCCACCCACATC	ARID1A_11.181180
ARID1A	chr1	CCGCTGGGAAAGGAGCTG	GCCTAGGGCCCGCTTC	ARID1A_1.1.20289
ARID1A	chr1	CTATGCCTCTATGTGTCTGTGAAG	GTACCACATGAAGCCAGTGAGTAC	ARID1A_11.248116
ARID1A	chr1	ACAACTCTACTACCCAACC	CTGCTGAGCGAAGGACGA	ARID1A_1.1.2481
ARID1A	chr1	CTCCAGAAATCCAGTTCTTCTACTACA	ATAGAGGTCCAGAGGTTTCTACC	ARID1A_11.279375
ARID1A	chr1	CTCAGCAGGCTTCGGG	GGGCCCGCCACTGTAGT	ARID1A_1.1.36612
ARID1A	chr1	CTCGGAGCTGAAGAAAGCCG	GCTCTCGGCCCGCTCT	ARID1A_1.1.38056
ARID1A	chr1	GAGCCGTCTGCCGTCG	GGAGTGTACTGGTGGTTGGG	ARID1A_1.1.42139
ARID1A	chr1	GGCCCCAGCAGAAGCTCTCAC	AGCCCGGAGTGCCACCTC	ARID1A_1.1.52554
ARID1A	chr1	GGCTGCCGGCTCCAAGC	GCTGGCGACGTGAGCA	ARID1A_1.1.54514
ARID1A	chr1	GGGATCATGGCCGCGCA	CCGGCGGCTGCCTTCAT	ARID1A_1.1.54590
ARID1A	chr1	TTATCTGGCCTTCACTGAGGAGAA	CTCACCTGAGTCAATCCACCAAT	ARID1A_11.550938
ARID1A	chr1	AGCCGGACTGAAGAAGCTCG	GGCCCGGCTGAGTGAG	ARID1A_1.1.6484
ARID1A	chr1	CTCGCCCGGACCCCTCAG	GCCAGACAATGGCAGCTCC	ARID1A_1.2.19161
ARID1A	chr1	GGGTACCAGGGCTACCC	GGGCTCATGGGCGCTG	ARID1A_1.2.26067
ARID1A	chr1	GATATACCTCGACTCCTTTGGTTTGG	AGGGTCTTCTCCCGTTCAAT	ARID1A_12.293039
ARID1A	chr1	GCCAGCTCCTTGAAAAGCAGTATATC	GACCCATCCTTACCAGGAGAG	ARID1A_12.311881
ARID1A	chr1	AGACATCTTTCAGCTGTCTGATT	CACAGATCCTTGGCATATCCTGTTG	ARID1A_12.73402
ARID1A	chr1	CCGGCGGACATGGCCTC	CCTCCCACTCAGCTGTGTA	ARID1A_1.2.9363
ARID1A	chr1	CTCAACTTGTATCTCTGTCCACAGC	CTGCTCTGGCCTTACCTCATG	ARID1A_13.224100
ARID1A	chr1	CTCCTGCGTGTCTTTGTTATATTGG	TGGAGTCATGGAATCCGCTT	ARID1A_13.228066
ARID1A	chr1	GAGGAGACTTAAAGCCACCAACTC	CAAGGAGTCCCATGCACTTATCT	ARID1A_13.262576
ARID1A	chr1	GCCTTGTAGATCCTCTGCTAAGAAG	GCCCTGCATAGATCCTGATCC	ARID1A_13.286741
ARID1A	chr1	CTTAATGATGGAAGTACTCCACATTC	CAAGTCAAATAGCAATCAGATCAGTCA	ARID1A_14.234479
ARID1A	chr1	TGACTCAAACCTGGGTATCA	CATTTCACTGGCCCTGTCTTACG	ARID1A_14.440936
ARID1A	chr1	GACCACGACAGCACTATCCCTA	TCATGTTCCCTCAGGCCCTATT	ARID1A_15.209989
ARID1A	chr1	TCACCCTTGCCTTTCTACG	TCACTGTGCATAAGGACCTCCA	ARID1A_15.321878
ARID1A	chr1	CCAATTTTGTAGGACGGAGCCT	CACCGAGACCAGGCTTACTC	ARID1A_15.99688

ARID1A	chr1	CTAATCCTGTGTTCTTTGCCTCCT	TTTTCAAGGCGAACCTGCATG	ARID1A_16.147847
ARID1A	chr1	GGATGTATTCTCCTAGCCGCTAC	TTGGGTGGAGAACTGATTGCCATA	ARID1A_16.243588
ARID1A	chr1	AGCGTGCCATACAGCACT	GGCAGTGGCAGGATAGGCA	ARID1A_18.122838
ARID1A	chr1	AACCGCACCTCTCCTAGC	TCCCGCGAATCATGGG	ARID1A_18.17117
ARID1A	chr1	CAGATGAAATGCTGCACACAGATC	GATACCTGAGGAATGTGATTCTGCAT	ARID1A_18.249269
ARID1A	chr1	CAGGTATCCAGCCCTGCTC	TGCTATGTGCGAGGCAGGT	ARID1A_18.260793
ARID1A	chr1	CCACTGCCACAGCTGCTAC	GCTGAGCAACCTCAGCTGAT	ARID1A_18.303487
ARID1A	chr1	AAGGCTCGTGGCCTTCCC	GTGCGGTTCTCCATTGGC	ARID1A_18.33212
ARID1A	chr1	CTGTGTCCACCAAGCATCTGG	GGCACGCTGTACATCTCC	ARID1A_18.457891
ARID1A	chr1	GCAAACATGCCACCACAAATGATG	TGTTCCGGTTCACGCCATGATAG	ARID1A_18.536845
ARID1A	chr1	GCCTTCCCCTCAGCAAGATGTATA	GGTCTCGGCCAAACTGGAATG	ARID1A_18.584475
ARID1A	chr1	ACATAGCACCTGCCCTGT	GGGCAGATTAGGCAACCGAATG	ARID1A_18.63843
ARID1A	chr1	TGCTCAGCAAGGCACCATG	CGAGCCTTCGTGGTTGG	ARID1A_18.820768
ARID1A	chr1	TTGTCTCTGCCTTAGAATTACAAGCG	GCTGGGCAGCTTGTGCT	ARID1A_18.880618
ARID1A	chr1	AGACGACATGGAGGTTTATTCAGG	CCCAGGCACTGATACTCA	ARID1A_19.54023
ARID1A	chr1	ATCTTCAGAGTAGCTTCACTGATGGG	GTTGATGGTATCTAATGCCATGTG	ARID1A_19.79292
ARID1A	chr1	CAACATCCTGCTGTATGATGACAAC	GGCATGGAAGATATCTACAAGAGAGAAA	ARID1A_19.96133
ARID1A	chr1	ATCCTGGGAGGTTTCAGCAA	GAAGCTGGCTTGCCTTGC	ARID1A_20.1.247050
ARID1A	chr1	CCAGTTCAGAGAATAGTGAGGA	GCAGCAGGCCACTGTCAAA	ARID1A_20.1.351511
ARID1A	chr1	CCCTCGGAAGCATGTGACAAC	CTTGATGGCCTCTGAACCTTAGC	ARID1A_20.1.374770
ARID1A	chr1	CCTGCTGCACTGGCGGAT	GGCCCTCCTGGTCTGTTG	ARID1A_20.1.397870
ARID1A	chr1	CGAAGCCTGTCAATTTGTGCCA	GTTAGTGGTGCCTGCTTCCG	ARID1A_20.1.400147
ARID1A	chr1	CTGTTCTTAGGCCACTTTTCTCC	CCCAGGATCCAGTAGCGTT	ARID1A_20.1.464959
ARID1A	chr1	GAGGAAGTAGTTGAAAATGATGAGGAGA	TCCACCACAAATGGATCATTCTTCTGTA	ARID1A_20.1.565326
ARID1A	chr1	GCAGCAAGTTTCCATTGGCATTAG	AGGCTTCGAATGGTATTGGACAC	ARID1A_20.1.612574
ARID1A	chr1	GCCTGATTGAGATCTTTGGCATTAAAA	ACTTCTCTTCTTCTTCTTCTTAGTTTA	ARID1A_20.1.637352
ARID1A	chr1	GGGCCCCACCTGATGGA	GTTCCGGTGGCTCTGTGC	ARID1A_20.1.733579
ARID1A	chr1	GTGGTGGACTGCTCAGATAAGCT	AGCTCTGTCTTGTCTCGAAGT	ARID1A_20.1.787955
ARID1A	chr1	ACCGGAACATCAAGATCCTAGAG	CCCTGGGTGTTGGACATC	ARID1A_20.1.90003
ARID1A	chr1	ATGGTGCGCTTCTCAGT	CGGCAAGGCTGCTCTAG	ARID1A_20.2.152846
ARID1A	chr1	CAGTGCAAGAGGCGAGTATCG	CCGCATCATGTCCACACTAGTTG	ARID1A_20.2.222602
ARID1A	chr1	CCACTAATTATGAAAAGGAGGAGGAA	CCCGAGATGTTGGCGAGTGTA	ARID1A_20.2.247152
ARID1A	chr1	CCTTGCCGCCACACAGTT	CAACAGCCGTGATTCTGACA	ARID1A_20.2.313338
ARID1A	chr1	CTTGAGATGCTCCGGGAA	AGGGCAAACTGCCAGTGTA	ARID1A_20.2.409280
ARID1A	chr1	CTTCAGCTGAAGCCAGGAC	CGACCATAGTGTATACAACCTTCT	ARID1A_20.2.432258
ARID1A	chr1	AAACTCAGCATCCAGGACAACAAT	GCCAGGTTGGCCAGCAGTA	ARID1A_20.2.5295
ARID1A	chr1	ACCCAGGGCTGCTGCTCAT	TCTCAAGCAGTCCCACCA	ARID1A_20.2.54967
ARID1A	chr1	GGCTGTTGGACATCTCGGT	GTTTTGCATAAATAAGGGCAACAGTC	ARID1A_20.2.603909
ARID1A	chr1	GGGCAGTTGGACCTATCTCCATAC	CTGAGTTTGTGAGGGTTTCAA	ARID1A_20.2.613243
ARID1A	chr1	TGGACGAGAACCCTCAGAGTTTAC	GCTGTCTGACTGGCAATCAAAA	ARID1A_20.2.760156
ARID1A	chr1	CATGGGCGGCTCTTATAC	TAGTAGCACTGTAAATTAAGTCCCA	ARID1A_2.198073
ARID1A	chr1	CTAACCCATACTCGCAGCAACA	TCACAATCACCATCTACTGCTG	ARID1A_2.263887
ARID1A	chr1	GCCATCCAGTCCAATGGATCAG	CCTGCATGGTCTCGGGTAC	ARID1A_2.310812
ARID1A	chr1	AAACTGTGTACTTGGGTTATATATTCAGT	CCATATGGCTGAGGTTCTCATCTTG	ARID1A_2.6808
ARID1A	chr1	AGTCCAGCAAACCTGCCTATTC	ACCCAGAGTTAATTGGTCTTAAGTG	ARID1A_3.115759

ARID1A	chr1	CAGCAAAGTCTCACCTCAG	GGGATGGCTGCTGGGAGTAT	ARID1A_3.189854
ARID1A	chr1	CAGCCTCCACATCAGCAGTC	AGCCTGCTGGGAGAGCGT	ARID1A_3.203145
ARID1A	chr1	CAGGCTCAGTCTCCTTACCA	GCAGGAGGCAGGGATATCTT	ARID1A_3.210697
ARID1A	chr1	TGCTTCTATACTCATCATCAGTGCAT	CTTTGCTGGTTGTAATATGGAGTCTG	ARID1A_3.663071
ARID1A	chr1	TTTTCTTTCTACAGATTCCTCCTT	CTGCTGCTGATACGAAGGTTG	ARID1A_3.701387
ARID1A	chr1	AGCAGCAGCCACAGTCTCAA	TGAGCCTGTGGCTGTGAGTA	ARID1A_3.77267
ARID1A	chr1	CCATCACAGCTTTTGTCTTTCTGTGTAG	ACCTTCAGAAGGTGCAGAAATACT	ARID1A_4.173246
ARID1A	chr1	CTGGCCTTACATAATACTTTTCGC	GATGCCTGAGACCCAAATGAATC	ARID1A_4.215850
ARID1A	chr1	GAGGGCAAGAAGATATGAACCTGAG	AGGTCAAATTAGCTAAACTTCCAACCA	ARID1A_4.255932
ARID1A	chr1	GAGTCTGGAGTGAGCACATC	CGAGAGTGGTCTGAGCGA	ARID1A_5.220317
ARID1A	chr1	AGAATCTTCTGCCTAATATACTAATCCATG	AGGAGACTGAGCTGGATTACTCT	ARID1A_5.34011
ARID1A	chr1	AGTCTCTTTCTCTCCTACACT	CAGTCACTTTCCCTCTCCCTAA	ARID1A_5.70816
ARID1A	chr1	GATATGCTTATGTTGTTCTTTGTCTGGA	CACTCAAATGTCTGCCCTAGCTC	ARID1A_6.227771
ARID1A	chr1	AGCCATTTCTAGCTCTGAATTAACCTCC	TCGATCTTGGGCAATGCTTGAT	ARID1A_6.45476
ARID1A	chr1	CAGCCTTATCTCCGCGTCAG	ACTGTTTTCTCTCACCCTGAT	ARID1A_7.149596
ARID1A	chr1	CAGGATAAGGATGGAGAGCATTGTTC	TGTGTATCTGTCTCCGGAA	ARID1A_7.152412
ARID1A	chr1	CATGGCCAATATGCCACCTCA	ATAATACATTTCTTGCACTGACACCCT	ARID1A_8.210031
ARID1A	chr1	CCAATGCCAACTACCCAGTG	GGCCATGTTAGGGCCATAAGG	ARID1A_8.229785
ARID1A	chr1	GTTGCTAGTGAGTGACTAACCAAGTC	GGCTGTCCATGCATTTGACCTC	ARID1A_8.517555
ARID1A	chr1	AGGATGAGTCACGCCTCCATG	GGCCTTACCTGTTTTGGATAGAGTTG	ARID1A_8.91537
ARID1A	chr1	AGCACTATTTGGCTCCAGTTCAAATC	GGTTGATCATGCCAGCCATACTATTA	ARID1A_9.65769
BRAF	chr7	CATACTTACCATGCCACTTTCCCTT	TTTCTTTTCTGTTGGCTTGACTTGA	CHP2_BRAF_1
BRAF	chr7	CCACAAAATGGATCCAGACAACGT	GCTTGCTCTGATAGGAAAATGAGATCTA	CHP2_BRAF_2
CDKN2A	chr9	CACCAGCGTGTCCAGGAA	CCCTGGCTCTGACCATTCTGT	CHP2_CDKN2A_1
CDKN2A	chr9	CATCTATGCGGGCATGGTACT	CGCTGGTGGTGTCTG	CHP2_CDKN2A_2
CTNNB1	chr3	ACTGTTTCGTATTTATAGCTGATTTGATGGA	CCTCTTCTCAGGATTGCCTTT	CHP2_CTNNB1_1
EGFR	chr7	CCTCATTGCCCTCAACACAGT	TCAGTCCGGTTTTATTGTCATCATAGTT	CHP2_EGFR_1
EGFR	chr7	CACCAGTACCAGATGGATGT	CCCAAAGACTCTCCAAGATGGGATA	CHP2_EGFR_2
EGFR	chr7	AGACATGCATGAACATTTTTCTCCAC	TCCAGACCAGGGTGTGTTTTTC	CHP2_EGFR_3
EGFR	chr7	TGTGGAGCCTTTACACCCA	GTGCCAGGGACCTTACCTTATAC	CHP2_EGFR_4
EGFR	chr7	ACGTCTTCTCTCTCTGTCA	CTGAGGTTCAGAGCCATGGA	CHP2_EGFR_5
EGFR	chr7	CATGCGAAGCCACTGAC	ACATAGTCCAGGAGGCA	CHP2_EGFR_6
EGFR	chr7	GACTATGTCCGGGAACACAAGA	CCCATGGCAAACCTTGCTA	CHP2_EGFR_7
EGFR	chr7	CGCAGCATGTCAAGATCACAGAT	GCATGTGTTAAACAATACAGCTAGTG	CHP2_EGFR_8
FBXW7	chr4	TGACAATGTTTAAAGTGGTAGCTGTT	ACTCATTGATAGTTGGAACCAACACA	CHP2_FBXW7_1
FBXW7	chr4	CCTGTGACTGCTGACCAAACCTTTTA	CACATCTTCTTATAGGTGCTGAAAGG	CHP2_FBXW7_2
FBXW7	chr4	CCCAACCATGACAAGATTTTCCC	GGTCATCACAATGAGAGACAACATCA	CHP2_FBXW7_3
FBXW7	chr4	ACTAACAAACCCTCTGCCATCATA	TCTGCAGAGTTGTTAGCGGTT	CHP2_FBXW7_4
FBXW7	chr4	GTAGAATCTGCATTCCAGAGACAA	TCTCTTGATACATCAATCCGTGTTTGG	CHP2_FBXW7_5
FGFR2	chr10	CATCACTGTAACCTTGACAGACAAAC	TGGTCTCTCATTCTCCCATCCC	CHP2_FGFR2_1
FGFR2	chr10	CATCCTCTCTCAACTCCAACAGG	AGTGGATCAAGCACGTGGAAAA	CHP2_FGFR2_2
FGFR2	chr10	GCTTCTTGGTCTGTCTTCTTCTT	CTCCTCTGTGATCTGCAATCT	CHP2_FGFR2_3
FGFR2	chr10	TGGAAGCCAGCCATTTCTAAA	GATGATGAAGATGATTGGGAAACACAAG	CHP2_FGFR2_4
GNAS	chr20	TTGGTGAGATCCATTGACCTCAATTT	TGAATGTCAAGAAACCATGATCTCTGTT	CHP2_GNAS_1
GNAS	chr20	CCTCTGGAATAACAGCTGTCC	TGATCCCTAACAAACACAGAAGCAA	CHP2_GNAS_2

IDH1	chr2	CCAACATGACTTACTTGATCCCCAT	ATCACCAAATGGCACCATACGA	CHP2_IDH1_1
IDH2	chr15	ACCCTGGCCTACCTGGTC	AGTTCAAGCTGAAGAAGATGTGGAA	CHP2_IDH2_1
KRAS	chr12	CAAAGAATGGCTCGCACCAGTAATAT	AGGCCTGCTGAAAATGACTGAATATAA	CHP2_KRAS_1
KRAS	chr12	TCCTCATGTACTGGTCCCTCATT	GTAAAAGGTGCACTGTATAATCCAGACT	CHP2_KRAS_2
KRAS	chr12	CAGACTGTATTTATTTTCAGTGTACTTACCT	GACTCTGAAGATGTACCTATGGTCTTA	CHP2_KRAS_3
NRAS	chr1	CCTCACCTCTATGGTGGGATCATAT	GTTCTTGCTGGTGTGAAATGACTG	CHP2_NRAS_1
NRAS	chr1	TTGCCTGTCTCATGTATTGG	CACCCCAGGATTCTTACAGAAAA	CHP2_NRAS_2
NRAS	chr1	GCACAAATGCTGAAAGCTGTACC	CAAGTGTGATTGCCAACAAAGGA	CHP2_NRAS_3
PIK3CA	chr3	CCATAAAGCATGAACATTTTAAAGAAGCAAGA	GGTTGAAAAAGCCGAAGGTACAC	CHP2_PIK3CA_1
PIK3CA	chr3	TGGAATGCCAGAACTACAATCTTTTGAT	AAGATCCAATCCATTTTGTGTGC	CHP2_PIK3CA_10
PIK3CA	chr3	TGGATCTCCACACAATTAACAGCAT	TGCTGTTTATGGATTGTGCAATTC	CHP2_PIK3CA_11
PIK3CA	chr3	CCCTTTTTAAAGTAATTGAACCAAGTAGGC	TTTAAGATTACGAAGGTATTGGTTAGACAGAA	CHP2_PIK3CA_2
PIK3CA	chr3	GACGATTTCCACAGCTACAC	AGCATCAGCATTTGACTTTACCTTATCA	CHP2_PIK3CA_3
PIK3CA	chr3	CATAGGTGGAATGAATGGCTGAATTATG	TCAATCAGCGGTATAATCAGGAGTTTTT	CHP2_PIK3CA_4
PIK3CA	chr3	TCCCATTATTATAGAGATGATTGTTGAATTTTCT	CAAAACAAGTTTATATTTCCCATGCCA	CHP2_PIK3CA_5
PIK3CA	chr3	GCTTTGAATCTTTGGCCAGTACCT	CATAAGAGAGAAGGTTTGACTGCCATA	CHP2_PIK3CA_6
PIK3CA	chr3	CAGAGTAACAGACTAGCTAGAGACAATGA	GCACTTACCTGTGACTCCATAGAAA	CHP2_PIK3CA_7
PIK3CA	chr3	CACGATCTTTTAGATCTGAGATGCACA	CCTTTGTGTTTTCATCCTTCTCTCTG	CHP2_PIK3CA_8
PIK3CA	chr3	GATGCAGCCATTGACCTGTTTAC	AGAAAACCATTACTTGTCCATCGTCT	CHP2_PIK3CA_9
PTEN	chr10	GCCATCTCTCTCCTCTTTTCTT	GCCGCAGAAATGGATACAGGTC	CHP2_PTEN_1
PTEN	chr10	TGTTAATGGTGGCTTTTGTGTTTGT	TCTACCTCACTCTAACCAAGCAGATAACT	CHP2_PTEN_2
PTEN	chr10	CCATAACCCACACAGCTAGAA	TGCCCGATGTAATAAATATGCACAT	CHP2_PTEN_3
PTEN	chr10	GGCTACGACCCAGTTACCATAG	TGCCACTGGTCTATAATCCAGATGAT	CHP2_PTEN_4
PTEN	chr10	TGAGATCAAGATTGCAGATACAGAATCC	ACCTTTAGCTGGCAGACCAC	CHP2_PTEN_5
PTEN	chr10	AGGTGAAGATATATTCTCCAATTCAGGAC	TTGGATATTTCTCCAATGAAAGTAAAGTAC	CHP2_PTEN_6
PTEN	chr10	CACTTTTGGGTAATACATTCTCATACCAGGA	TATACTGCAAATGCTATCGA	CHP2_PTEN_7
PTEN	chr10	GCAGTATAGAGCGTGCAGATAATGA	CATCACATACATAAGTCAACAACCC	CHP2_PTEN_8
RNF43	chr17	CCAAACACATCTGGAGCACACT	GCCTGACCCTCAATGACCTCTT	RNF43_1.100174
RNF43	chr17	CCGCTTTTGTAGTGGTGGT	TGACTTTGACCCCTAGTGTACT	RNF43_2.1.213215
RNF43	chr17	ACAACCACTGGCTGTGAA	GCACCCAGCTTCCAGATT	RNF43_2.1.22754
RNF43	chr17	CGGTGTCAGAATCCATTAGAAAG	GACAAGAGGCTGTACCAGAAA	RNF43_2.1.264668
RNF43	chr17	CTCTCCCTACCACCCACTT	GTGGTTGTGCTGACTCCTC	RNF43_2.1.277654
RNF43	chr17	CTGGGTGCACAGTTGCATC	CCCTGGCCAGTTGACG	RNF43_2.1.308947
RNF43	chr17	GAAACCTGGGTTTCCCTGT	GGGTCCATGGCAGCAGTTC	RNF43_2.1.342797
RNF43	chr17	AAAGTCACTGCTTAGGGAGCT	AGAAAGCTATTGCACAGAACGC	RNF43_2.1.4249
RNF43	chr17	GGGACCAAGGATATGCCACACT	TGCAAAAATCCAGCCTCTCTGC	RNF43_2.1.479773
RNF43	chr17	GGGCACTGTGGTTAGAGAG	AAAAGCGTTCCAGTGGCA	RNF43_2.1.483268
RNF43	chr17	GTGACTTGCTGATCAGGAGAAGGT	GTTTCCAGCCATGTCCACTACC	RNF43_2.1.554471
RNF43	chr17	TTTTTGCAAGTTGAACAGACTGCT	CAAGTACCAGATCCAATCAGC	RNF43_2.1.716452
RNF43	chr17	CTCCAGATCCACTGCTGTCA	TTCCCAAGAGCTGCACATC	RNF43_2.2.168519
RNF43	chr17	GTAGGCTGATGTCCGTGCAG	GCTTGCCAGTGCCCTTA	RNF43_2.2.335644
RNF43	chr17	GTGCTGTGAGGTGGATTGGAG	CCCACAGCTGGTCCCTT	RNF43_2.2.348341
RNF43	chr17	GTGATGCCGAGGGCCCAT	CAGGTGCAAGACTCCACCTC	RNF43_2.2.359855
RNF43	chr17	AGGTGGTAGTGGGATGGC	TGCTTTTCTGAATGCATTCTGTAGG	RNF43_2.2.62203
RNF43	chr17	CCTCTACTGTGATGTTGAACATG	CCTGATTCTGGCAATCCTATGG	RNF43_3.144168

RNF43	chr17	AAGCCACATTCTAGACCTGTCTG	CTCTTTTCTCCAGGACTACGG	RNF43_3.9926
RNF43	chr17	TCCTCCAGACAGATGGCACA	CCCAATCTGAGCCCCATTCT	RNF43_4.332752
RNF43	chr17	TTCAATCTCCCCAGTCTGGTCAT	AGCTGGCCACCAGGAGGTA	RNF43_4.381754
RNF43	chr17	TACTCCTTCTTCTCCCTAACCAC	ATGATGTGTGGATCCTAATGACAGT	RNF43_5.252108
RNF43	chr17	AAGCCAGGATGATCACAAGATGG	CTCAAGGGAACCTCCAGTTAGCTAT	RNF43_5.9080
RNF43	chr17	CCCTGAGAGCTTATCTCTCCATC	GACCTCAGCCCAACCTCTACT	RNF43_6.126819
RNF43	chr17	GTCTGGAGGTCTAGTGTGCT	TGGGCACCTTCCCCCTGTA	RNF43_6.251138
RNF43	chr17	ATCAGCTTCTCAGCGTCATTACC	CTGGATGGAGGAAGATAAAGCTCTCA	RNF43_6.62210
RNF43	chr17	CACAGGACAAAGTAGGGCTAAGTG	AAGCTGATGGAGTTTGTGTACAAGAA	RNF43_6.83735
RNF43	chr17	CCAGCTTGACGATGCTGATGAAT	TGGTACTCTCCCTAGAAAATGGAGAG	RNF43_8.145848
RNF43	chr17	GTGTAGGGCGAAGTGTGAGTC	CCTAACCCAAGTCTGTCTCTCTG	RNF43_8.334246
RNF43	chr17	ATTTCCACTTCTCTCAGACCAAGTCAT	CCTGTCACTGGCTAGCAAGGTA	RNF43_8.99948
RNF43	chr17	GCAAACACACCTTCCAAAGTGAGATT	TGGACGCACAGGACTGGTAC	RNF43_9.251835
RNF43	chr17	ACAAAAGAAGAAAGACATATTTCAAACAGATG	TTATCAGAGTGATCCCTTGAAAATGG	RNF43_9.43347
RNF43	chr17	AGCTTTCTGTCTGCTGATCTTCA	GTATGTATGGTTGAAGTGCATTGCTG	RNF43_9.83487
SMAD4	chr18	CTCATGTGATCTATGCCGCT	AGTCTACTTACCAATCCAGGTGATACA	CHP2_SMAD4_1
SMAD4	chr18	TGCTACTTCTGAATTGAAATGGTTCA	GATTACTACCATTACTCTGCAGTGTT	CHP2_SMAD4_2
SMAD4	chr18	ATGGTGAAGGATGAATATGTGCATGA	GCTGGTAGCATTAGACTCAGATGG	CHP2_SMAD4_3
SMAD4	chr18	GTGAAGGACTGTTGCAGATAGCAT	AAGGCCACATGGGTTAATTTG	CHP2_SMAD4_4
SMAD4	chr18	TTTCTTTAGGGCTTTCACAATGA	CTGAGAAGTGACCCATAATCCATT	CHP2_SMAD4_5
SMAD4	chr18	GCTCCTGAGTATTGGTGTCCAT	CCTGTGGACATTGGAGAGTTGA	CHP2_SMAD4_6
SMAD4	chr18	TGTAATTTCTTTTTCTTCTAAGGTTGCACATAG	ACTTGGGTAGATCTTATGAACAGCAT	CHP2_SMAD4_7
SMAD4	chr18	AGGCTTTGATTGCGTCAGTGT	GCTGGAGCTATCCACTACTG	CHP2_SMAD4_8
SMAD4	chr18	GCTGCTGGAATTGGTGTGATG	AGTACTCGTCTAGGAGCTGGAG	CHP2_SMAD4_9
STK11	chr19	GAGCTGATGTCGGTGGGTAT	CTCCGAGTCCAGCACCTC	CHP2_STK11_1
STK11	chr19	CTCCAGGCAGCTGCAA	CCGGTGGTGAGCAGCAG	CHP2_STK11_2
STK11	chr19	CCGGTGGCACCTCAA	CTGGTCCGGCAGGTGTC	CHP2_STK11_3
STK11	chr19	AACATCACACGGGTCTGTAC	GATGAGGCTCCACCTTCAG	CHP2_STK11_4
STK11	chr19	GAAGAAACATCCTCCGGCTGAA	ACCGTGAAGTCTGAGTGTAGA	CHP2_STK11_5
TP53	chr17	TCCACTCACAGTTTCCATAGGTCT	GTTGGAAGTGTCTCATGCTGGAT	CHP2_TP53_1
TP53	chr17	GGCTGTCCAGAATGCAAGAA	GATGAAGCTCCAGAATGCCA	CHP2_TP53_2
TP53	chr17	TGCACAGGGCAGGTCTTG	CCGTCTCCAGTTGCTTTATCTGT	CHP2_TP53_3
TP53	chr17	ACCAGCCTGTCTCTCT	GTGCAGCTGGGTTGATTC	CHP2_TP53_4
TP53	chr17	CCAGTTGCAAACAGACCTCA	AGGCCTTGATTCCTCACTGAT	CHP2_TP53_5
TP53	chr17	GGCTCCTGACCTGGAGTCTT	CTCATCTTGGGCTGTATTATCTC	CHP2_TP53_6
TP53	chr17	CGCTTCTGTCTGCTTCT	TTCTTTTTCTATCTGAGTAGTGGT	CHP2_TP53_7
TP53	chr17	GGAAGGGGCTGAGGTCACT	CCCCTCTCTGTTGCTGC	CHP2_TP53_8
VHL	chr3	CTCCAGGTCATCTTCTGCAAT	GTACCTCGGTAGCTGTGGATG	CHP2_VHL_1
VHL	chr3	GTGGCTTTTAAACCTTTGCT	GTCAGTACCTGGCAGTGTGATA	CHP2_VHL_2
VHL	chr3	GGCAAAGCCTCTTGTCTGTTTC	TGACGATGTCCAGTCTCTGTAAT	CHP2_VHL_3

1

1 **Supplementary table 3: Mutation profile of precursor lesions detected by targeted NGS.**

Grade	Gene	Sample	Variant	VAF [%]	Variant Effect	Transcript
low-grade PanIN	<i>ARID1A</i>	<b>113</b>	Gln802fs	4.83	frameshift/insertion	NM_006015.5
	<i>CDKN2A</i>	74	Arg58Ter	3.48	nonsense	NM_001195132.1
	<i>GNAS</i>	127	Arg201His	20.17	missense	NM_000516.5
	<i>KRAS</i>	52	Gly12Val	15.38	missense	NM_033360.3
		<b>55</b>	Gly12Val	9.66	missense	NM_033360.3
		<b>56</b>	Gly12Asp	6.13	missense	NM_033360.3
		69	Gln61His	4.08	missense	NM_033360.3
		74	Gly12Asp	12.05	missense	NM_033360.3
		<b>111</b>	Gly12Val	11.19	missense	NM_033360.3
		125	Gly12Val	4.29	missense	NM_033360.3
		127	Gly12Asp	18.24	missense	NM_033360.3
		128	Gly12Asp	3.42	missense	NM_033360.3
		129	Gly12Asp	3.7	missense	NM_033360.3
		<b>113</b>	Gly12Arg	4.18	missense	NM_033360.3
	<b>113</b>	Gly12Val	8.75	missense	NM_033360.3	
	<b>43</b>	Gly12Val	12.88	missense	NM_033360.3	
	<i>PIK3CA</i>	68	Arg349Ter	3.74	nonsense	NM_006218.3
127		Phe83fs	4.52	frameshift/deletion	NM_006218.3	
<i>PTEN</i>		128	Asn323fs	22.37	frameshift/deletion	NM_000314.6
high-grade PanIN	<i>ARID1A</i>	73	Trp2091Ter	7.46	nonsense	NM_006015.4
	<i>GNAS</i>	96	Arg201His	3.42	missense	NM_000516.5
	<i>KRAS</i>	73	Gly12Asp	8.29	missense	NM_033360.3
		<b>80</b>	Gly12Val	16.59	missense	NM_033360.3
		101	Gly12Asp	13.7	missense	NM_033360.3
		<b>104</b>	Gly12Asp	5.15	missense	NM_033360.3
		<b>114</b>	Gly12Val	18.3	missense	NM_033360.3

	<i>TP53</i>	<b>80</b>	Arg213Ter	34.5	nonsense	NM_000546.5
		<b>104</b>	Arg196Ter	4.04	nonsense	NM_000546.5
low-grade IPMN gastric	<i>ARID1A</i>	21	Asp1850fs	7.45	frameshift/insertion	NM_006015.5
	<i>GNAS</i>	<b>2</b>	Arg201His	33.98	missense	NM_000516.5
		<b>7</b>	Arg201Cys	11.34	missense	NM_000516.5
		<b>35</b>	Arg201His	41.52	missense	NM_000516.5
		<b>62</b>	Arg201Cys	15.56	missense	NM_000516.5
		<b>86</b>	Arg201His	30.46	missense	NM_000516.5
		89	Arg201His	5.56	missense	NM_000516.5
		<b>94</b>	Arg201His	21.97	missense	NM_000516.5
		<b>97</b>	Arg201Cys	33.81	missense	NM_000516.5
		<b>99</b>	Arg201His	25.08	missense	NM_000516.5
		<b>110</b>	Arg201Cys	22.37	missense	NM_000516.5
		<b>112</b>	Arg201His	24.32	missense	NM_000516.5
		<b>54</b>	Arg201Cys	23.16	missense	NM_000516.5
	<i>KRAS</i>	21	Gly12Val	18.86	missense	NM_033360.3
		<b>2</b>	Gly12Val	35.1	missense	NM_033360.3
		<b>7</b>	Gly12Val	12.14	missense	NM_033360.3
		<b>35</b>	Gly12Asp	38.57	missense	NM_033360.3
		<b>39</b>	Gly12Val	35	missense	NM_033360.3
		<b>61</b>	Gly12Val	18.03	missense	NM_033360.3
		<b>62</b>	Gly12Val	18.5	missense	NM_033360.3
		64	Gly12Val	9.01	missense	NM_033360.3
		<b>86</b>	Gly12Val	27.81	missense	NM_033360.3
		89	Gln61His	36.49	missense	NM_033360.3
		<b>94</b>	Gly12Asp	21.16	missense	NM_033360.3
		<b>97</b>	Gly12Asp	33.68	missense	NM_033360.3

		<b>99</b>	Gly12Val	26.83	missense	NM_033360.3
		<b>110</b>	Gly12Val	24.76	missense	NM_033360.3
		<b>57</b>	Gly12Arg	6.96	missense	NM_033360.3
	<i>STK11</i>	<b>61</b>	Tyr60Ter	61.89	nonsense	NM_000455.4
high-grade IPMN gastric	<i>ARID1A</i>	130	Gln2115Ter	30.84	nonsense	NM_006015.5
	<i>GNAS</i>	51	Arg201Cys	31.03	missense	NM_000516.5
	<i>KRAS</i>	51	Gly12Val	33.12	missense	NM_033360.3
		65	Gly12Asp	16.51	missense	NM_033360.3
		66	Gly12Asp	33.64	missense	NM_033360.3
		130	Gly12Asp	22.65	missense	NM_033360.3
		131	Gly12Asp	23.98	missense	NM_033360.3
	<i>TP53</i>	65	Arg248Trp	17.99	missense	NM_000546.5
low-grade IPMN intestinal	<i>GNAS</i>	<b>92</b>	Arg201Cys	80.59	missense	NM_000516.5
	<i>KRAS</i>	<b>92</b>	Gly12Arg	37.95	missense	NM_033360.3
high-grade IPMN intestinal	<i>GNAS</i>	<b>33</b>	Arg201Cys	45.42	missense	NM_000516.5
		<b>88</b>	Arg201Cys	36.81	missense	NM_000516.5
		<b>90</b>	Arg201His	35.51	missense	NM_000516.5
		17	Gln227Lys	42.36	missense	NM_000516.5
	<i>KRAS</i>	<b>88</b>	Gly12Ser	33.81	missense	NM_033360.3
	<i>TP53</i>	<b>88</b>	Met237Thr	49.16	missense	NM_000546.5

1 PanIN/IPMN in cases without associated/concomitant PDAC are indicated in bold.

2

3

4

5

1 **Supplementary table 4. Distribution of CNV-positive and negative precursor lesions**  
 2 **according to the degree of dysplasia.**

		<i>CNV pos</i>	<i>CNV neg</i>
<i>PanIN</i>	<b>Low-grade</b>	16 (57%)	12 (43%)
	<b>High-grade</b>	6 (75%)	2 (25%)
<i>Gastric IPMN</i>	<b>Low-grade</b>	22 (76%)	7 (24%)
	<b>High-grade</b>	6 (75%)	3 (25%)
<i>Intestinal IPMN</i>	<b>Low-grade</b>	8 (100%)	0
	<b>High-grade</b>	13 (100%)	0

3 Percentages refers to the total number of cases in each group

4

5

6

7

8

9

10

11

12

13

14

**Supplementary table 5: Overview of log2 copy number ratios sorted in ascending order. Values of genomic alterations were detected by low-coverage sequencing (n=28) and DNA methylation data (n=67), respectively.**

Genomic location	affected samples (n)	PanIN (n=36)	gIPMN (n=38)			iIPMN (n=21)		
<b>deleted regions</b>								
chr01:010875000-013052998	3					-0.26	-0.25	-0.24
chr01:015375000-016825000	3					-0.26	-0.25	-0.20
chr06:074175000-074375000	5		-0.29	-0.22	-0.21	-0.44	-0.24	
chr06:133664400-143100000	5		-0.37	-0.28		-0.50	-0.45	-0.28
chr06:143620678-151100000	7	-0.21	-0.37	-0.34	-0.29	-0.50	-0.45	-0.28
chr09:005958053-023802212	5	-0.23	-0.51	-0.36	-0.36	-0.24		
chr10:071075000-120925000	6		-0.45	-0.22		-0.36	-0.30	-0.28
chr10:120925000-125869472	5		-0.30			-0.41	-0.30	-0.28
chr11:057325000-058807232	4					-0.44	-0.40	-0.27
chr11:058807232-069089801	5					-0.44	-0.40	-0.28
chr11:096437584-114325000	5					-0.51	-0.44	-0.40
chr11:114325000-134898258	4					-0.51	-0.44	-0.28
chr17:006225000-009675000	4		-0.50	-0.32	-0.21	-0.23		
chr17:009675000-012500000	5		-0.53	-0.31	-0.21	-0.50	-0.22	
chr17:015792977-021566608	6		-0.58	-0.23	-0.21	-0.49	-0.32	-0.25
<b>amplified regions</b>								
chr01:035225000-037325000	3					0.25	0.33	0.61

chr03:176225000-188875000	6	0.26	0.21	0.23	0.28	0.38	0.44					
chr05:028950000-044925000	5				0.24	0.25	0.31	0.74	0.79			
chr06:024125000-033575000	5		0.25	0.36	0.31	0.35	0.56					
chr06:033575000-042725000	4		0.42		0.32	0.34	0.56					
chr07:000282484-007150000	5				0.22	0.30	0.32	0.36	0.41			
chr07:054725000-055775000	5				0.21	0.26	0.27	0.33	0.36			
chr07:061967157-074715724	4				0.27	0.32	0.36	0.37				
chr07:112425436-130154523	5				0.21	0.33	0.36	0.38	0.57			
chr07:139404377-142048195	5				0.22	0.32	0.36	0.33	0.58			
chr07:143397897-154270634	5				0.24	0.33	0.34	0.38	0.59			
chr08:086726451-089550000	3				0.21	0.31	0.36					
chr08:127450000-129175000	7	0.42			0.21	0.27	0.29	0.36	0.56	0.66		
chr09:001992685-035698318	3				0.24	0.32	0.61					
chr09:070835468-092343416	4				0.22	0.26	0.32	0.60				
chr09:096718222-097575000	4				0.21	0.24	0.32	0.60				
chr09:097775000-114750000	4				0.22	0.26	0.32	0.61				
chr09:124994207-133073060	3				0.22	0.32	0.61					
chr12:006475000-007169938	8	0.21			0.24	0.33	0.56	0.71	0.88	0.89	1.70	
chr12:024993545-028938805	4	0.21			0.21	0.38	1.32					
chr14:020700000-022050000	3				0.21	0.28	0.33					
chr14:022800000-050175000	3				0.22	0.25	0.35					
chr14:097258910-107289540	3				0.25	0.22	0.36					
chr17:061125000-062410760	3				0.32	0.32	0.74					
chr17:062775000-063525000	3				0.32	0.34	0.49					
chr17:068117898-077546461	3				0.21	0.32	0.38					

chr20:008050000-016400000	7	0.24	0.22	0.23	0.24	0.26	0.33	0.84
chr20:016625000-021300000	7	0.25	0.22	0.23	0.25	0.28	0.33	0.82
chr20:030025000-034897085	7	0.26	0.22	0.22	0.23	0.31	0.33	0.81
chr20:036958189-042991501	6	0.26	0.22	0.23	0.35	0.33	0.79	
chr20:052650000-061091437	7	0.23	0.22	0.22	0.23	0.33	0.35	0.80
chr21:032825000-034475000	3		0.21	0.26	0.30			

1

1 **Supplementary table 6a: Differentially methylated probes in low- and high-grade pancreatic**  
 2 **cancer precursors.**

	Low-grade samples	High-grade samples	DMPs (hypermethylated in high-grade)	DMP associated genes (hypermethylated in high-grade)
iPMN	8	12	0	0
gIPMN	24	8	0	0
PanIN	20	7	86 (62)	59 (45)

3 iIPMN: intestinal IPMN; gIPMN: gastric IPMN

4

5 **Supplementary table 6b: Genes associated with significantly hyper- or hypomethylated CpG**  
 6 **in PanIN high-grade**

Genes associated with at least one significantly hypermethylated CpG	Genes associated with at least one significantly hypomethylated
TAC1	GLRX
AKAP13	BCL11B
POLR1D	ITFG3
GLYATL3	IFT140
HOXA5	CTNNA3
ZIC2	RUNX1
SIM2	SPARCL1
ARID4B	PHLDB1
MON2	NINJ2
CNKSR3	METTL9
SP8	SLC51A
ADD2	EMID2
HOXB1	CACNA1A
ST3GAL6	C19orf35
FBN2	
ZIK1	
LRP1B	
NTRK3	
GLI3	
NTM	
RASGRF1	
FAM46C	

NXPH1	
LBX2	
LOC101929710	
ADRA1A	
GRIK3	
PARP8	
KIAA1026	
SLC6A15	
IRX1	
GRIA4	
TLE4	
DGKI	
PACSIN2	
DOK5	
ZIC4	
MYLK	
DAPK1	
C5orf66-AS1	
AMER3	
CPEB1	
ST6GAL2	
INA	
AP2A2	

1

## 1 **Supplementary Figure Legends**

### 2 **Supplementary figure 1: Overview of lesions and methods**

3 55 PanINs, 46 gastric IPMNs (gIPMN) and 21 intestinal IPMNs (iIPMN) were subjected to 4  
4 main analyses: targeted next generation sequencing (n=52), low-coverage whole-genome  
5 sequencing (n=28), genome-wide DNA methylation analysis (n=79) and transcriptome analysis  
6 (n=34). Each circle of the diagram represents one of the mentioned methods and includes the  
7 number of samples used for related analyses. The samples that could not be placed into the  
8 diagram were shown at the right bottom corner of the figure. Pancreatobiliary and mixed-type  
9 IPMNs were excluded from further analyses due to small sample size.

### 10 **Supplementary figure 2: Allele frequency of *KRAS* and *GNAS* mutations in different precursor 11 lesions.**

12 (A) VAF of *KRAS* mutations; (B) VAF of *GNAS* mutations; (C) scatterplot of the VAF of the *KRAS*  
13 mutations (G12) against the VAF of *GNAS* mutations (R201) detected in low- and high-grade  
14 gastric IPMN. The grey lines represent the 95% confidence interval of the Pearson's correlation  
15 coefficient  $r$  (n=9). (Kruskal-Wallis-test \*  $p < 0.05$ ; \*\*  $p < 0.01$ ; \*\*\*  $p < 0.001$ ).

16

### 17 **Supplementary figure 3: Morphology of lesions with different genetic status according to 18 targeted NGS**

19 Representative HE images of low- and high-grade PanINs, gastric IPMNs and intestinal IPMNs  
20 with variable mutation profiles detected by targeted NGS are shown. No specific morphology  
21 was identified related to the mutation status between the samples in the same diagnostic  
22 group. In particular, gastric lesions with *GNAS* mutations (case 127, 96, 99 and 112) did not  
23 show relevant intestinal differentiation; only in case 112, focal (<5% of the cells) expression of  
24 *MUC2* and *CDX2* was observed (not shown). Scale bars represent 200  $\mu\text{m}$ . Detailed mutation  
25 profile of the samples is provided in Suppl. Table 3.

### 26 **Supplementary figure 4: Quality control of DNA methylation data derived from normal 27 pancreas cell preparations.**

28 (A) Multi-dimensional scaling of the 1000 most variable probes. (B) Hierarchical clustering of  
29 probes for known acinar and ductal marker genes.

1

2 **Supplementary figure 5: Proliferation activity, expression of TFF3 and of MUCL3 protein in**  
3 **PanIN, IPMN and PDAC.**

4 Representative images (A) and related graphs (B-D) of IHC staining performed in whole tissue  
5 sections in 31 PanIN, 28 gastric IPMN, 20 intestinal IPMN and 24 PDAC. Intestinal IPMNs and  
6 PDACs showed higher proliferation rates with Ki67 staining than PanIN and gastric IPMN. TFF3  
7 was strongly expressed in intestinal IPMN. Gastric IPMN revealed higher expression of MUCL3  
8 compared to PanIN. Scale bars represent 100  $\mu$ m. (IRS: immunoreactivity score) (\* $p < 0.05$ ).

9

10 **Supplementary figure 6: Hierarchical clustering of DNA methylation data based on published**  
11 **marker genes for distinct normal pancreas cell populations.** The mean methylation beta-  
12 value for all gene associated probes is displayed, respectively.

13

14 **Supplementary figure 7: Differentially activated gene sets.** Displayed pathways were  
15 detected by pairwise comparison between the indicated lesions. Odds ratios below 0.8  
16 indicate the activation in the first listed lesion whereas 1.1 is associated with the second  
17 group. The analyzed gene sets based on the KEGG pathway (A) and hallmarks (B) from  
18 the MSigDB.

19

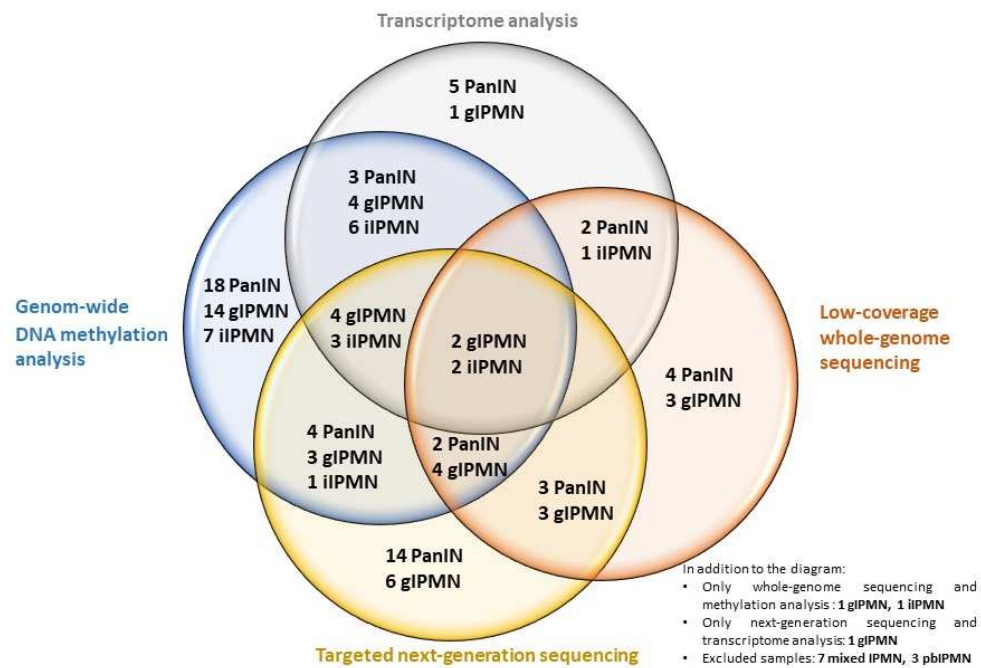
20

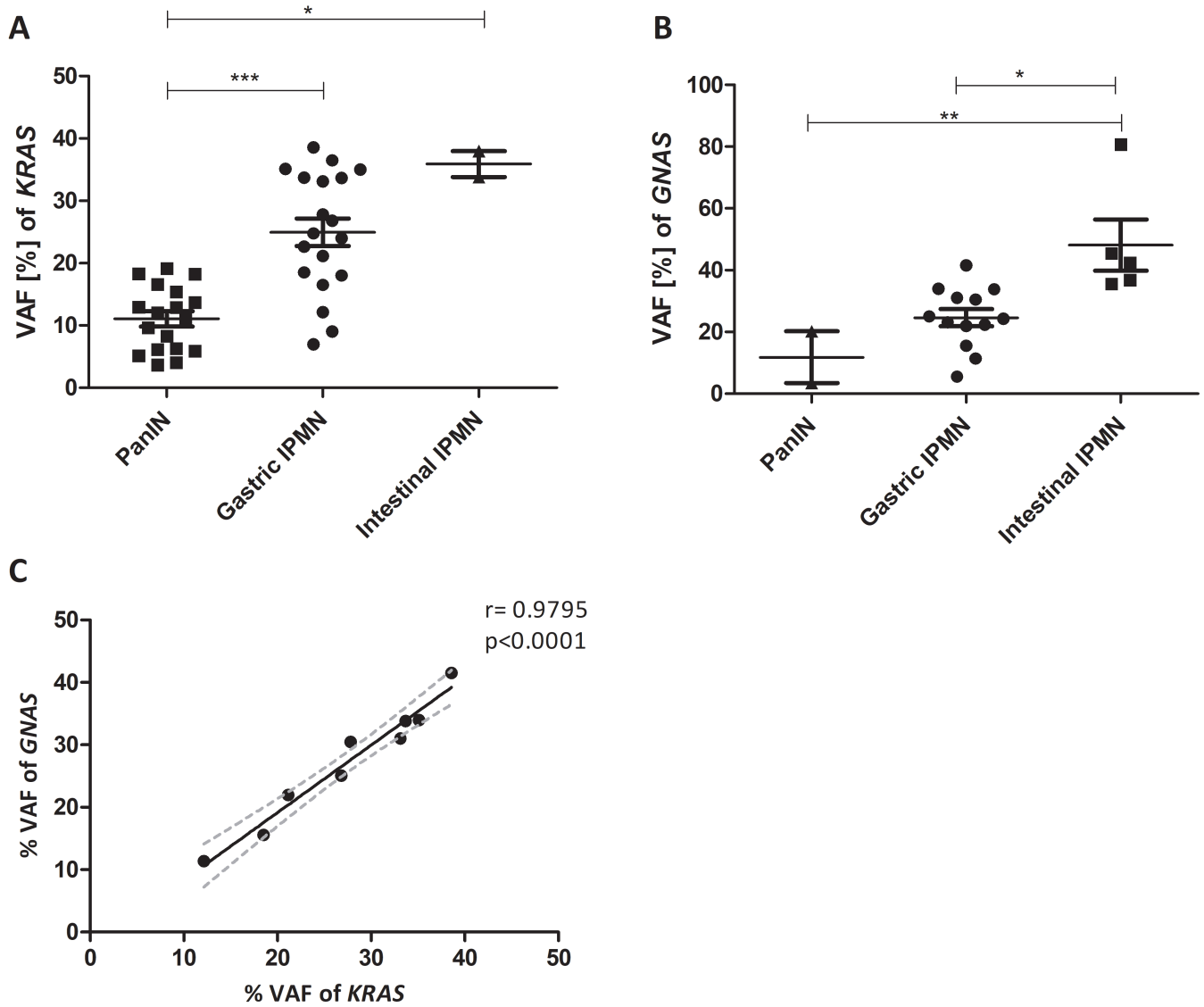
21

22

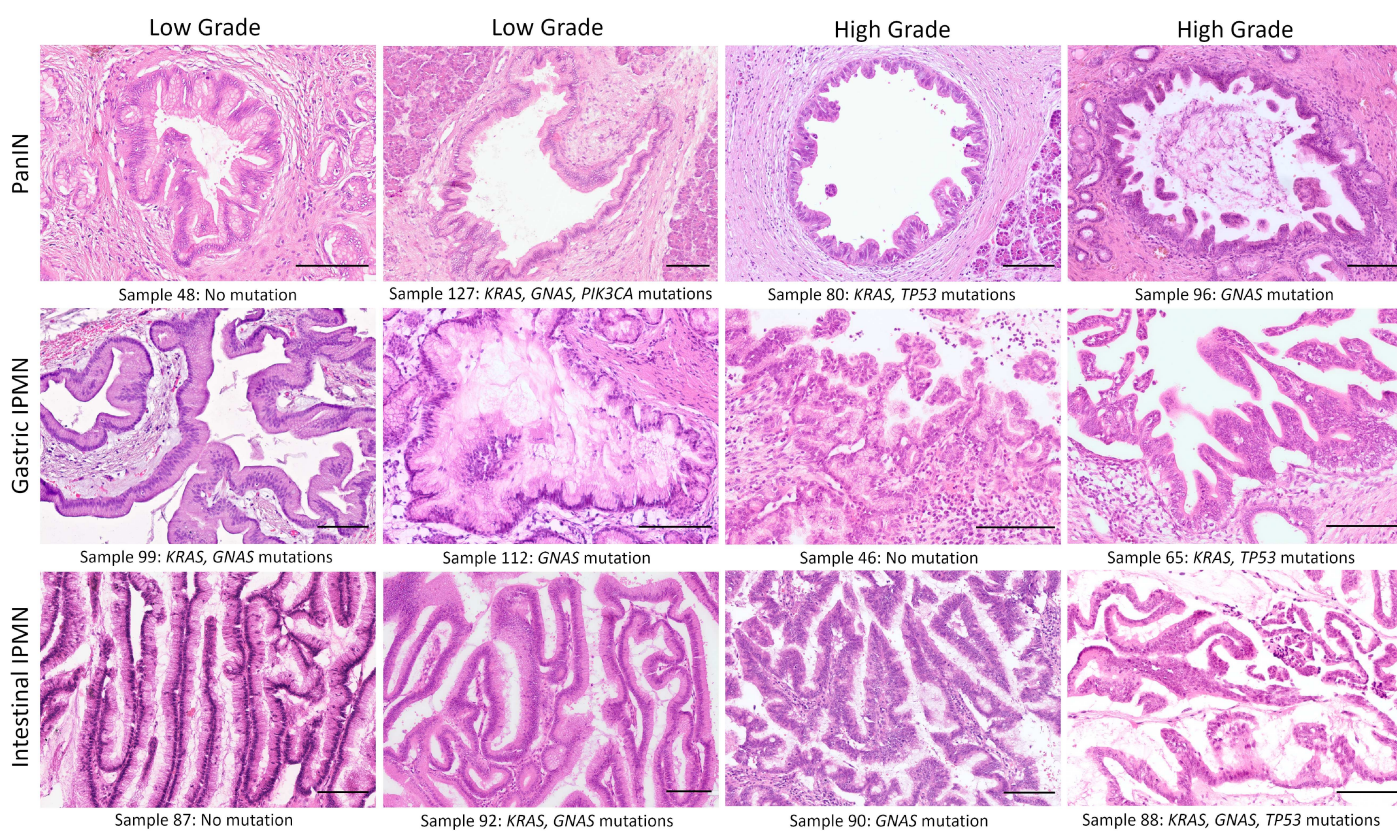
23

## Suppl. Figure 1.jpg

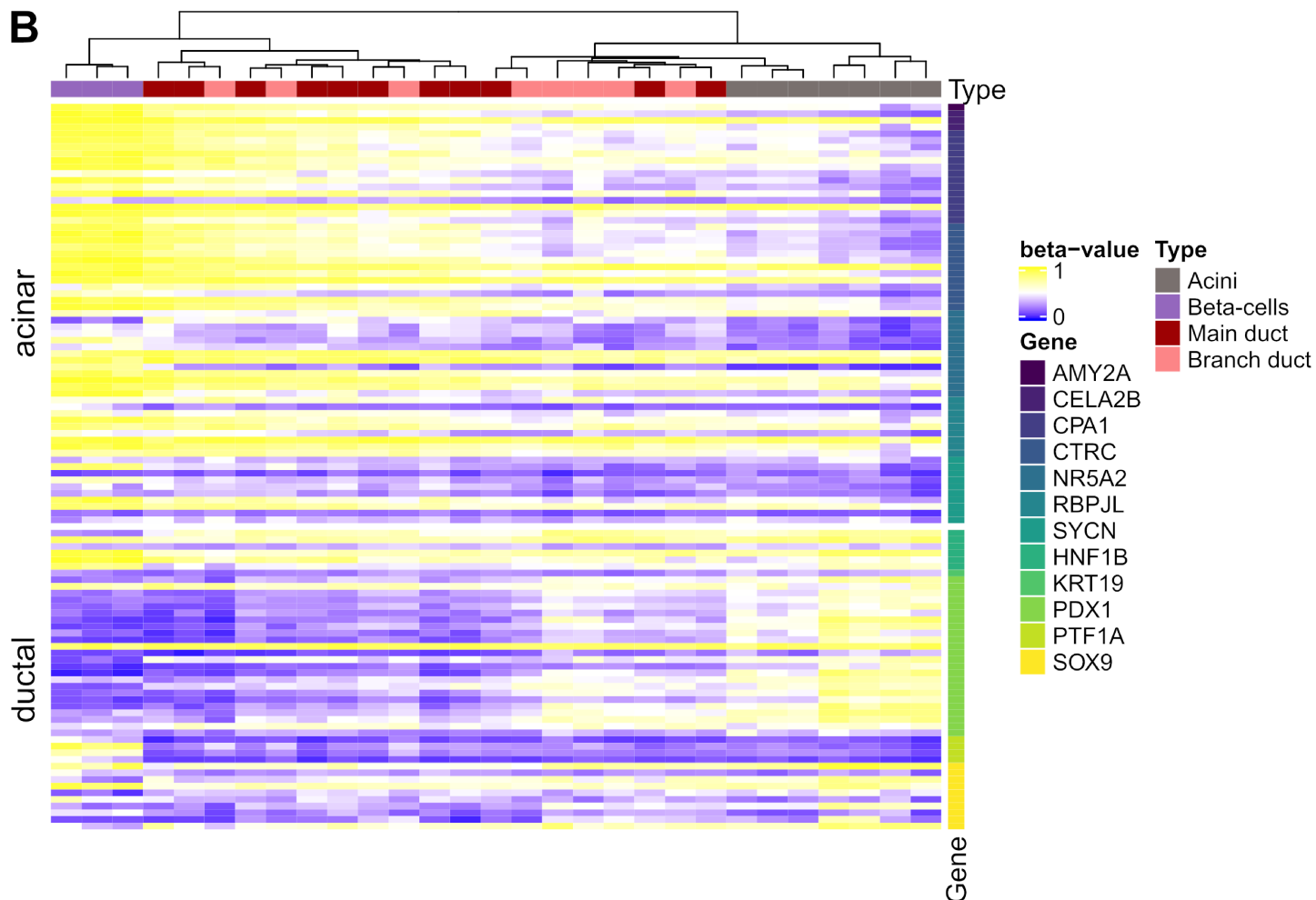
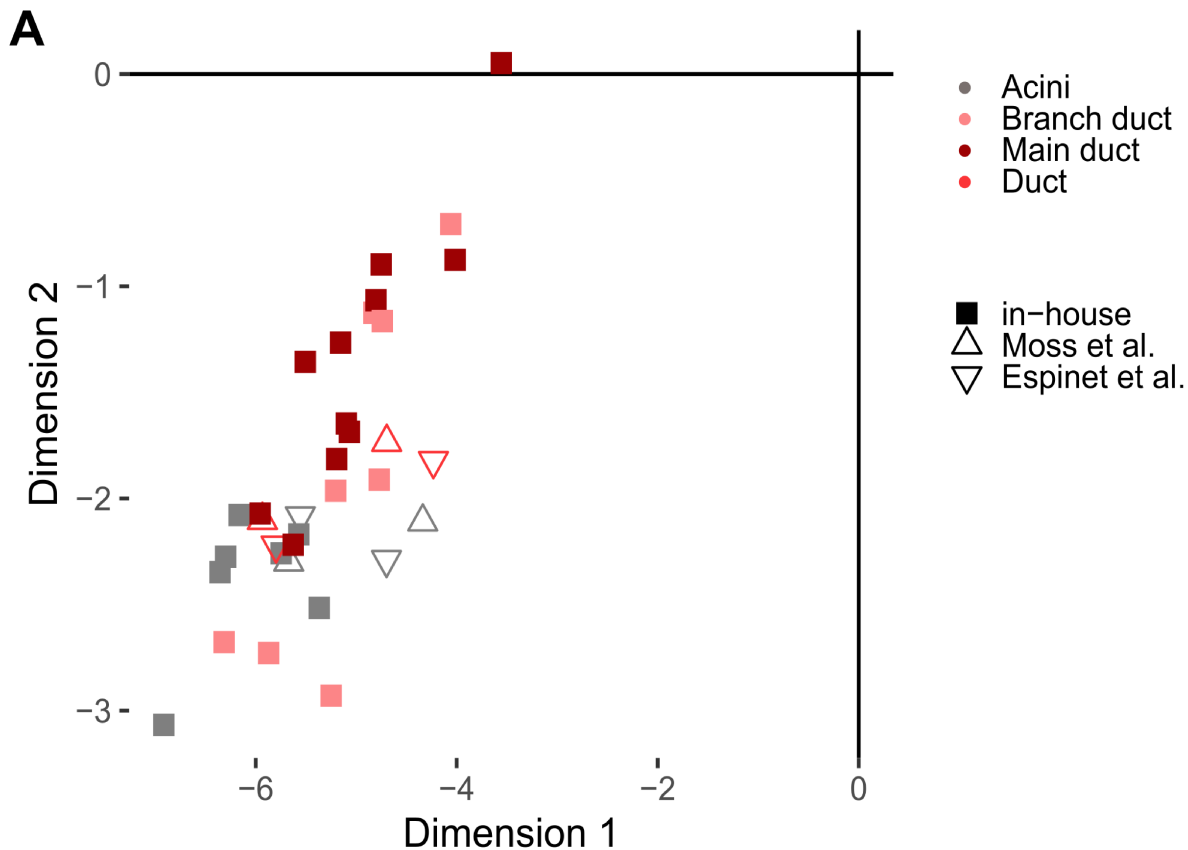


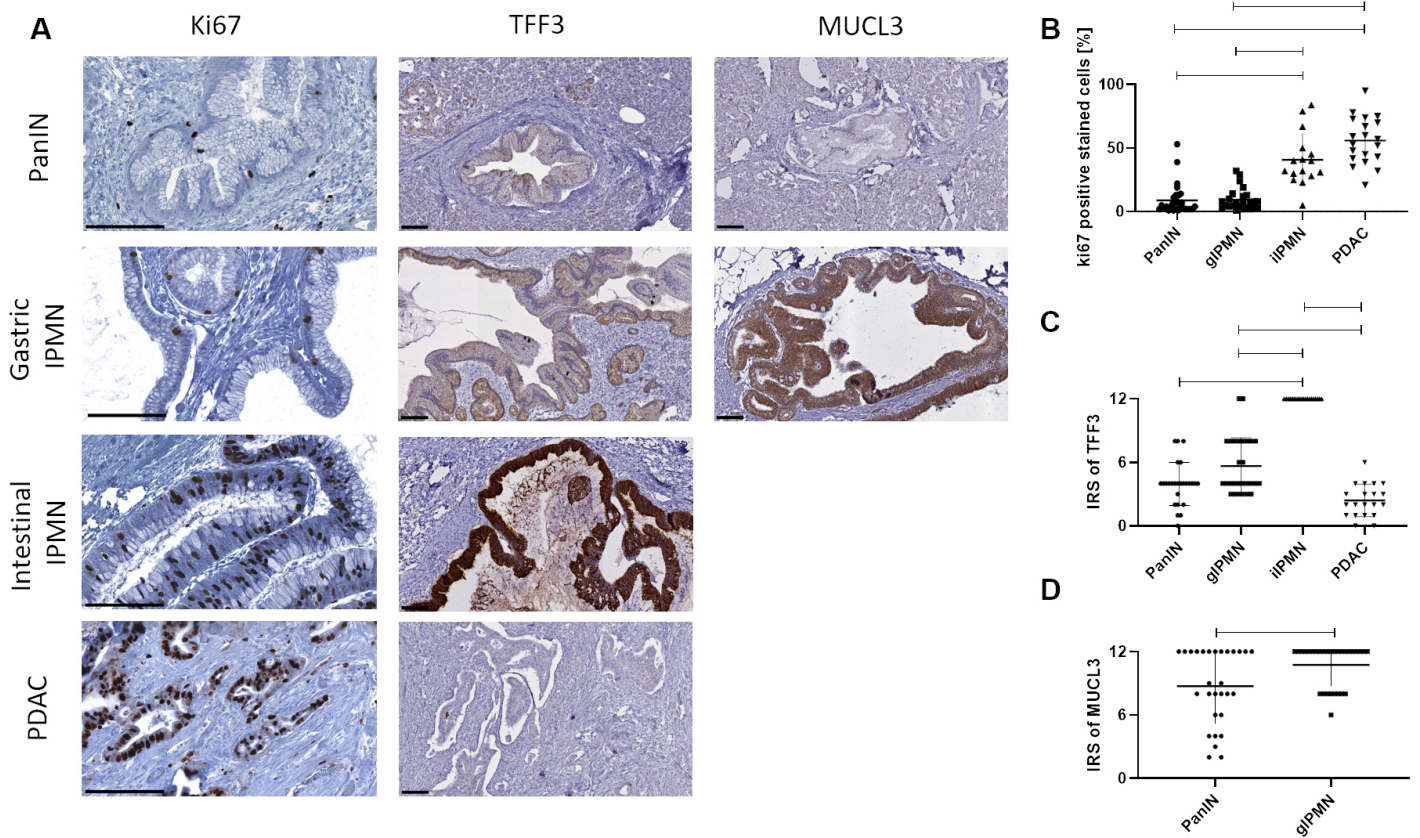


Suppl. Figure 3.tif

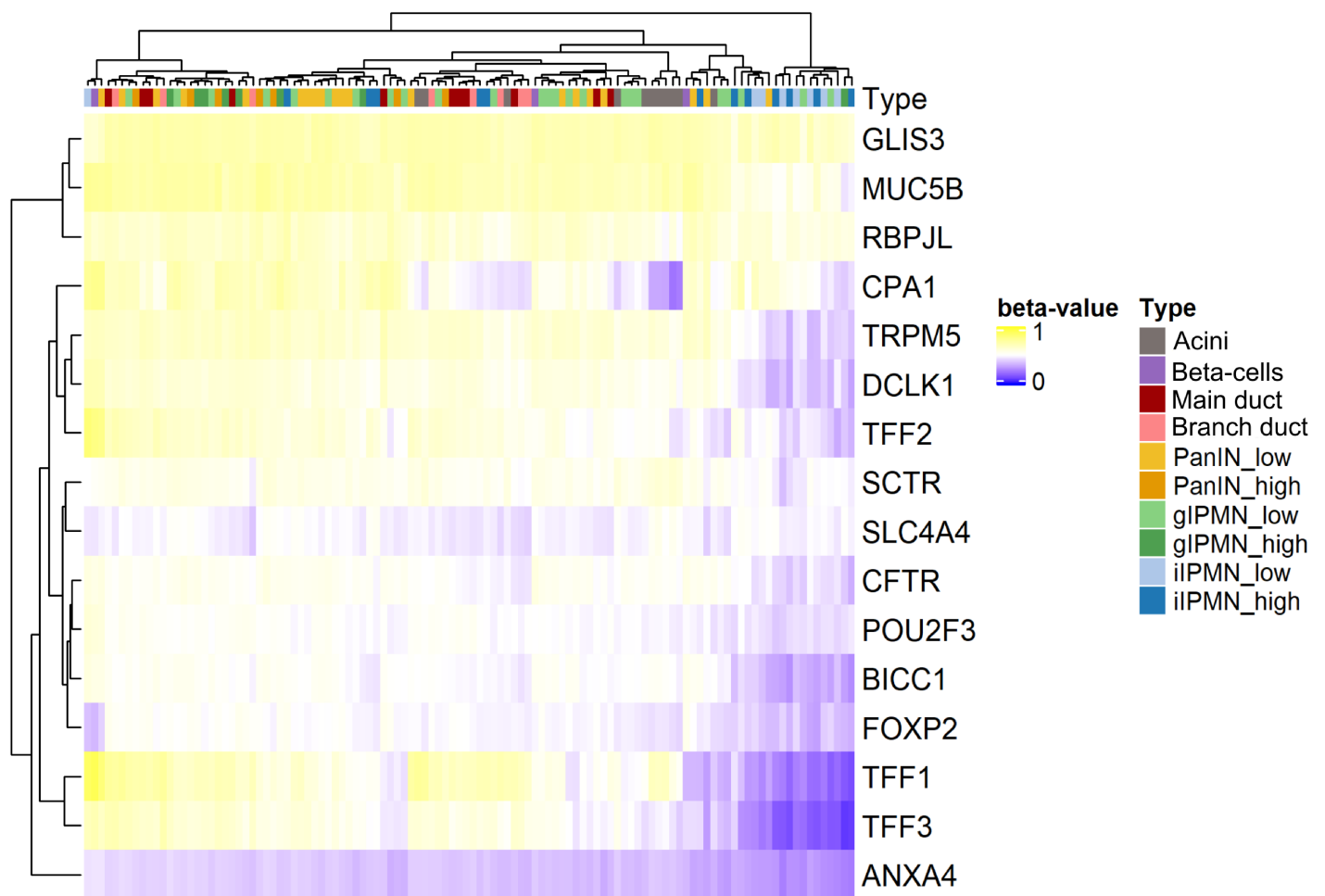


Layer



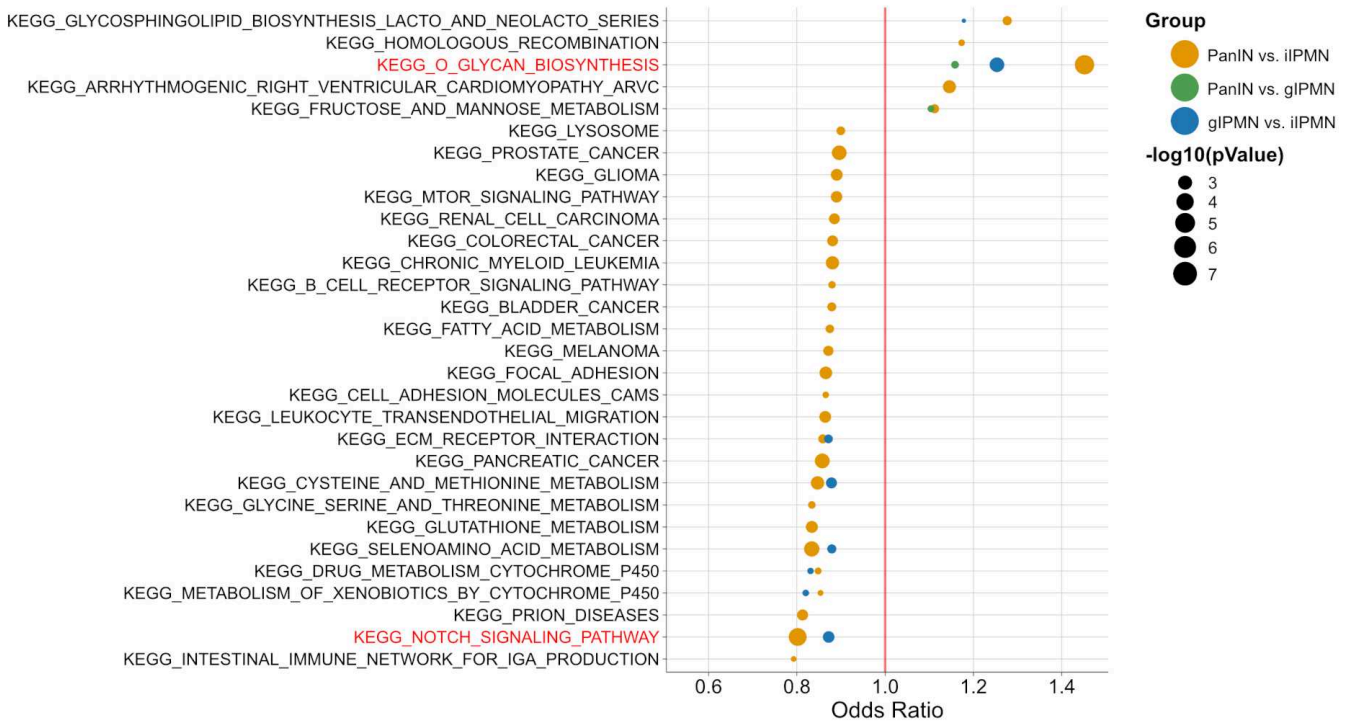


Layer

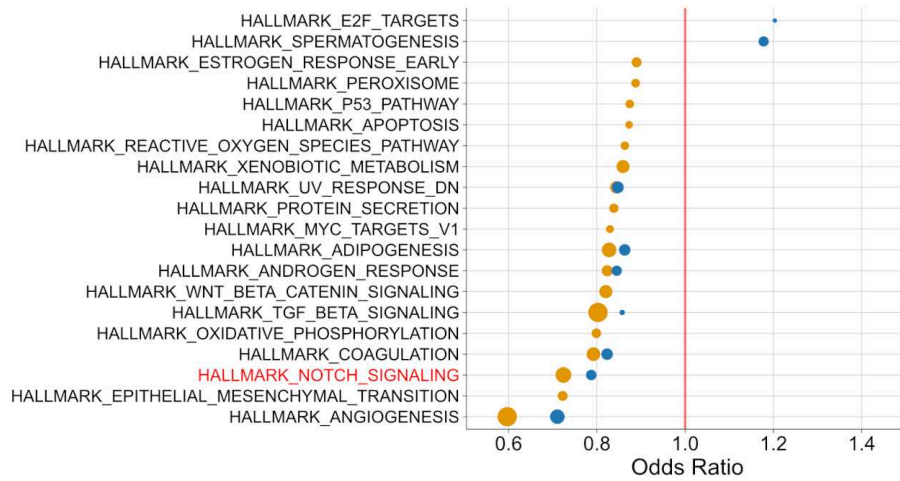


Suppl. Figure 7.tiff

**A**



**B**



## 1 Supplemental data

## 2 Methods

### 3 Immunohistochemistry

4 Staining was performed manually or using the Ventana BenchMark Ultra automated IHC/ISH  
5 slide staining system (Ventana Medical Systems Inc., Tucson, USA) (suppl. table 1a). The  
6 cytoplasmic expression of TFF3 and MUCL3 was evaluated using the immunoreactivity scoring  
7 system (IRS) based on staining intensity (0: negative, 1: mild, 2: moderate, 3: intense) and the  
8 percentage of stained cells (0: no positive cells, 1: <10% positive cells, 2: 10-50% positive cells,  
9 3: 51-80% positive cells, 4: >80% positive cells). The final score (0-12) was found by multiplying  
10 the positive cells proportion score (0-4) and the staining intensity score (0-3). The mean value  
11 of Ki67 proliferation rate of five randomly selected high power (40x) fields (HPFs) was  
12 calculated using the percentage of stained cells.

### 13 DNA/ RNA Isolation from FFPE samples

14 For genomic DNA or total RNA Isolation, 5-8 8- $\mu$ m-thick tissue sections were prepared, and  
15 lesions were dissected manually or by laser-capture microdissection (LMD), depending on  
16 their size to ensure adequate cellularity (>80%) for subsequent molecular analysis. For LMD,  
17 cresyl violet staining was done before using the Palm Microbeam System (Carl Zeiss,  
18 Oberkochen, Germany) according to the manufacturer's instructions. In some samples  
19 containing larger lesions, manual microdissection was used, as previously described.[1] The  
20 obtained cell clusters were isolated using the QIAamp DNA micro Kit or the GeneRead FFPE  
21 DNA Kit for DNA and the RNeasy FFPE Kit for RNA (all from Qiagen, Hilden, Germany) following  
22 the manufacturer's instructions. The genomic DNA quality control was performed by  
23 quantitative PCR using the Power SYBR™ Green PCR Master Mix on a StepOnePlus™ Real-Time  
24 PCR System. Quantification was performed with a self-designed primer assay (HML-2 for: 5'  
25 AAACGCCAATCCTGAGTGTC-3'; HML-2 rev: 5' CATAGCTCCTCCGATCCAT-3'). These primers  
26 are complementary to long terminal repeats (LTRs) of the HML 2 human endogenous  
27 retroviruses and have a length of about 115 bp.

## 1 Targeted NGS

2 A PDAC-Panel with two primer pools was created by the Ion AmpliSeq™ Designer (v5.6,  
3 ThermoFisher Scientific, Dreieich, Germany). The panel consists of 217 amplicons of 21 genes  
4 covering hot-spot mutational sites of 18 and the whole coding sequence of 3 (*ARID1A*, *TP53*  
5 and *RNF43*) additional genes relevant for PDAC (suppl. table 2). Barcoded libraries from gDNA  
6 (up to 10 ng per pool) were prepared using the Ion AmpliSeq Library kit 2.0 with Ion Xpress™  
7 Barcode adapters. The Ion library TaqMan™ Quantitation Kit was used for quantification of  
8 the libraries. The libraries were pooled and amplified in an emulsion PCR reaction using the  
9 Ion 520™ & Ion 530™ Kit-OT2. The resulting Ion Sphere particles (ISPs) were loaded on a 520™  
10 or 530™ Chip and sequenced on the Ion S5™ system (all reagents from ThermoFisher).

11 The results of the next generation sequencing from the Ion S5™ system were aligned to the  
12 human reference genome (GRCh37/hg19) using the S5 Ion Torrent Server VM (ThermoFisher).  
13 The Ion Reporter software (Version 5.12.0.0) was used for variant calling and annotations of  
14 the DNA panel sequencing. The parameters for variant calling were set equal for all samples.  
15 Following thresholds were defined: 3% allele frequency with a minimum coverage of 500 and  
16 a Phred Score of  $\geq 30$ . Detected variants were validated using the Integrative Genomics Viewer  
17 (IGV), ClinVar database from National Institutes of Health (NIH) and University of California  
18 Santa Cruz (UCSC) Genome Browser. Variants not present in the above mentioned databases  
19 were classified according to the American College of Medical Genetics and Genomics (ACMG)  
20 guidelines using the ACMG database (varsome.com; v7.3.7).[2]

## 21 Fusion transcript analysis

22 50 ng of isolated RNA were used for cDNA synthesis by QuantiTect Reverse Transcription Kit  
23 (Qiagen) and were subsequently subjected to library preparation using the Oncomine  
24 Comprehensive Assay Plus RNA (ThermoFisher) targeting over 1,300 isoforms of 49 tumor  
25 driver genes including approximately 200 known *BRAF* fusion transcripts. NGS was performed  
26 (as described above) and data analysis was done using the Oncomine Comprehensive Plus  
27 w2.1 - Fusion workflow implemented within the IonReporter Software package (V5.18;  
28 ThermoFisher).

## 29 Isolation of epithelial cells from the main pancreatic duct and from peripheral (branch) ducts

1 Specimens were obtained fresh from the operating theater and immediately subjected to  
2 gross examination. The main pancreatic duct was probed, and the specimen dissected by a  
3 pathologist along the probe. The main duct was then carefully dissected with a scissor and  
4 then fixed in 10% buffered formalin and embedded in paraffin. Peripheral tissue blocks were  
5 prepared, and branch-ducts were isolated by LMD, as described above. DNA extraction was  
6 performed as described above.

### 7 **Generation of $\beta$ -cells**

8  $\beta$ -cell populations from FFPE tissue were generated from 50- $\mu$ m-thick sections. Tissue sections  
9 were dewaxed with xylol and rehydrated in descending ethanol concentrations. Antigen  
10 retrieval was done at 80°C for one hour in a pressure cooker before tissue was digested with  
11 1% (w/v) collagenase Ia (Sigma, Steinheim, Germany) and 1%(w/v) dispase (Gibco, Grand  
12 Island, USA) for 45 min at 37°C to obtain single cells. The cell suspension was subsequently  
13 filtered (30  $\mu$ m mesh) and the cells were collected by centrifugation. Single cells were stained  
14 Insulin (Abcam, Cambridge, UK; 1:200). The stained cells were sorted with a BD FACS Aria™  
15 III System. DNA was isolated from the sorted cells as described above.

### 16 **Transcriptome analysis**

17 After total RNA isolation, the samples were shipped to Macrogen (Seoul, Korea) for  
18 sequencing. Libraries from total RNA were prepared using the Illumina TruSeq™ Stranded  
19 mRNA Library Prep kit and sequenced with 2 x 100 bp on the Illumina NovaSeq 6000 (Illumina  
20 Inc, San Diego, USA). The raw data processing of the transcriptome data was performed by  
21 Macrogen. Briefly, adapter and low-quality base trimming was carried out with Trimmomatic  
22 (v0.38).[3] Trimmed reads were mapped against the GRCh38/hg38 human reference genome  
23 using the Bowtie2 (v2.3.4.1) aligner.[4] Afterwards, the aligned reads were assembled with  
24 Cufflinks (v2.2.1).[5] After assembly the abundance of gene was calculated in read counts per  
25 gene. Before differential gene expression analysis lowly expressed genes were filtered from  
26 the data set. Therefore, genes which showed a lower read count as 0.5 transcripts per million  
27 reads and were missing in more than one sample per group were excluded from further  
28 analysis. The filtered raw count matrix was normalized and batch-corrected using the DESeq2  
29 package (v3.14).[6] Finally, differentially expressed genes were calculated pairwise and  
30 defined as followed  $\log_2$  fold change of  $< -1$  and  $> 1$ , respectively, and the significance level of

1 the adjusted p-value was set to < 0.05. PCA, heatmap and expression plots were calculated  
2 based on the variance stabilizing transformation output of DESeq2

### 3 **Pathway analysis**

4 Gene set enrichment analysis

5 For methylation data, enrichment of KEGG terms was estimated for all differentially  
6 methylated probes (DMP) in a pair-wise manner. DMPs were defined as displaying a beta  
7 value change of 0.4 and an adjusted p-value < 0.05. Gene set enrichment was calculated with  
8 the gometh function of the missMethyl package (v.1.26.1).[7]

9 The single sample Gene Set Enrichment Analysis (ssGSEA) was performed only for RNA seq  
10 derived data. Briefly, the normalized enrichment scores (NES) were calculated on the variance  
11 stabilized transformation data with the GSVA package (v.1.40.1).[8] Differentially activated  
12 gene sets were calculated between the different precursor lesions as described by Larsen *et*  
13 *al.* with a p-value of < 0.05.[9]

14 VIPER analysis

15 The activation of transcription factors was calculated with the VIPER algorithm (v1.26.0).[9]  
16 For the analysis, the paad regulon was taken from the arcane.networks package (1.18.0).  
17 Activated transcription factors were defined as displaying a p-value < 0.005 and a NES score  
18 of >3 or >-3.

### 19 **Statistical analysis**

20 Statistical analysis was performed using the GraphPad Prism 8 software (GraphPad Software  
21 Inc., San Diego, USA) or R v. 3.6.0 (R Core Team 2018). Statistical significance in  
22 immunohistochemistry was determined by Kruskal-Wallis test with Dunn's multiple  
23 comparison test. Results are presented as means  $\pm$  standard error of the mean (SEM). P values  
24 less than 0.05 were considered statistically significant (\* p < 0.05; \*\* p < 0.01; \*\*\* p < 0.001).

## 1 References

- 2 1 Schlitter AM, Born D, Bettstetter M, *et al.* Intraductal papillary neoplasms of the bile  
3 duct: Stepwise progression to carcinoma involves common molecular pathways. *Mod*  
4 *Pathol* 2014;27:73–86.
- 5 2 Richards S, Aziz N, Bale S, *et al.* Standards and guidelines for the interpretation of  
6 sequence variants: a joint consensus recommendation of the American College of  
7 Medical Genetics and Genomics and the Association for Molecular Pathology. *Genet*  
8 *Med* 2015;17:405–24.
- 9 3 Bolger AM, Lohse M, Usadel B. Trimmomatic: a flexible trimmer for Illumina sequence  
10 data. *Bioinformatics*. 2014;30:2114-2120.
- 11 4 Langmead B, Salzberg SL. Fast gapped-read alignment with Bowtie 2. *Nat Methods*  
12 2012;9:357-9.
- 13 5 Li H, Handsaker B, Wysoker A, *et al.* The sequence alignment/map format and  
14 SAMtools. *Bioinformatics* 2009;25:2078-9.
- 15 6 Love MI, Huber W, Anders S. Moderated estimation of fold change and dispersion for  
16 RNA-seq data with DESeq2. *Genome Biol* 2014;15:550.
- 17 7 Phipson B, Maksimovic J, Oshlack A. missMethyl: an R package for analyzing data from  
18 Illumina's HumanMethylation450 platform. *Bioinformatics* 2016;32:286-8.
- 19 8 Hänzelmann S, Castelo R, Guinney J. GSVA: gene set variation analysis for microarray  
20 and RNA-seq data. *BMC Bioinformatics* 2013;14:7.
- 21 9 Larsen BM, Kannan M, Langer LF, *et al.* A pan-cancer organoid platform for precision  
22 medicine. *Cell Rep* 2021;36:109429.
- 23 10 Alvarez MJ, Shen Y, Giorgi FM, *et al.* Functional characterization of somatic mutations  
24 in cancer using network-based inference of protein activity. *Nat Genet* 2016;48:838-  
25 47.

26

1 **Supplementary tables**2 **Supplementary table 1a: Antibodies and protocols for immunohistochemistry.**

Antibody	Type	Dilution	Antigen Demasking	Source
Anti-MUC1	Mo Mono	1:100	CC1	Biocare
Anti-MUC2	Mo Mono	1:100	CC1	Dako
Anti-MUC5AC	Mo Mono	1:1000	CC1	Chemicon
Anti-CDX2	Mo Mono	1:40	CC1	BioGenex
Anti-MIB1	Mo Mono	1:100	CC1	Dako
Anti-TFF3	Rb Mono	1:2000	EDTA buffer pH 9	Abcam
Anti-MUCL3	Rb Poly	1:500	Citrate buffer pH 6	LSBio

3 \*Rb: rabbit. Mo: mouse Mono: monoclonal. Poly: polyclonal. CC1: Cell Conditioning 1 (Ventana Medical System, Tucson, AZ,  
4 USA).

5 **Supplementary table 1b: Tissue collective used for Ki67, TFF3 and anti-MUC13 staining.**

Type of lesion	Number of lesions
<b>PanIN</b>	<b>31</b>
Low grade	26
High grade	5
<b>Gastric IPMN</b>	<b>28</b>
Low grade	20
High grade	8
<b>Intestinal IPMN</b>	<b>20</b>
Low grade	9
High grade	11
<b>PDAC</b>	<b>24</b>

6

## 1 Supplementary table 2: Genes and amplicons in targeted NGS.

Gene Symbol	Chr	Ion AmpliSeq Fwd Primer (5'-3')	Ion AmpliSeq Rev Primer (5'-3')	Amplicon ID
ALK	chr2	TCTCTCGGAGGAAGGACTTGAG	GCCCAGACTCAGCTCAGTTAAT	CHP2_ALK_1
ALK	chr2	ACAGGGTACCAGGAGATGATGTAAG	GGAAGAGTGGCCAAGATTGGA	CHP2_ALK_2
APC	chr5	GAGAGAACGCGGAATTGGTCTA	GTATGAATGGCTGACACTTCTCCA	CHP2_APC_1
APC	chr5	AGCACTGATGATAAACACCTCAAGTT	ATCTTCTTGACACAAAGACTGGCT	CHP2_APC_2
APC	chr5	TTCAATATCATCTTTGTCATCAGCTGAA	TTTGGTTCTAGGGTGTGTGAC	CHP2_APC_3
APC	chr5	GCAGACTGCAGGGTTCTAGTT	GTGAAGTACAGAAAGTACATCTGCT	CHP2_APC_4
APC	chr5	AGCCCCAGTGTCTCCAGATA	CCCTCTGAAGTGCAGCATTACT	CHP2_APC_5
APC	chr5	AGAGGGTCCAGGTTCTCCA	TCATTTCTGAACTGGAGGCATT	CHP2_APC_6
APC	chr5	ATGAAACAGAATCAGAGCAGCCTAAA	CGTGATGACTTTGTTGGCATGG	CHP2_APC_7
ARID1A	chr1	CAAAATGAACAACAAGGCAGATGGG	TCAGAGACTATCTAGTCCGGTGTCT	ARID1A_10.112972
ARID1A	chr1	CAGCTAACTTACTGGACTTGAGAATTTTT	GAGTCAAGACAAAAATCACTACCTTGG	ARID1A_10.135473
ARID1A	chr1	CATGATGGGAACTGGACCTCCTTA	TTAGCTGTGATGTGACTCTGAAGAAAT	ARID1A_10.143283
ARID1A	chr1	CCCCAGCCTACGGCTTC	CCCCCGTAGGGCTCCA	ARID1A_1.1.15178
ARID1A	chr1	CCTAGGCCCGCCCTGA	GGCTCCGGCCGTAGGGT	ARID1A_1.1.16654
ARID1A	chr1	CAGTCAAGAGACTTCTGAGACCCTTA	CAGATAACGGTCCACCCACATC	ARID1A_11.181180
ARID1A	chr1	CCGCTGGGAAAGGAGCTG	GCCTAGGGCCCGCTTC	ARID1A_1.1.20289
ARID1A	chr1	CTATGCCTCTATGTGTCTGTGAAG	GTACCACATGAAGCCAGTGAGTAC	ARID1A_11.248116
ARID1A	chr1	ACAACTCTACTACCCCAACC	CTGCTGAGCGAAGGACGA	ARID1A_1.1.2481
ARID1A	chr1	CTCCAGAAATCCAGTTCTTCTACTACA	ATAGAGGTCCAGAGGTTTCTACC	ARID1A_11.279375
ARID1A	chr1	CTCAGCAGCGCTTCGGG	GGGCCCGCCACTGTAGT	ARID1A_1.1.36612
ARID1A	chr1	CTCGGAGCTGAAGAAAGCCG	GCTCTCGGCCCGCTCT	ARID1A_1.1.38056
ARID1A	chr1	GAGCCGTCTGCCGTCG	GGAGTGTACTGGTGGTTGGG	ARID1A_1.1.42139
ARID1A	chr1	GGCCCCAGCAGAAGCTCTCAC	AGCCCGGAGTGCCACCTC	ARID1A_1.1.52554
ARID1A	chr1	GGCTGCCGGCTCCAAGC	GCTGGCGACGTGAGCA	ARID1A_1.1.54514
ARID1A	chr1	GGGATCATGGCCGCGCA	CCGGCGGCTGCCTTCAT	ARID1A_1.1.54590
ARID1A	chr1	TTATCTGGCCTTCACTGAGGAGAA	CTCACCTGAGTCAATCCACCAAT	ARID1A_11.550938
ARID1A	chr1	AGCCGGACTGAAGAAGCTCG	GGCCCGGCTGAGTGAG	ARID1A_1.1.6484
ARID1A	chr1	CTCGCCCGGACCCCTCAG	GCCAGACAATGGCAGCTCC	ARID1A_1.2.19161
ARID1A	chr1	GGGTACCAGGGCTACCC	GGGCTCATGGGCGCTG	ARID1A_1.2.26067
ARID1A	chr1	GATATACCTCGACTCCTTTGGTTTGG	AGGGTCTTCTCCCGTTCAAT	ARID1A_12.293039
ARID1A	chr1	GCCAGCTCCTTGAAAAGCAGTATATC	GACCCATCCTTACCAGGAGAG	ARID1A_12.311881
ARID1A	chr1	AGACATCTTTCAGCTGTGATT	CACAGATCCTTGGCATATCCTGTTG	ARID1A_12.73402
ARID1A	chr1	CCGGCGGACATGGCCTC	CCTCCCACTCAGCTGTGTA	ARID1A_1.2.9363
ARID1A	chr1	CTCAACTTGATCTCTGTCCACAGC	CTGCTCTGGCCTTACCTCATG	ARID1A_13.224100
ARID1A	chr1	CTCCTGCGTGTCTTTGTTATATTGG	TGGAGTCATGGAATCCGCTT	ARID1A_13.228066
ARID1A	chr1	GAGGAGACTTAAAGCCACCAACTC	CAAGGAGTCCCATGCACTTATCT	ARID1A_13.262576
ARID1A	chr1	GCCTTGATAGCTCTGCTAAGAAG	GCCCTGCATAGATCCTGATCC	ARID1A_13.286741
ARID1A	chr1	CTTAATGATGGAAGTACTCCACATTC	CAAGTCAAATAGCAATCAGATCAGTCA	ARID1A_14.234479
ARID1A	chr1	TGACTCAAACCTGGGTATCA	CATTTCACTGGCCCTGTCTTACG	ARID1A_14.440936
ARID1A	chr1	GACCACGACAGCACTATCCCTA	TCATGTTCCCTCAGGCCCTATT	ARID1A_15.209989
ARID1A	chr1	TCACCCTTGCCTTTCTACG	TCACTGTGCATAAGGACCTCCA	ARID1A_15.321878
ARID1A	chr1	CCAATTTTGTAGGACGGAGCCT	CACCGAGACCAGGCTTACTC	ARID1A_15.99688

ARID1A	chr1	CTAATCCTGTGTTCTTTGCCTCCT	TTTTCAAGGCGAACCTGCATG	ARID1A_16.147847
ARID1A	chr1	GGATGTATTCTCCTAGCCGCTAC	TTGGGTGGAGAACTGATTGCCATA	ARID1A_16.243588
ARID1A	chr1	AGCGTGCCATACAGCACT	GGCAGTGGCAGGATAGGCA	ARID1A_18.122838
ARID1A	chr1	AACCGCACCTCTCCTAGC	TCCCGCGAATCATGGG	ARID1A_18.17117
ARID1A	chr1	CAGATGAAATGCTGCACACAGATC	GATACCTGAGGAATGTGATTCTGCAT	ARID1A_18.249269
ARID1A	chr1	CAGGTATCCAGCCCTGCTC	TGCTATGTGCGAGGCAGGT	ARID1A_18.260793
ARID1A	chr1	CCACTGCCACAGCTGCTAC	GCTGAGCAACCTCAGCTGAT	ARID1A_18.303487
ARID1A	chr1	AAGGCTCGTGGCCTTCCC	GTGCGGTTCTCCATTGGC	ARID1A_18.33212
ARID1A	chr1	CTGTGTCCACCAAGCATCTGG	GGCACGCTGTACATCTCC	ARID1A_18.457891
ARID1A	chr1	GCAAACATGCCACCACAAATGATG	TGTTCCGTTCCAGCCATGATAG	ARID1A_18.536845
ARID1A	chr1	GCCTTCCCCTCAGCAAGATGTATA	GGTCTCGGCCAACTGGAATG	ARID1A_18.584475
ARID1A	chr1	ACATAGCACCTGCCCTGT	GGGAGATTAGGCAACCGAATG	ARID1A_18.63843
ARID1A	chr1	TGCTCAGCAAGGCACCATG	CGAGCCTTCGTGGTTGG	ARID1A_18.820768
ARID1A	chr1	TTGTCTCTGCCTTAGAATTACAAGCG	GCTGGGCAGCTTGTGCT	ARID1A_18.880618
ARID1A	chr1	AGACGACATGGAGGTTTATTCAGG	CCCAGGCACTGATACTCA	ARID1A_19.54023
ARID1A	chr1	ATCTTCAGAGTAGCTTCACTGATGGG	GTTGATGGTATCTAATGCCATGTG	ARID1A_19.79292
ARID1A	chr1	CAACATCCTGCTGTATGATGACAAC	GGCATGGAAGATATCTACAAGAGAGAAA	ARID1A_19.96133
ARID1A	chr1	ATCCTGGGAGGTTTCAGCAA	GAAGCTGGCTTGCCTTGC	ARID1A_20.1.247050
ARID1A	chr1	CCAGTTCAGAGAATAGTGAGGA	GCAGCAGGCCACTGTCAAA	ARID1A_20.1.351511
ARID1A	chr1	CCCTCGGAAGCATGTGACAAC	CTTGATGGCCTCTGAACCTTAGC	ARID1A_20.1.374770
ARID1A	chr1	CCTGCTGCACTGGCGGAT	GGCCCTCCTGGTCTGTTG	ARID1A_20.1.397870
ARID1A	chr1	CGAAGCCTGTCAATTTGTGCCA	GTTAGTGGTGCCTGCTTCCG	ARID1A_20.1.400147
ARID1A	chr1	CTGTTCTTAGGCCACTTTTCTCC	CCCAGGATCCAGTAGCGTT	ARID1A_20.1.464959
ARID1A	chr1	GAGGAAGTAGTTGAAAATGATGAGGAGA	TCCACCACAAATGGATCATTCTTCTGTA	ARID1A_20.1.565326
ARID1A	chr1	GCAGCAAGTTTCCATTGGCATTAG	AGGCTTCGAATGGTATTGGACAC	ARID1A_20.1.612574
ARID1A	chr1	GCCTGATTGAGATCTTTGGCATTAAAA	ACTTCTCTTCTTCTCTTCTTAGTTTA	ARID1A_20.1.637352
ARID1A	chr1	GGGCCCCACCTGATGGA	GTTCCGGTGGCTCTGTGC	ARID1A_20.1.733579
ARID1A	chr1	GTGGTGGACTGCTCAGATAAGCT	AGCTCTGTCTTGTCTCGAAGT	ARID1A_20.1.787955
ARID1A	chr1	ACCGGAACATCAAGATCCTAGAG	CCCTGGGTGTTGGACATC	ARID1A_20.1.90003
ARID1A	chr1	ATGGTGCGCTTCTCAGT	CGGCAAGGCTGCTCTAG	ARID1A_20.2.152846
ARID1A	chr1	CAGTGCAAGGCGAGTATCG	CCGCATCATGTCCACACTAGTTG	ARID1A_20.2.222602
ARID1A	chr1	CCACTAATTATGAAAAGGAGGAGGAA	CCGAGATGTTGGCGAGTGTA	ARID1A_20.2.247152
ARID1A	chr1	CCTTGCCGCCACACAGTT	CAACAGCCGTGATTCTGACA	ARID1A_20.2.313338
ARID1A	chr1	CTTGAGATGCTCCGGGAA	AGGGCAAACTGCCAGTGTA	ARID1A_20.2.409280
ARID1A	chr1	CTTCAGCTGAAGCCAGGAC	CGACCATAGTGTATACAATTCT	ARID1A_20.2.432258
ARID1A	chr1	AAACTCAGCATCCAGGACAACAAT	GCCAGGTTGGCCAGCAGTA	ARID1A_20.2.5295
ARID1A	chr1	ACCCAGGGCTGCTGCTCAT	TCTCAAGCAGTCCCACCA	ARID1A_20.2.54967
ARID1A	chr1	GGCTGTTGGACATCTCGGT	GTTTTGCATAAATAAGGGCAACAGTC	ARID1A_20.2.603909
ARID1A	chr1	GGGCAGTTGGACCTATCTCCATAC	CTGAGTTTGTGAGGGTTTCAA	ARID1A_20.2.613243
ARID1A	chr1	TGGACGAGAACCCTCAGAGTTTAC	GCTGTCTGACTGGCAATCAAAA	ARID1A_20.2.760156
ARID1A	chr1	CATGGGCGGCTCTTATAC	TAGTAGCACTGTAAATTAAGTCCCA	ARID1A_2.198073
ARID1A	chr1	CTAACCCATACTCGCAGCAACA	TCACAATCACCATCTACTGCTG	ARID1A_2.263887
ARID1A	chr1	GCCATCCAGTCCAATGGATCAG	CCTGCATGGTCTCGGGTAC	ARID1A_2.310812
ARID1A	chr1	AAACTGTGTACTTGGGTTATATATTCAGT	CCATATGGCTGAGGTTCTCATCTTG	ARID1A_2.6808
ARID1A	chr1	AGTCCAGCAAACTGCCTATTC	ACCAGAGTTAATTGGTCTTAAGTG	ARID1A_3.115759

ARID1A	chr1	CAGCAAAGTCTCACCTCAG	GGGATGGCTGCTGGGAGTAT	ARID1A_3.189854
ARID1A	chr1	CAGCCTCCACATCAGCAGTC	AGCCTGCTGGGAGAGCGT	ARID1A_3.203145
ARID1A	chr1	CAGGCTCAGTCTCCTTACCA	GCAGGAGGCAGGGATATCTT	ARID1A_3.210697
ARID1A	chr1	TGCTTCTATACTCATCATCAGTGCAT	CTTTGCTGGTTGTAATATGGAGTCTG	ARID1A_3.663071
ARID1A	chr1	TTTTCTTTCTACAGATTCCTCCTT	CTGCTGCTGATACGAAGGTTG	ARID1A_3.701387
ARID1A	chr1	AGCAGCAGCCACAGTCTCAA	TGAGCCTGTGGCTGTGAGTA	ARID1A_3.77267
ARID1A	chr1	CCATCACAGCTTTTGTCTTTCTGTGTAG	ACCTTCAGAAGGTGCAGAAATACT	ARID1A_4.173246
ARID1A	chr1	CTGGCCTTACATAATACTTTTCGC	GATGCCTGAGACCCAAATGAATC	ARID1A_4.215850
ARID1A	chr1	GAGGGCAAGAAGATGAACCTGAG	AGGTCAAATTAGCTAAACTTCCAACCA	ARID1A_4.255932
ARID1A	chr1	GAGTCTGGAGTGAGCACATC	CGAGAGTGGTCTGAGCGA	ARID1A_5.220317
ARID1A	chr1	AGAATCTTTCTGCCTAATATACTAATCCATG	AGGAGACTGAGCTGGATTACTCT	ARID1A_5.34011
ARID1A	chr1	AGTCTCTTTCTCTCCTCATACCT	CAGTCACTTTCCCTCTCCCTAA	ARID1A_5.70816
ARID1A	chr1	GATATGCTTATGTTGTTCTTTGTCTGGA	CACTCAAATGTCTGCCCTAGCTC	ARID1A_6.227771
ARID1A	chr1	AGCCATTTCTAGCTCTGAATTAACCTCC	TCGATCTTGGGCAATGCTTGAT	ARID1A_6.45476
ARID1A	chr1	CAGCCTTATCTCCGCGTCAG	ACTGTTTTCTCTCACCCTGAT	ARID1A_7.149596
ARID1A	chr1	CAGGATAAGGATGGAGAGCATTGTTC	TGTGTATCTGTCTCCGGAA	ARID1A_7.152412
ARID1A	chr1	CATGGCCAATATGCCACCTCA	ATAATACATTTCTTGCACTGACACCCT	ARID1A_8.210031
ARID1A	chr1	CCAATGCCAACTACCCAGTG	GGCCATGTTAGGGCCATAAGG	ARID1A_8.229785
ARID1A	chr1	GTTGCTAGTGAGTGACTAACCAAGTC	GGCTGTCCATGCATTTGACCTC	ARID1A_8.517555
ARID1A	chr1	AGGATGAGTCACGCCTCCATG	GGCCTTACCTGTTTTGGATAGAGTTG	ARID1A_8.91537
ARID1A	chr1	AGCACTATTTGGCTCCAGTTCAAATC	GGTTGATCATGCCAGCCATACTATTA	ARID1A_9.65769
BRAF	chr7	CATACTTACCATGCCACTTTCCCTT	TTTCTTTTCTGTTGGCTTGACTTGA	CHP2_BRAF_1
BRAF	chr7	CCACAAAATGGATCCAGACAACCTGT	GCTTGCTCTGATAGGAAAATGAGATCTA	CHP2_BRAF_2
CDKN2A	chr9	CACCAGCGTGTCCAGGAA	CCCTGGCTCTGACCATTCTGT	CHP2_CDKN2A_1
CDKN2A	chr9	CATCTATGCGGGCATGGTACT	CGCTGGTGGTGTCTG	CHP2_CDKN2A_2
CTNNB1	chr3	ACTGTTTCGTATTTATAGCTGATTTGATGGA	CCTCTTCTCAGGATTGCCTTT	CHP2_CTNNB1_1
EGFR	chr7	CCTCATTGCCCTCAACACAGT	TCAGTCCGGTTTTATTGTCATCATAGTT	CHP2_EGFR_1
EGFR	chr7	CACCAGTACCAGATGGATGT	CCCAAAGACTCTCCAAGATGGGATA	CHP2_EGFR_2
EGFR	chr7	AGACATGCATGAACATTTTTCTCCAC	TCCAGACCAGGGTGTGTTTTTC	CHP2_EGFR_3
EGFR	chr7	TGTGGAGCCTTTACACCCA	GTGCCAGGGACCTTACCTTATAC	CHP2_EGFR_4
EGFR	chr7	ACGTCTTCTCTCTCTGTCA	CTGAGGTTCAGAGCCATGGA	CHP2_EGFR_5
EGFR	chr7	CATGCGAAGCCACACTGAC	ACATAGTCCAGGAGGCA	CHP2_EGFR_6
EGFR	chr7	GACTATGTCCGGGAACACAAAGA	CCCATGGCAAACCTTGCTA	CHP2_EGFR_7
EGFR	chr7	CGCAGCATGTCAAGATCACAGAT	GCATGTGTTAAACAATACAGCTAGTG	CHP2_EGFR_8
FBXW7	chr4	TGACAATGTTTAAAGTGGTAGCTGTT	ACTCATTGATAGTTGTAACCAACACA	CHP2_FBXW7_1
FBXW7	chr4	CCTGTGACTGCTGACCAAACCTTTTA	CACATCTTCTTATAGGTGCTGAAAGG	CHP2_FBXW7_2
FBXW7	chr4	CCCAACCATGACAAGATTTTCCC	GGTCATCACAATGAGAGACAACATCA	CHP2_FBXW7_3
FBXW7	chr4	ACTAACAAACCCTCTGCCATCATA	TCTGCAGAGTTGTTAGCGGTT	CHP2_FBXW7_4
FBXW7	chr4	GTAGAATCTGCATTCCAGAGACAA	TCTCTTGATACATCAATCCGTGTTTGG	CHP2_FBXW7_5
FGFR2	chr10	CATCACTGTAAACCTTGAGACAAAAC	TGGTCTCTCATTCTCCCATCCC	CHP2_FGFR2_1
FGFR2	chr10	CATCCTCTCTCAACTCCAACAGG	AGTGGATCAAGCACGTGGAAAA	CHP2_FGFR2_2
FGFR2	chr10	GCTTCTTGGTCTGTTCTTCATT	CTCCTCTGTGATCTGCAATCT	CHP2_FGFR2_3
FGFR2	chr10	TGGAAGCCAGCCATTTCTAAA	GATGATGAAGATGATGGGAAACACAAG	CHP2_FGFR2_4
GNAS	chr20	TTGGTGAGATCCATTGACCTCAATTT	TGAATGTCAAGAAACCATGATCTCTGTT	CHP2_GNAS_1
GNAS	chr20	CCTCTGGAATAACAGCTGTCC	TGATCCCTAACAAACACAGAAGCAA	CHP2_GNAS_2

IDH1	chr2	CCAACATGACTTACTTGATCCCCAT	ATCACCAAATGGCACCATACGA	CHP2_IDH1_1
IDH2	chr15	ACCCTGGCCTACCTGGTC	AGTTCAAGCTGAAGAAGATGTGGAA	CHP2_IDH2_1
KRAS	chr12	CAAAGAATGGCTGCACCAGTAATAT	AGGCCTGCTGAAAATGACTGAATATAA	CHP2_KRAS_1
KRAS	chr12	TCCTCATGTACTGGTCCCTCATT	GTAAAAGGTGCACTGTATAATCCAGACT	CHP2_KRAS_2
KRAS	chr12	CAGACTGTATTTATTTTCAGTGTACTTACCT	GACTCTGAAGATGTACCTATGGTCTTA	CHP2_KRAS_3
NRAS	chr1	CCTCACCTCTATGGTGGGATCATAT	GTTCTTGCTGGTGTGAAATGACTG	CHP2_NRAS_1
NRAS	chr1	TTGCCTGTCTCATGTATTGG	CACCCCAGGATTCTTACAGAAAA	CHP2_NRAS_2
NRAS	chr1	GCACAAATGCTGAAAGCTGTACC	CAAGTGTGATTTGCCAACAAAGGA	CHP2_NRAS_3
PIK3CA	chr3	CCATAAAGCATGAACTATTTAAAGAAGCAAGA	GGTTGAAAAAGCCGAAGGTCAC	CHP2_PIK3CA_1
PIK3CA	chr3	TGGAATGCCAGAACTACAATCTTTTGAT	AAGATCCAATCCATTTTGTGTGC	CHP2_PIK3CA_10
PIK3CA	chr3	TGGATCTCCACACAATTAACAGCAT	TGCTGTTCATGGATTGTCAATTC	CHP2_PIK3CA_11
PIK3CA	chr3	CCCTTTTTAAAGTAATTGAACCAAGTAGGC	TTTAAGATTACGAAGGATTGGTTAGACAGAA	CHP2_PIK3CA_2
PIK3CA	chr3	GACGATTTCCACAGCTACAC	AGCATCAGCATTTGACTTTACCTTATCA	CHP2_PIK3CA_3
PIK3CA	chr3	CATAGGTGGAATGAATGGCTGAATTATG	TCAATCAGCGGTATAATCAGGAGTTTTT	CHP2_PIK3CA_4
PIK3CA	chr3	TCCCATTATTATAGAGATGATTGTTGAATTTTCT	CAAAACAAGTTTATATTTCCCATGCCA	CHP2_PIK3CA_5
PIK3CA	chr3	GCTTTGAATCTTTGGCCAGTACCT	CATAAGAGAGAAGGTTTGACTGCCATA	CHP2_PIK3CA_6
PIK3CA	chr3	CAGAGTAACAGACTAGCTAGAGACAATGA	GCACTTACCTGTGACTCCATAGAAA	CHP2_PIK3CA_7
PIK3CA	chr3	CACGATCTTTTAGATCTGAGATGCACA	CCTTTGTGTTTCATCCTTCTCTCTG	CHP2_PIK3CA_8
PIK3CA	chr3	GATGCAGCCATTGACCTGTTTAC	AGAAAACCATTACTTGTCCATCGTCT	CHP2_PIK3CA_9
PTEN	chr10	GCCATCTCTCTCCTCTTTTCTT	GCCGCAGAAATGGATACAGGTC	CHP2_PTEN_1
PTEN	chr10	TGTTAATGGTGGCTTTTGTGTTGTTGT	TCTACCTCACTCTAACAAAGCAGATAACT	CHP2_PTEN_2
PTEN	chr10	CCATAACCCACCACAGCTAGAA	TGCCCGATGTAATAAATATGCACAT	CHP2_PTEN_3
PTEN	chr10	GGCTACGACCCAGTTACCATAG	TGCCACTGGTCTATAATCCAGATGAT	CHP2_PTEN_4
PTEN	chr10	TGAGATCAAGATTGCAGATACAGAATCC	ACCTTTAGCTGGCAGACCAC	CHP2_PTEN_5
PTEN	chr10	AGGTGAAGATATATTCTCCAATTCAGGAC	TTGGATATTTCTCCAATGAAAGTAAAGTAC	CHP2_PTEN_6
PTEN	chr10	CACTTTTGGGTAATACATTCTCATACCAGGA	TATACTGCAAATGCTATCGA	CHP2_PTEN_7
PTEN	chr10	GCAGTATAGAGCGTGCAGATAATGA	CATCACATACATAAAGTCAACAACCC	CHP2_PTEN_8
RNF43	chr17	CCAAACACATCTGGAGCACACT	GCCTGACCCTCAATGACCTCTT	RNF43_1.100174
RNF43	chr17	CCGCTTTTGTAGTGGTGGT	TGACTTTGACCCCTAGTGTACT	RNF43_2.1.213215
RNF43	chr17	ACAACCACACTGGCTGTGAA	GCACCAGCTTGCCAGATT	RNF43_2.1.22754
RNF43	chr17	CGGTGTCAGAATCCATTAGAAAG	GACAAGAGGCTGCTACCAGAAA	RNF43_2.1.264668
RNF43	chr17	CTCTCCCTACCACACCCACTT	GTGGTTGTGCTGACTCCTC	RNF43_2.1.277654
RNF43	chr17	CTGGGTGCACAGTTGCATC	CCCTGGCCAGTTGACG	RNF43_2.1.308947
RNF43	chr17	GAAACCTGGGTTTCCCTGT	GGGTCCATGGCAGCAGTTC	RNF43_2.1.342797
RNF43	chr17	AAAGTCACTGCTTAGGGAGCT	AGAAAGCTATTGCACAGAACGC	RNF43_2.1.4249
RNF43	chr17	GGGACCAAGGATATGCCACACT	TGCAAAAATCCAGCCTCTCTGC	RNF43_2.1.479773
RNF43	chr17	GGGCACTGTGGTTAGAGAG	AAAAGCGGTTCCAGTGGCA	RNF43_2.1.483268
RNF43	chr17	GTGACTTGCTGATCAGGAGAAGGT	GTTTCCAGCCATGTCCACTACC	RNF43_2.1.554471
RNF43	chr17	TTTTTGCAAGTTGAACAGACTGCT	CAAGTACCAGATCCAATCAGC	RNF43_2.1.716452
RNF43	chr17	CTCCAGATCCACTGCTGTCA	TTCCCCAGAGCTGCACATC	RNF43_2.2.168519
RNF43	chr17	GTAGGCTGATGTCCGTGCAG	GCTTGCCAGTGCCCTTA	RNF43_2.2.335644
RNF43	chr17	GTGCTGTGAGGTGGATTGGAG	CCCACGACCTGGTCCCTT	RNF43_2.2.348341
RNF43	chr17	GTGATGCCGAGGGCCCAT	CAGGTGCAAGACTCCACCTC	RNF43_2.2.359855
RNF43	chr17	AGGTGGTAGTGGGATGGC	TGTCTTTCTGAATGCATTCTGTAGG	RNF43_2.2.62203
RNF43	chr17	CCTCTACCTGTGATGTTGAACATG	CCTGATTCTGGCAATCCTATGG	RNF43_3.144168

RNF43	chr17	AAGCCACATTCTAGACCTGTCTG	CTCTTTTCTCCAGGACTACGG	RNF43_3.9926
RNF43	chr17	TCCTCCAGACAGATGGCACA	CCCAATCTGAGCCCCATTCT	RNF43_4.332752
RNF43	chr17	TTCAATCTCCCCAGTCTGGTCAT	AGCTGGCCACCAGGAGGTA	RNF43_4.381754
RNF43	chr17	TACTCCTTCTTCTCCCTAACCCAC	ATGATGTGTGGATCCTAATGACAGT	RNF43_5.252108
RNF43	chr17	AAGCCAGGATGATCACAAGATGG	CTCAAGGGAACCTCCAGTTAGCTAT	RNF43_5.9080
RNF43	chr17	CCCTGAGAGCTTTATCTTCTCCATC	GACCTCAGCCCAACCTCTACT	RNF43_6.126819
RNF43	chr17	GTCTGGAGGTCTAGTGTGCT	TGGGCACCTTCCCCCTGTA	RNF43_6.251138
RNF43	chr17	ATCAGCTTCTCAGCGTCATTACC	CTGGATGGAGGAAGATAAAGCTCTCA	RNF43_6.62210
RNF43	chr17	CACAGGACAAAGTAGGGCTAAGTG	AAGCTGATGGAGTTTGTGTACAAGAA	RNF43_6.83735
RNF43	chr17	CCAGCTTGACGATGCTGATGAAT	TGGTACTCTCCCTAGAAAATGGAGAG	RNF43_8.145848
RNF43	chr17	GTGTAGGGCGAAGTGTGAGTC	CCTAACCCAAGTCTGTCTCTCTG	RNF43_8.334246
RNF43	chr17	ATTTCCACTTCTCTCAGACCAAGTCAT	CCTGTCACTGGCTAGCAAGGTA	RNF43_8.99948
RNF43	chr17	GCAAACACACCTTCCAAAGTGAGATT	TGGACGCACAGGACTGGTAC	RNF43_9.251835
RNF43	chr17	ACAAAAGAAGAAAGACATATTTCAAACAGATG	TTATCAGAGTGATCCCTTGAAAATGG	RNF43_9.43347
RNF43	chr17	AGCTTTCTGTCTGCTGATCTTCA	GTATGTATGGTTGAAGTGCATTGCTG	RNF43_9.83487
SMAD4	chr18	CTCATGTGATCTATGCCGCT	AGTCTACTTACCAATCCAGGTGATACA	CHP2_SMAD4_1
SMAD4	chr18	TGCTACTTCTGAATTGAAATGGTTCA	GATTACTACCATTACTCTGCAGTGTT	CHP2_SMAD4_2
SMAD4	chr18	ATGGTGAAGGATGAATATGTGCATGA	GCTGGTAGCATTAGACTCAGATGG	CHP2_SMAD4_3
SMAD4	chr18	GTGAAGGACTGTTGCAGATAGCAT	AAGGCCACATGGGTTAATTTG	CHP2_SMAD4_4
SMAD4	chr18	TTTCTTTAGGGCTTTCACAATGA	CTGAGAAGTGACCCATAATCCATT	CHP2_SMAD4_5
SMAD4	chr18	GCTCCTGAGTATTGGTGTCCAT	CCTGTGGACATTGGAGAGTTGA	CHP2_SMAD4_6
SMAD4	chr18	TGTAATTTCTTTTTCTTCTAAGGTTGCACATAG	ACTTGGGTAGATCTTATGAACAGCAT	CHP2_SMAD4_7
SMAD4	chr18	AGGCTTTGATTGCGTCAGTGT	GCTGGAGCTATTCCACTACTG	CHP2_SMAD4_8
SMAD4	chr18	GCTGCTGGAATTGGTGTGATG	AGTACTCGTCTAGGAGCTGGAG	CHP2_SMAD4_9
STK11	chr19	GAGCTGATGTCGGTGGGTAT	CTCCGAGTCCAGCACCTC	CHP2_STK11_1
STK11	chr19	CTCCAGGCAGCTGCAA	CCGGTGGTGAGCAGCAG	CHP2_STK11_2
STK11	chr19	CCGGTGGCACCTCAA	CTGGTCCGGCAGGTGTC	CHP2_STK11_3
STK11	chr19	AACATCACACGGGTCTGTAC	GATGAGGCTCCACCTTCAG	CHP2_STK11_4
STK11	chr19	GAAGAAACATCCTCCGGCTGAA	ACCGTGAAGTCTGAGTGTAGA	CHP2_STK11_5
TP53	chr17	TCCACTCACAGTTTCCATAGGTCT	GTTGGAAGTGTCTCATGCTGGAT	CHP2_TP53_1
TP53	chr17	GGCTGTCCAGAATGCAAGAA	GATGAAGCTCCAGAATGCCA	CHP2_TP53_2
TP53	chr17	TGCACAGGGCAGGTCTTG	CCGTCTCCAGTTGCTTTATCTGT	CHP2_TP53_3
TP53	chr17	ACCAGCCTGTCTCTCT	GTGCAGCTGTGGTTGATTC	CHP2_TP53_4
TP53	chr17	CCAGTTGCAAACAGACCTCA	AGGCCTCTGATTCCTCACTGAT	CHP2_TP53_5
TP53	chr17	GGCTCCTGACCTGGAGTCTT	CTCATCTTGGGCTGTGTTATCTC	CHP2_TP53_6
TP53	chr17	CGCTTCTGTCTGCTTCT	TTCTTTTTCTATCTGAGTAGTGGT	CHP2_TP53_7
TP53	chr17	GGAAGGGGCTGAGGTCACT	CCCCTCTCTGTTGCTGC	CHP2_TP53_8
VHL	chr3	CTCCAGGTCATCTTCTGCAAT	GTACCTCGGTAGCTGTGGATG	CHP2_VHL_1
VHL	chr3	GTGGCTCTTAAACCTTTGCT	GTCAGTACCTGGCAGTGTGATA	CHP2_VHL_2
VHL	chr3	GGCAAAGCCTCTTGTCTGTTTC	TGACGATGTCCAGTCTCCTGTAAT	CHP2_VHL_3

1

1 **Supplementary table 3: Mutation profile of precursor lesions detected by targeted NGS.**

Grade	Gene	Sample	Variant	VAF [%]	Variant Effect	Transcript
low-grade PanIN	<i>ARID1A</i>	<b>113</b>	Gln802fs	4.83	frameshift/insertion	NM_006015.5
	<i>CDKN2A</i>	74	Arg58Ter	3.48	nonsense	NM_001195132.1
	<i>GNAS</i>	127	Arg201His	20.17	missense	NM_000516.5
	<i>KRAS</i>	52	Gly12Val	15.38	missense	NM_033360.3
		<b>55</b>	Gly12Val	9.66	missense	NM_033360.3
		<b>56</b>	Gly12Asp	6.13	missense	NM_033360.3
		69	Gln61His	4.08	missense	NM_033360.3
		74	Gly12Asp	12.05	missense	NM_033360.3
		<b>111</b>	Gly12Val	11.19	missense	NM_033360.3
		125	Gly12Val	4.29	missense	NM_033360.3
		127	Gly12Asp	18.24	missense	NM_033360.3
		128	Gly12Asp	3.42	missense	NM_033360.3
		129	Gly12Asp	3.7	missense	NM_033360.3
		<b>113</b>	Gly12Arg	4.18	missense	NM_033360.3
		<b>113</b>	Gly12Val	8.75	missense	NM_033360.3
		<b>43</b>	Gly12Val	12.88	missense	NM_033360.3
	<i>PIK3CA</i>	68	Arg349Ter	3.74	nonsense	NM_006218.3
127		Phe83fs	4.52	frameshift/deletion	NM_006218.3	
<i>PTEN</i>		128	Asn323fs	22.37	frameshift/deletion	NM_000314.6
high-grade PanIN	<i>ARID1A</i>	73	Trp2091Ter	7.46	nonsense	NM_006015.4
	<i>GNAS</i>	96	Arg201His	3.42	missense	NM_000516.5
	<i>KRAS</i>	73	Gly12Asp	8.29	missense	NM_033360.3
		<b>80</b>	Gly12Val	16.59	missense	NM_033360.3
		101	Gly12Asp	13.7	missense	NM_033360.3
		<b>104</b>	Gly12Asp	5.15	missense	NM_033360.3
		<b>114</b>	Gly12Val	18.3	missense	NM_033360.3

	<i>TP53</i>	<b>80</b>	Arg213Ter	34.5	nonsense	NM_000546.5
		<b>104</b>	Arg196Ter	4.04	nonsense	NM_000546.5
low-grade IPMN gastric	<i>ARID1A</i>	21	Asp1850fs	7.45	frameshift/insertion	NM_006015.5
	<i>GNAS</i>	<b>2</b>	Arg201His	33.98	missense	NM_000516.5
		<b>7</b>	Arg201Cys	11.34	missense	NM_000516.5
		<b>35</b>	Arg201His	41.52	missense	NM_000516.5
		<b>62</b>	Arg201Cys	15.56	missense	NM_000516.5
		<b>86</b>	Arg201His	30.46	missense	NM_000516.5
		89	Arg201His	5.56	missense	NM_000516.5
		<b>94</b>	Arg201His	21.97	missense	NM_000516.5
		<b>97</b>	Arg201Cys	33.81	missense	NM_000516.5
		<b>99</b>	Arg201His	25.08	missense	NM_000516.5
		<b>110</b>	Arg201Cys	22.37	missense	NM_000516.5
		<b>112</b>	Arg201His	24.32	missense	NM_000516.5
		<b>54</b>	Arg201Cys	23.16	missense	NM_000516.5
	<i>KRAS</i>	21	Gly12Val	18.86	missense	NM_033360.3
		<b>2</b>	Gly12Val	35.1	missense	NM_033360.3
		<b>7</b>	Gly12Val	12.14	missense	NM_033360.3
		<b>35</b>	Gly12Asp	38.57	missense	NM_033360.3
		<b>39</b>	Gly12Val	35	missense	NM_033360.3
		<b>61</b>	Gly12Val	18.03	missense	NM_033360.3
		<b>62</b>	Gly12Val	18.5	missense	NM_033360.3
		64	Gly12Val	9.01	missense	NM_033360.3
		<b>86</b>	Gly12Val	27.81	missense	NM_033360.3
		89	Gln61His	36.49	missense	NM_033360.3
		<b>94</b>	Gly12Asp	21.16	missense	NM_033360.3
		<b>97</b>	Gly12Asp	33.68	missense	NM_033360.3

		<b>99</b>	Gly12Val	26.83	missense	NM_033360.3
		<b>110</b>	Gly12Val	24.76	missense	NM_033360.3
		<b>57</b>	Gly12Arg	6.96	missense	NM_033360.3
	<i>STK11</i>	<b>61</b>	Tyr60Ter	61.89	nonsense	NM_000455.4
high-grade IPMN gastric	<i>ARID1A</i>	130	Gln2115Ter	30.84	nonsense	NM_006015.5
	<i>GNAS</i>	51	Arg201Cys	31.03	missense	NM_000516.5
	<i>KRAS</i>	51	Gly12Val	33.12	missense	NM_033360.3
		65	Gly12Asp	16.51	missense	NM_033360.3
		66	Gly12Asp	33.64	missense	NM_033360.3
		130	Gly12Asp	22.65	missense	NM_033360.3
		131	Gly12Asp	23.98	missense	NM_033360.3
	<i>TP53</i>	65	Arg248Trp	17.99	missense	NM_000546.5
low-grade IPMN intestinal	<i>GNAS</i>	<b>92</b>	Arg201Cys	80.59	missense	NM_000516.5
	<i>KRAS</i>	<b>92</b>	Gly12Arg	37.95	missense	NM_033360.3
high-grade IPMN intestinal	<i>GNAS</i>	<b>33</b>	Arg201Cys	45.42	missense	NM_000516.5
		<b>88</b>	Arg201Cys	36.81	missense	NM_000516.5
		<b>90</b>	Arg201His	35.51	missense	NM_000516.5
		17	Gln227Lys	42.36	missense	NM_000516.5
	<i>KRAS</i>	<b>88</b>	Gly12Ser	33.81	missense	NM_033360.3
	<i>TP53</i>	<b>88</b>	Met237Thr	49.16	missense	NM_000546.5

1 PanIN/IPMN in cases without associated/concomitant PDAC are indicated in bold.

2

3

4

5

1 **Supplementary table 4. Distribution of CNV-positive and negative precursor lesions**  
 2 **according to the degree of dysplasia.**

		<i>CNV pos</i>	<i>CNV neg</i>
<i>PanIN</i>	<b>Low-grade</b>	16 (57%)	12 (43%)
	<b>High-grade</b>	6 (75%)	2 (25%)
<i>Gastric IPMN</i>	<b>Low-grade</b>	22 (76%)	7 (24%)
	<b>High-grade</b>	6 (75%)	3 (25%)
<i>Intestinal IPMN</i>	<b>Low-grade</b>	8 (100%)	0
	<b>High-grade</b>	13 (100%)	0

3 Percentages refers to the total number of cases in each group

4

5

6

7

8

9

10

11

12

13

14

**Supplementary table 5: Overview of log<sub>2</sub> copy number ratios sorted in ascending order. Values of genomic alterations were detected by low-coverage sequencing (n=28) and DNA methylation data (n=67), respectively.**

Genomic location	affected samples (n)	PanIN (n=36)	gIPMN (n=38)			iIPMN (n=21)		
<b>deleted regions</b>								
chr01:010875000-013052998	3					-0.26	-0.25	-0.24
chr01:015375000-016825000	3					-0.26	-0.25	-0.20
chr06:074175000-074375000	5		-0.29	-0.22	-0.21	-0.44	-0.24	
chr06:133664400-143100000	5		-0.37	-0.28		-0.50	-0.45	-0.28
chr06:143620678-151100000	7	-0.21	-0.37	-0.34	-0.29	-0.50	-0.45	-0.28
chr09:005958053-023802212	5	-0.23	-0.51	-0.36	-0.36	-0.24		
chr10:071075000-120925000	6		-0.45	-0.22		-0.36	-0.30	-0.28
chr10:120925000-125869472	5		-0.30			-0.41	-0.30	-0.28
chr11:057325000-058807232	4					-0.44	-0.40	-0.27
chr11:058807232-069089801	5					-0.44	-0.40	-0.28
chr11:096437584-114325000	5					-0.51	-0.44	-0.40
chr11:114325000-134898258	4					-0.51	-0.44	-0.28
chr17:006225000-009675000	4		-0.50	-0.32	-0.21	-0.23		
chr17:009675000-012500000	5		-0.53	-0.31	-0.21	-0.50	-0.22	
chr17:015792977-021566608	6		-0.58	-0.23	-0.21	-0.49	-0.32	-0.25
<b>amplified regions</b>								
chr01:035225000-037325000	3					0.25	0.33	0.61

chr03:176225000-188875000	6	0.26	0.21	0.23	0.28	0.38	0.44				
chr05:028950000-044925000	5				0.24	0.25	0.31	0.74	0.79		
chr06:024125000-033575000	5		0.25	0.36	0.31	0.35	0.56				
chr06:033575000-042725000	4		0.42		0.32	0.34	0.56				
chr07:000282484-007150000	5				0.22	0.30	0.32	0.36	0.41		
chr07:054725000-055775000	5				0.21	0.26	0.27	0.33	0.36		
chr07:061967157-074715724	4				0.27	0.32	0.36	0.37			
chr07:112425436-130154523	5				0.21	0.33	0.36	0.38	0.57		
chr07:139404377-142048195	5				0.22	0.32	0.36	0.33	0.58		
chr07:143397897-154270634	5				0.24	0.33	0.34	0.38	0.59		
chr08:086726451-089550000	3				0.21	0.31	0.36				
chr08:127450000-129175000	7	0.42			0.21	0.27	0.29	0.36	0.56	0.66	
chr09:001992685-035698318	3				0.24	0.32	0.61				
chr09:070835468-092343416	4				0.22	0.26	0.32	0.60			
chr09:096718222-097575000	4				0.21	0.24	0.32	0.60			
chr09:097775000-114750000	4				0.22	0.26	0.32	0.61			
chr09:124994207-133073060	3				0.22	0.32	0.61				
chr12:006475000-007169938	8	0.21			0.24	0.33	0.56	0.71	0.88	0.89	1.70
chr12:024993545-028938805	4	0.21			0.21	0.38	1.32				
chr14:020700000-022050000	3				0.21	0.28	0.33				
chr14:022800000-050175000	3				0.22	0.25	0.35				
chr14:097258910-107289540	3				0.25	0.22	0.36				
chr17:061125000-062410760	3				0.32	0.32	0.74				
chr17:062775000-063525000	3				0.32	0.34	0.49				
chr17:068117898-077546461	3				0.21	0.32	0.38				

chr20:008050000-016400000	7	0.24	0.22	0.23	0.24	0.26	0.33	0.84
chr20:016625000-021300000	7	0.25	0.22	0.23	0.25	0.28	0.33	0.82
chr20:030025000-034897085	7	0.26	0.22	0.22	0.23	0.31	0.33	0.81
chr20:036958189-042991501	6	0.26	0.22	0.23	0.35	0.33	0.79	
chr20:052650000-061091437	7	0.23	0.22	0.22	0.23	0.33	0.35	0.80
chr21:032825000-034475000	3		0.21	0.26	0.30			

1

1 **Supplementary table 6a: Differentially methylated probes in low- and high-grade pancreatic**  
 2 **cancer precursors.**

	Low-grade samples	High-grade samples	DMPs (hypermethylated in high-grade)	DMP associated genes (hypermethylated in high-grade)
iPMN	8	12	0	0
gIPMN	24	8	0	0
PanIN	20	7	86 (62)	59 (45)

3 iIPMN: intestinal IPMN; gIPMN: gastric IPMN

4

5 **Supplementary table 6b: Genes associated with significantly hyper- or hypomethylated CpG**  
 6 **in PanIN high-grade**

Genes associated with at least one significantly hypermethylated CpG	Genes associated with at least one significantly hypomethylated
TAC1	GLRX
AKAP13	BCL11B
POLR1D	ITFG3
GLYATL3	IFT140
HOXA5	CTNNA3
ZIC2	RUNX1
SIM2	SPARCL1
ARID4B	PHLDB1
MON2	NINJ2
CNKSR3	METTL9
SP8	SLC51A
ADD2	EMID2
HOXB1	CACNA1A
ST3GAL6	C19orf35
FBN2	
ZIK1	
LRP1B	
NTRK3	
GLI3	
NTM	
RASGRF1	
FAM46C	

NXPH1	
LBX2	
LOC101929710	
ADRA1A	
GRIK3	
PARP8	
KIAA1026	
SLC6A15	
IRX1	
GRIA4	
TLE4	
DGKI	
PACSIN2	
DOK5	
ZIC4	
MYLK	
DAPK1	
C5orf66-AS1	
AMER3	
CPEB1	
ST6GAL2	
INA	
AP2A2	

1

## 1 **Supplementary Figure Legends**

### 2 **Supplementary figure 1: Overview of lesions and methods**

3 55 PanINs, 46 gastric IPMNs (gIPMN) and 21 intestinal IPMNs (iIPMN) were subjected to 4  
4 main analyses: targeted next generation sequencing (n=52), low-coverage whole-genome  
5 sequencing (n=28), genome-wide DNA methylation analysis (n=79) and transcriptome analysis  
6 (n=34). Each circle of the diagram represents one of the mentioned methods and includes the  
7 number of samples used for related analyses. The samples that could not be placed into the  
8 diagram were shown at the right bottom corner of the figure. Pancreatobiliary and mixed-type  
9 IPMNs were excluded from further analyses due to small sample size.

### 10 **Supplementary figure 2: Allele frequency of *KRAS* and *GNAS* mutations in different precursor 11 lesions.**

12 (A) VAF of *KRAS* mutations; (B) VAF of *GNAS* mutations; (C) scatterplot of the VAF of the *KRAS*  
13 mutations (G12) against the VAF of *GNAS* mutations (R201) detected in low- and high-grade  
14 gastric IPMN. The grey lines represent the 95% confidence interval of the Pearson's correlation  
15 coefficient  $r$  (n=9). (Kruskal-Wallis-test \*  $p < 0.05$ ; \*\*  $p < 0.01$ ; \*\*\*  $p < 0.001$ ).

16

### 17 **Supplementary figure 3: Morphology of lesions with different genetic status according to 18 targeted NGS**

19 Representative HE images of low- and high-grade PanINs, gastric IPMNs and intestinal IPMNs  
20 with variable mutation profiles detected by targeted NGS are shown. No specific morphology  
21 was identified related to the mutation status between the samples in the same diagnostic  
22 group. In particular, gastric lesions with *GNAS* mutations (case 127, 96, 99 and 112) did not  
23 show relevant intestinal differentiation; only in case 112, focal (<5% of the cells) expression of  
24 *MUC2* and *CDX2* was observed (not shown). Scale bars represent 200  $\mu\text{m}$ . Detailed mutation  
25 profile of the samples is provided in Suppl. Table 3.

### 26 **Supplementary figure 4: Quality control of DNA methylation data derived from normal 27 pancreas cell preparations.**

28 (A) Multi-dimensional scaling of the 1000 most variable probes. (B) Hierarchical clustering of  
29 probes for known acinar and ductal marker genes.

1

2 **Supplementary figure 5: Proliferation activity, expression of TFF3 and of MUCL3 protein in**  
3 **PanIN, IPMN and PDAC.**

4 Representative images (A) and related graphs (B-D) of IHC staining performed in whole tissue  
5 sections in 31 PanIN, 28 gastric IPMN, 20 intestinal IPMN and 24 PDAC. Intestinal IPMNs and  
6 PDACs showed higher proliferation rates with Ki67 staining than PanIN and gastric IPMN. TFF3  
7 was strongly expressed in intestinal IPMN. Gastric IPMN revealed higher expression of MUCL3  
8 compared to PanIN. Scale bars represent 100  $\mu$ m. (IRS: immunoreactivity score) (\* $p < 0.05$ ).

9

10 **Supplementary figure 6: Hierarchical clustering of DNA methylation data based on published**  
11 **marker genes for distinct normal pancreas cell populations.** The mean methylation beta-  
12 value for all gene associated probes is displayed, respectively.

13

14 **Supplementary figure 7: Differentially activated gene sets.** Displayed pathways were  
15 detected by pairwise comparison between the indicated lesions. Odds ratios below 0.8  
16 indicate the activation in the first listed lesion whereas 1.1 is associated with the second  
17 group. The analyzed gene sets based on the KEGG pathway (A) and hallmarks (B) from  
18 the MSigDB.

19

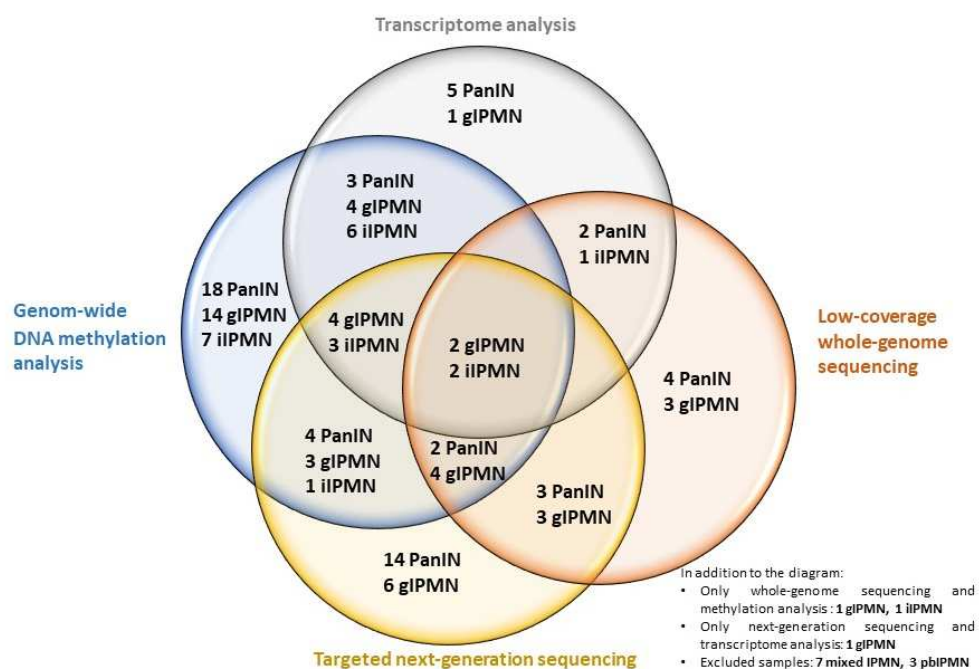
20

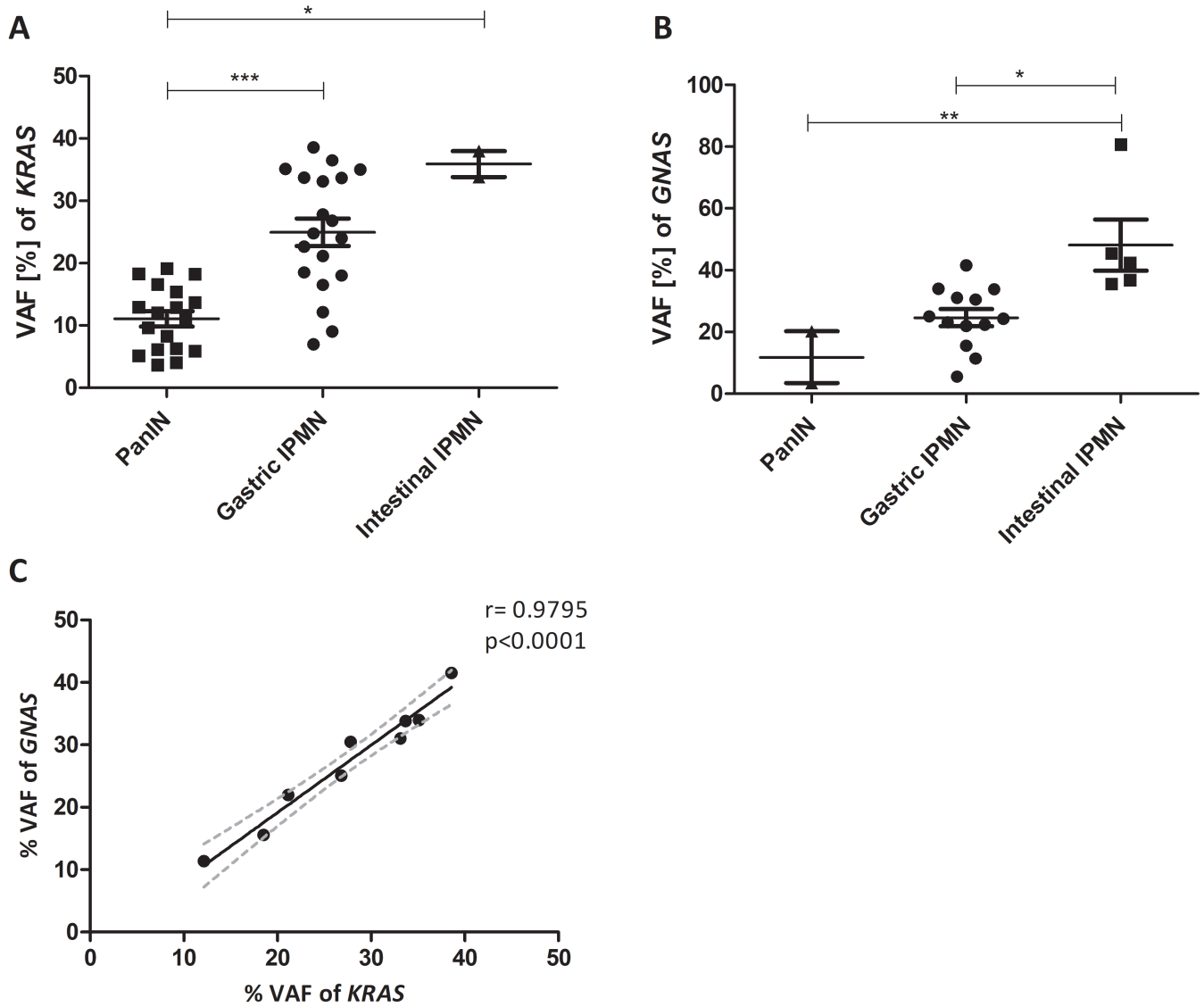
21

22

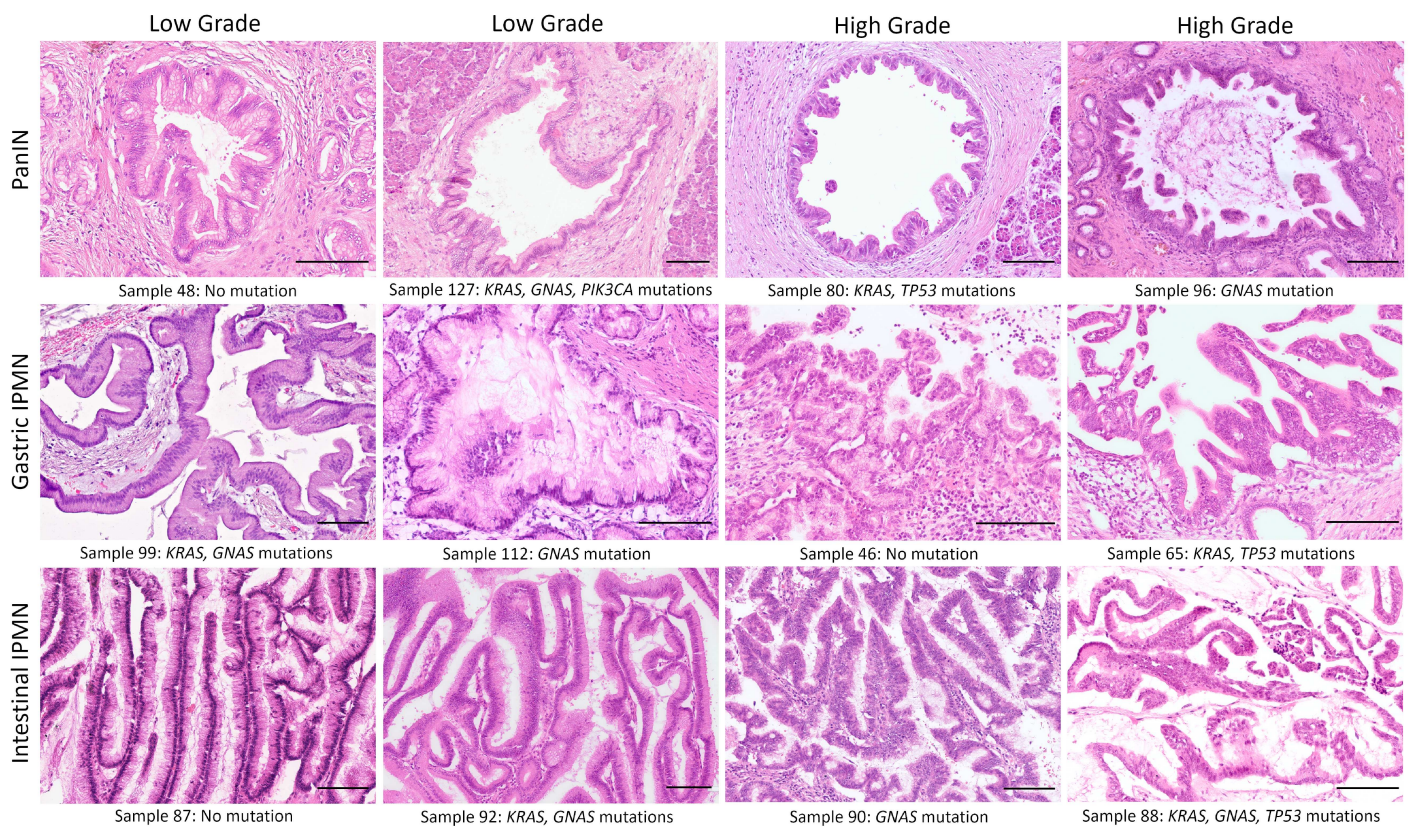
23

## Suppl. Figure 1.jpg

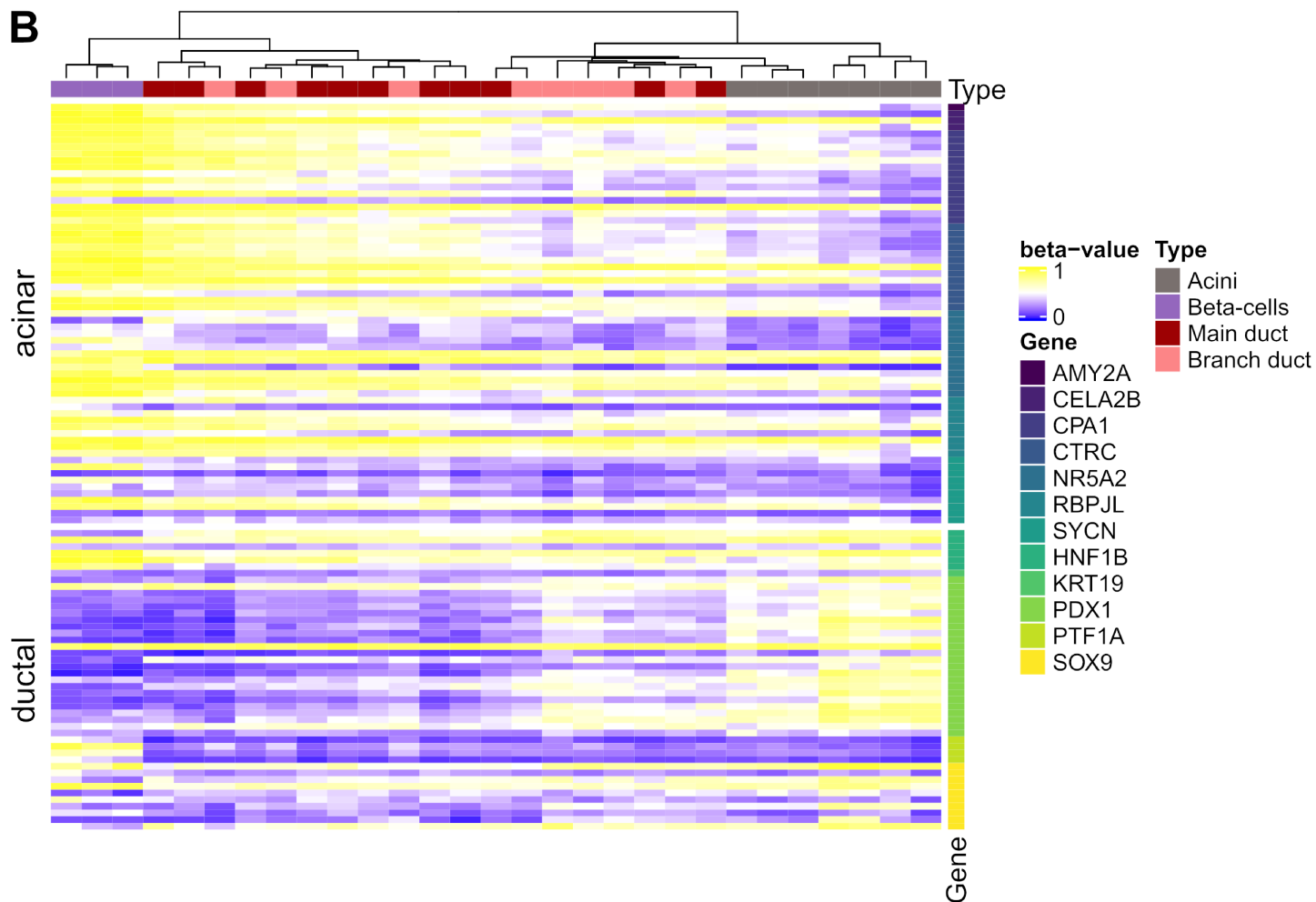
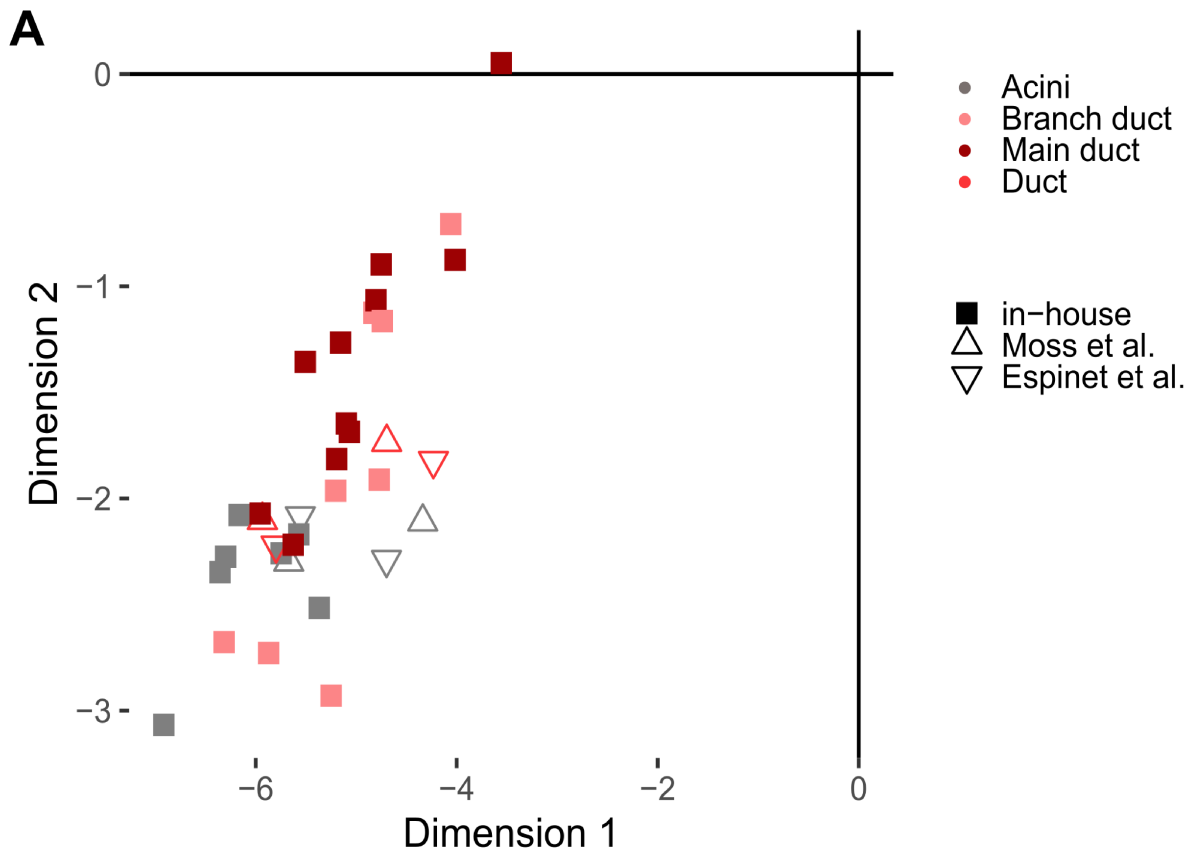


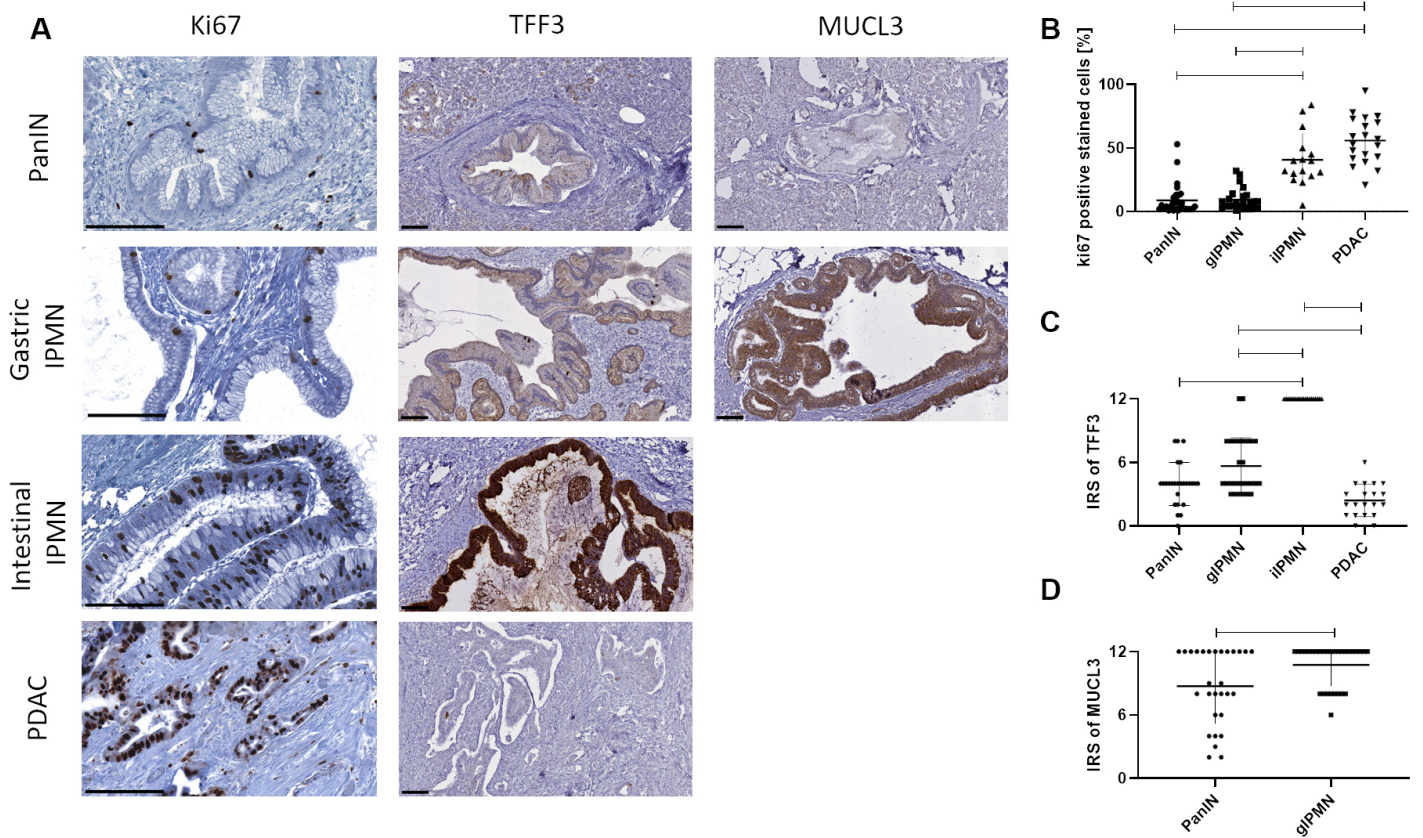


Suppl. Figure 3.tif

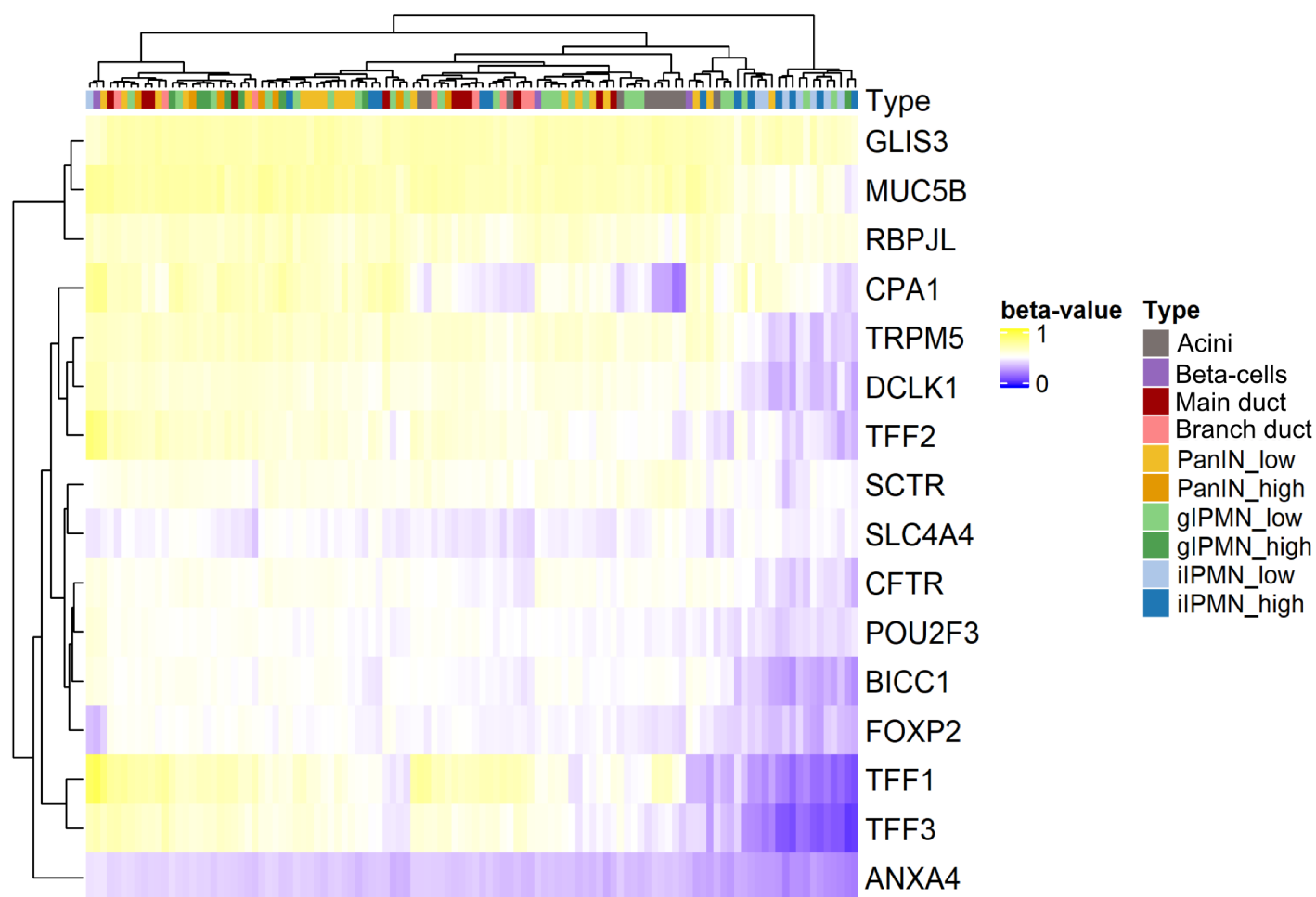


Layer





Layer



Suppl. Figure 7.tiff

